Author:
Felton, Harry

Title:
Improving user-interaction with material extrusion prototypes through emulation of mass properties

Improving User-Interaction With Material Extrusion Prototypes Through Emulation of Mass Properties

Submitted: 19/07/2022

Harry James Felton

A dissertation submitted to the University of Bristol in accordance with the requirements for award of the degree of PhD Mechanical Engineering in the Faculty of Engineering.

Word Count: 41,127

Abstract

Additive manufacturing is widely used as a method for prototyping products – especially in early-stage design. The most common method is Material Extrusion (MEX), which deposits filament using a heated nozzle. The method is widely used due to its low cost, ease of use, wide range of processable materials, and safety. While the method allows an accurate geometric form of a prototype to be fabricated relatively quickly, the mass properties of the fabricated product are often poorly represented. This discrepancy between the 'as-designed' mass properties and the fabricated prototype can, depending on use, have a significant impact on a user's perception of the product and ultimately the quality and commercial success of the final design. To address this shortcoming, this thesis develops a method that enables the fabrication of MEX prototypes that better emulate mass properties of the as-designed product.

The thesis begins with a user study to investigate the influence of each mass property (mass, mass balance, rotational inertia) on user perception of mass. The study reveals that, for consumer products, the principal rotational inertia has very little influence. Given this, the strategy for mass emulation aims at matching the mass and centre of mass position. Physical methods for modifying the mass properties were reviewed and down-selected based on their potential advantages and disadvantages. The use of variable infill was selected as full automation is possible and the method can be performed on multi-material printers – a capability that is becoming commonplace. The method was initially developed on a simple primitive, with a range of process parameters adjusted and tested spanning computation and manufacturing constraints. The process uses a directed search method, that iterates through potential centres of mass within the internal volume. Mass distributions are then generated and evaluated through Monte Carlo optimisation, using an exponential probability distribution.

The developed method was applied to three prototypical products – a games controller, electric hand drill and laser pointer – with results compared to a nominal fabrication. The case studies demonstrated that mass and centre of mass position can be emulated to high accuracy (in most instances to within 1% of the "as-designed" value, determined from the CAD model). Example prototypes were then manufactured using the method, further demonstrating encouraging results. Scope for improvement is, however, identified, and future work is discussed.

In summary, a novel process has been developed that allows mass properties to be emulated in MEX fabrications of prototypes of consumer goods. The process has been applied to specific use cases, demonstrating significant improvement in mass property accuracy compared to the typical fabrications. The scientific contribution of this thesis is three-fold:

1. Characterisation of the influence of mass properties on user perception of mass.
2. Creation of a method for emulating the as-designed mass properties of a 3D printed prototype.
3. Application and demonstration of the methodology in the MEX workflow for a range of consumer products.

Acknowledgements

First of all, I would like to thank Dr Jason Yon and Professor Ben Hicks for their supervision, mentorship and assistance throughout my PhD study. Without them, I would not have reached this stage of my PhD. Thank you also to Professor Aydin Nassehi for being my reviewer; providing invaluable feedback and direction throughout the last few years.

To the rest of the Design and Manufacturing Futures lab; thank you for the writing retreats, chess, support, discussion, coffee and generally being a fantastic group of people to work with. I wish you all every good fortune for the rest of your careers, and will always be available if you want a catch up. Please don't become strangers!

To my family and friends, thank you for putting up with me talking your ears off about 3D printing and prototyping, and providing me with opportunities for distraction and motivation - even over a pandemic. To my parents especially - thank you for helping me get here over the last 27 years. It really wouldn't have been possible without you.

Finally, to Laura. Thank you for putting up with me, distracting me, and always being with me. I am so lucky to be with you. I can't wait for all the adventures that await us.

Author's Declaration

I declare that the work in this dissertation was carried out in accordance with the requirements of the University's Regulations and Code of Practice for Research Degree Programmes and that it has not been submitted for any other academic award. Except where indicated by specific reference in the text, the work is the candidate's own work. Work done in collaboration with, or with the assistance of, others, is indicated as such. Any views expressed in the dissertation are those of the author.

SIGNED: DATE: 19/07/2022

Publications

A summary of the first author publications produced during the course of the PhD research are summarised below.

Journal Papers

1. **Felton, H.**, Yon, J. and Hicks, B. (In Review), *Improving Feel in 3D Printed Prototypes: A Numeric Methodology for Controlling Mass Properties Using Infill Structures* In: *To Be Confirmed*.
2. **Felton, H.**, Hughes, R.R. and Gaxiola, A. (2021), *Negligible-cost microfluidic device fabrication using 3D-printed interconnecting channel scaffolds* In: *PLOS One*. doi: https://doi.org/10.1371/journal.pone.0245206

Conference Papers and Posters

1. **Felton, H.**, Yon, J., Hicks, B. (2020), *Investigating strategies for mass property replication in 3D Printed Prototypes* At: *Design Computing and Cognition '20* (Poster)
2. **Felton, H.**, Yon, J. and Hicks, B. (2020), *Looks like but does it feel like? Investigating the influence of mass properties on user perceptions of rapid prototypes* In: *Proceedings of the Design Society: DESIGN Conference, 1, 1425-1434*. doi: https://doi.org/10.1017/dsd.2020.111

Claims

This thesis presents work completed at the University of Bristol within the Faculty of Engineering. The principal contributions claimed by the author are as follows:

1. The construction of a set of user and industrial data demonstrating that mass properties are important considerations in early-stage prototyping.
2. An assessment of the effect of principal rotational inertia on a user's perception of a prototype such that rotational inertia could be neglected in emulation methods.
3. An assessment of the potential emulation methods that may be integrated into the current material extrusion 3D printing workflow.
4. The development and characterisation of a method to allow mass properties to be emulated in material extrusion prototypes using variable infill density.
5. The application of the developed method to a series of case studies, demonstrating applicability in real-world cases and tuning of the method.
6. The development of a fabrication method for 3D printed prototypes with emulated mass properties by variable infill.

Contents

List of Figures

List of Tables

Acronyms

3MF 3D Manufacture Format.

ALM Additive Layer Manufacturing.

AM Additive Manufacturing.

AMF Additive Manufacture Format.

AR Augmented Reality.

CAD Computer Aided Design.

CAE Computer Aided Engineering.

CNC Computer Numeric Control.

CoM Centre of Mass.

DfA Design for Assembly.

DfAM Design for Additive Manufacture.

FDM Fused Deposition Modelling.

FFF Fused Filament Fabrication.

GC Geometric Centre.

HSS High Speed Steel.

IQR Interquartile Range.

ISO International Organization for Standardization.

LED Light Emitting Diode.

MCO Monte Carlo Optimisation.

MDR Material Density Ratio.

MEX Material Extrusion.

MR Mixed Reality.

PCB Printed Circuit Board.

PDS Problem Definition Specification.

PLA Polylactic Acid.

RAM Random Access Memory.

RI Rotational Inertia.

RP Rapid Prototyping.

RQ Research Question.

SI Système Internationale.

SLS Selective Laser Sintering.

VR Virtual Reality.

Chapter 1
Introduction

A prototype provides detailed insight into the way a future product may look, function, or otherwise exist [1]. They are regarded as crucial to the success of product development [2, 3] and there has been significant research into their use.

In practice, they are widely used in the development of products. Dyson, for example, are famous for their use of prototypes in the development of products. In the development of the DC01, 5127 prototypes were used [4]. These prototypes ranged from sketches to physical fabrications of parts or all of the products. Some of these fabrications used the same materials as the final product, whilst many did not. A range of testing is then undertaken with these prototypes to develop deeper understanding. Figure 1.1 shows some of these prototypes within the prototyping process at Dyson [5]. Here, sketches, cardboard, 3D prints and previous product components and assemblies are being used.

Figure 1.1: Dyson prototyping using sketches, cardboard, 3D prints and previous products as product prototypes (credit BBC [5]).

Colloquially, prototypes are often referred to by their design stage. For example, "proof-of-concept" models are often understood to be prototypes. However, Ullman demonstrates how there are several other design stages for which prototypes are useful [3]. These are proof-of-

product (to refine a design), proof-of-process (to verify a design) and proof-of-production (to verify a final production process). This is supported by Blomkvist and Holmlid in similar work [6].

Alternatively, other authors suggest the purpose of the prototype as the classification mechanism. One of the most famous of these is that by Houde and Hill [1]. In this work, it is suggested that prototypes can be classified within a continuum bounded by three points: look and feel, implementation, and role, as in Figure 1.2.

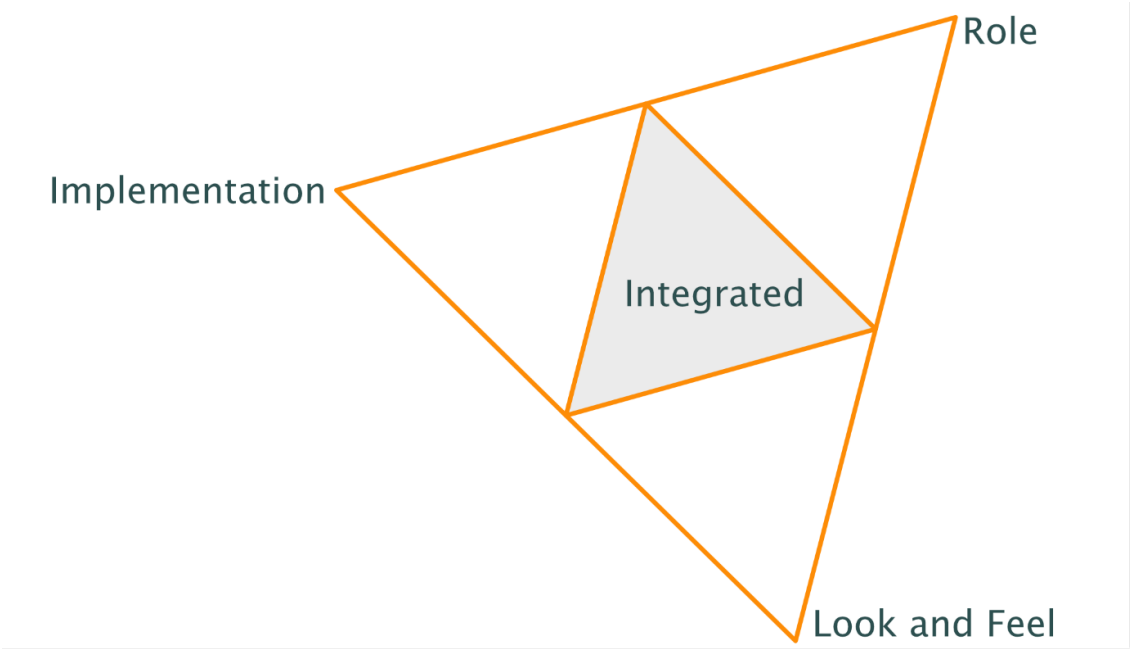

Figure 1.2: Prototype classification as defined by Houde and Hill [1]

Look and feel prototypes, as one would expect, look and feel like the intended design. Role prototypes behave as intended, but may not achieve this through the same methods as the intended design. Implementation prototypes work as intended, but do not look nor behave as intended. All prototypes are hypothesised to exist within this continuum, with those in the centre of this space considered integrated prototypes (demonstrating significant parts of more than one aspect). Similar classification proposals have been suggested by other authors [7–9].

Classification by fidelity is less well defined, though somewhat plays into the other classification methods proposed [10]. This classification mechanism works by considering the accuracy of the prototype relative to the intended design. Although this is often recognised as an important part of how prototypes are received [2, 6, 10–15], there are difficulties in evaluating a prototype's fidelity. Work has been done that looks to provide a framework for this [14], though it remains a challenge.

Whilst it is important to understand how a prototype is classified, it is also necessary to understand how they should be fabricated [13]. Depending on the required use, resources available, and environment [9], the prototype construction should be directed such that the process is as efficient as possible. This allows fabrication of a larger number of prototypes; a benefit for designers [11]. Although virtual and mixed methods of fabrication have become more widely used, physical prototypes continue to offer a unique tangiblity [16–19]. Physical fabrication methods range from cardboard modelling [4], to high-value Computer Numeric Control (CNC) manufacture [20]. For each fabrication method, the advantages and disadvantages should be considered such that efficient fabrication can be achieved.

In the past 40 years, the advent of Additive Manufacturing (AM) has changed the landscape through which physical prototypes are fabricated [8]. The technology, itself encompassing many manufacturing methods, allows for high-accuracy geometric forms to be manufactured with a high level of autonomy [8, 13]. Of the constiuent technologies, Material Extrusion (MEX) is the most widely used [21]. This method is also regularly referred to as Fused Deposition Modelling (FDM) and Fused Filament Fabrication (FFF), though MEX is the term recommended by International Organization for Standardization (ISO) [22].

The MEX method works by systematically extruding material through an orifice to build up a model in layers, generally using thermoplastics [23]. The process is graphically presented in Figure 1.3. Thanks to its simple operation and high level of safety, the technology has been found to be "office-friendly", which is particularly useful for a design office [24]. This enables the rapid manufacture and use of prototypes within the design process, improving the chance of successful product design. However, MEX methods often produce parts that do not feel like the intended design. This is because of three reasons:

1. The use of thermoplastics rather than metals, ceramics or other materials reduces the mass of the fabricated artefact.
2. The use of infill structures that only form a part of the internal volume reduces the overall volume filled with material.
3. The removal of internal components and simplification of geometry reduces the overall volume correctly filled with high-density material.

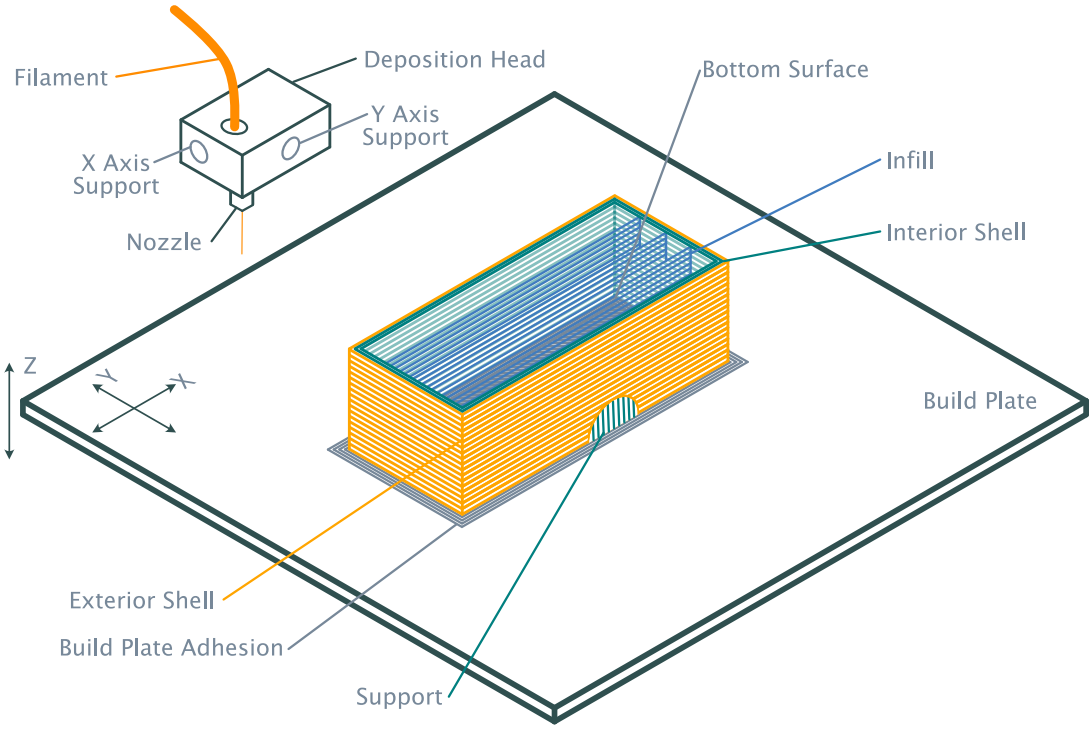

Figure 1.3: The basic material extrusion print set up and fabrication.

Houde and Hill have previously demonstrated how mass is an important consideration in the design process [1], using the example of a brick in a pizza box to emulate a laptop. This work required a user to carry the brick and pizza box to understand how the geometry and mass properties affected the user throughout the day. Other authors have also investigated how mass can have an effect on the user perception of a prototype, namely on the perceived feel [25, 26]. This work shows that mass properties have a clear effect on the user-interaction (feel) and performance, as applicable, on the use of prototypes. This poses a limitation on the usefulness of prototypes fabricated through the use of MEX which exhibit mass properties that are different to those of the intended product.

It is hypothesised, that the availability of a method through which a product's mass properties may be emulated within MEX prototypes would be advantageous. In particular, this is thought true for products that function with a high-level of interactivity. As such, this PhD study focussed on the development, characterisation and application of such a method. To investigate the hypothesis, a thesis aim was developed:

Improve the influence of mass properties in user-interaction of MEX prototypes.

To present the research undertaken as part of this aim, this thesis is formed of 10 chapters and 3 appendices, answering three Research Questions (RQs). The rest of this introductory chapter aims to outline the thesis and associated PhD study. This is done through review of RQs. The thesis structure is further presented graphically.

1.1 Research Questions

To investigate the aim, three RQs were decided upon that, if answered, would demonstrate the aim was achieved. These were:

1. How important are mass properties of MEX prototypes?
    - This investigates the first half of the thesis aim with the value of mass properties considered in MEX prototypes.
2. How can mass properties be emulated in MEX prototypes?
    - This provides initial investigation into the second half of the thesis aim, with the methods for emulation considered.
3. How can mass property emulation be embedded into the MEX workflow?
    - This question considers the difficulty of integration, are thereby usefulness, of the developed methodology into the current MEX and prototyping workflow – building on the second half of the thesis aim and RQ2.

The three RQs are intrinsically linked, and generally require solutions to the earlier RQs to provide sufficient solution. For this reason, the thesis detailed within is linearly presented.

1.2 Thesis Structure

The remainder of the thesis has a structure as detailed below:

Chapter 2 introduces prototyping through review of literature. The chapter assesses and discusses the difference between prototypes and prototyping, the motivation to fabricate a prototype, classification of developed prototypes and current methods for prototype fabrication.

Chapter 3 evaluates the current AM – and more specifically MEX – landscape through review of literature. The various methods, benefits and limitations are discussed, before a more thorough analysis of the MEX process is presented.

Chapter 4 reviews the definition of each of the mass properties – mass, mass balance and Rotational Inertia (RI) – for reference throughout the remainder of the thesis. The chapter then assesses how users perceive these mass properties when interacting with consumer goods, and hence, starts to establish the relative importance of each mass property in future emulation methods. The chapter concludes by stating the objective function that is used throughout the rest of the thesis. This chapter aims to develop an answer for RQ1.

Chapter 5 introduces and compares three potential methods for mass property emulation in MEX prototypes. These methods are the use of variable infill patterns, the use of particulates and/or fluids, and the use of lumped masses. The chapter compares these methods through application of a design process before discussing how the selected method (variable infill) may be set-up. Requirements around meshing, internal volume composition and hardware changes are considered, providing initial investigation into RQs 2 and 3.

Chapter 6 presents the development of the selected (variable infill) methodology. Initial sections consider the appropriate optimisation strategy, with a directed approach identified and developed. Application of the method to a primitive form – a cube - is then undertaken for identification of parameter effects. The chapter concludes by presenting an initial set of results for the primitive and a baseline set of process parameters. The work within this chapter builds on developing an answer to RQ2.

Chapter 7 evaluates the feasibility of the method developed through application to three prototypical products – a games controller, an electric hand drill, and a laser pointer. It is shown that the performance of the method varies with case study, with factors affecting this accuracy discussed. A set of initial results – from the baseline parameter set – and theoretical results – neglecting some Design for Additive Manufacture (DfAM) and computational limitations – are presented showing improvement in mass property emulation relative to nominal MEX prototypes. This finalises the answer to RQ2.

Chapter 8 demonstrates the fabrication of the three case study products from Chapter 7. This is done through discussion of the slicing methodology, fabrication quality, and mass property emulation accuracy. It is found that emulation accuracy does not achieve the predicted accuracy but that there is good improvement relative to nominal MEX fabrications of the three case study products. Further, it is recognised that calibration of the MEX process and changes to the print path planning would improve the result. This finalises the answer to RQ3.

Chapters 9 presents a discussion of the work, considering the achievements and limitations of the method working and application. **Chapter 10** then concludes and summarises the work presented within the thesis. The thesis aim and RQs are reviewed and future work streams are identified.

The structure is summarised in Figure 1.4 with references to how each RQ relates to the presented work.

Figure 1.4: Summary of thesis structure. The chapters in which each RQ is considered is highlighted (as in the key).

Chapter 2
A Review of Prototyping

2.1 Chapter Overview

This chapter introduces concepts from literature that consider prototypes in-depth, aiming to demonstrate the importance of prototypes and identify how they are commonly used. Further, methods for prototype fabrication are discussed and presented. The chapter aims to develop an answer to this chapter's research questions; "what are the important characteristics of prototypes?" and "how are prototypes fabricated?".

2.2 Prototyping (and Prototypes)

In literature, the term "prototype" has no single definition [27, 28]. Jensen *et al.* discuss this in their work which presents 19 definitions [27]. Many authors describe a prototype as a representation of design intent or a design idea [1, 2, 8, 29–35]. Houde and Hill put this simply as:

> *"We define a prototype as any representation of a design idea – regardless of medium" [1]*

This definition is poorly bounded but supports one of the main conclusions from their work – that prototypes should be broadly defined [1]. This is balanced by individual prototypes targeting the efficient development of answers for designers' most important questions. This approach is supported by many authors (such as [1, 8, 36, 37]), though others suggest prototypes can be used for learning (more generally) [38, 39], to raise questions of their own [35, 40, 41] or for communication [7, 42].

When considering the *purpose* a *prototype* has, it is important to also consider the definition of *prototyping*. Generally, this is defined as the activity of creating and using a prototype [27, 28, 43]. It is therefore beneficial for the *prototyping objective* and the associated *prototype(s) purpose* to be closely aligned [1].

In this thesis, a *prototype* will be considered as per Houde and Hill's definition, as a representation of a design idea. Further, *prototyping* will be considered the activity of constructing and using a prototype. Both definitions will, however, be limited to the design of products, rather than services or software.

2.3 Prototype Classification Frameworks

If a prototype, or associated prototyping activity, is to have a specific purpose, it is often categorised as such. Other options have also been proposed, with prototype stage, process and method also regularly used. This section explores these classifications.

2.3.1 Prototype Classification by Purpose

In one of the seminal works in the prototyping field, Houde and Hill defined a continuum within which prototypes could be classified. This continuum took a triangular form, as in Figure 1.2, with the vertices classified as extremities of prototype purpose. These purposes were Role, Look and Feel, and Implementation (Houde and Hill, 1997).

Role prototypes are those that should behave in the same way as the intended design, but the method through which this is achieved may be substantially different. For example, if a die were being prototyped, a computer generating a number between 1 and 6 (inclusive) from a uniform distribution could be considered a role prototype. Role prototypes are particularly useful when considering how a prototype is going to be employed.

Implementation prototypes are those that function as expected, but do not necessarily behave nor look like the intended design. For example, a Printed Circuit Board (PCB) that lights up an Light Emitting Diode (LED) when temperature exceeds a limit may be considered an implementation prototype for an air conditioning unit that is triggered by the same PCB. Implementation prototypes are commonly used when new technologies, manufacturing methods and/or assembly methods are to be tested.

Look and feel prototypes are, as the name implies, those that look and feel like the intended design (but do not necessarily function or behave as intended).

Additionally, a fourth prototype classification is proposed for prototypes that demonstrate all of the other three classifications. These prototypes are considered “Integrated” prototypes. Prototypes in this classification would classically be constructed towards the end of the design process and more-closely resemble the final-product.

Buchenau and Suri [7] propose a very similar (but discretised) classification system to that defined by Houde and Hill. These classifications are defined as “looks like”, “behaves like” and “works like”, with these being closely aligned to the “look and feel”, “role” and “implementation” purposes respectively. Ulrich and Eppinger [8] and Hallgrimsson [9] refer to similar classifications.

Alternatively, Ulrich and Eppinger also propose a continuum for prototype classification that uses two axes [8]. These axes refer to the prototype scope (purpose) and its tangibility, as in Figure 2.1. Although this provides insight into the prototype, it is hard to accurately identify a prototypes’ purpose from these axes alone. Instead, an additional note describing the prototype is required.

Further, Ulrich and Eppinger propose a continuum within which products lie, bounded by the terms “technology-driven” and “user-driven”. It is of note that this is intended for application to products, but it is thought that this can be extended to prototypes. Through understanding of the product driver, the aspects prototypes should target can be better understood. Technology-driven products are those that provide value through its technology and/or its ability to accomplish specific technical tasks. For example, Random Access Memory (RAM) modules in a computer leverage technology to provide benefit to a user. Although the form of the product may be important, the core value is driven by technology.

In comparison, user-driven products are those that provide value through the form of the product and/or its functionality. For example, a spectacle case provides its core value through its form.

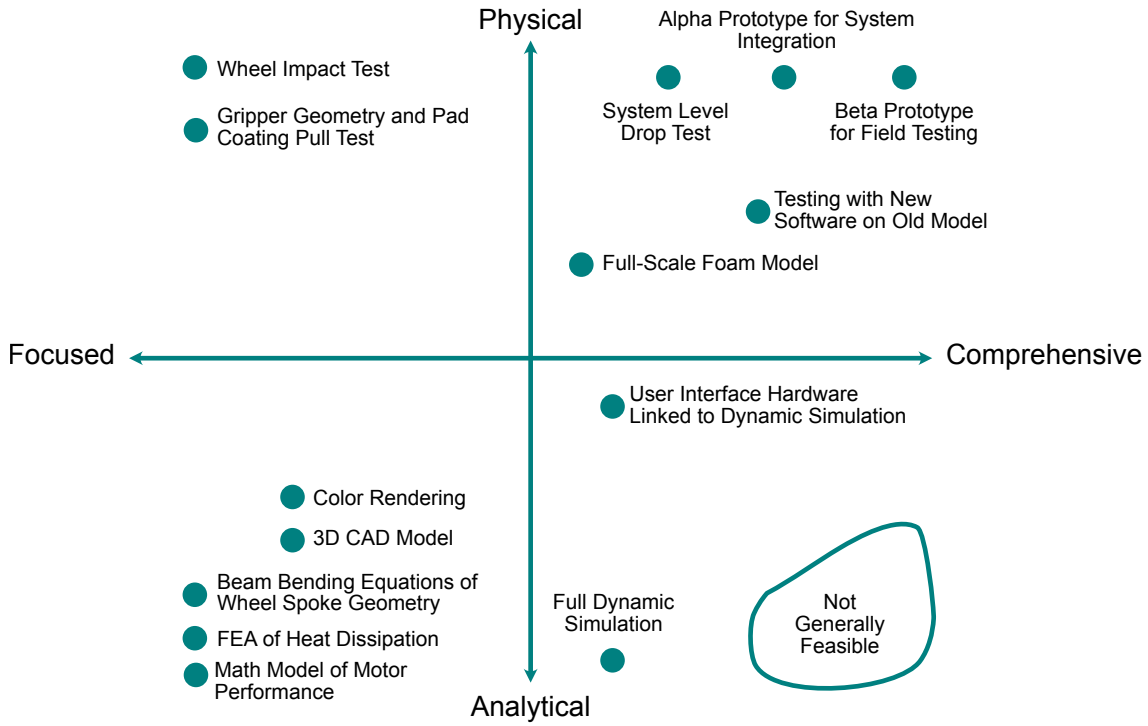

Figure 2.1: The two axes of prototyping, with examples, from “Product Design and Development” [8] figs. 14-5

Between these two ends of the spectrum lies all other products, with a balance between the included technology and the form of the product. One clear example here is the wristwatch. This is particularly true in recent years with the development of the smartwatch, where technology has developed to allow elevated functionality – activity tracking, etc.. Of course, the watch may be worn for aesthetic reasons and should therefore be aesthetically appealing. Other products would also be classified centrally in this spectrum. An example is presented in Figure 2.2, adapted from Ulrich and Eppinger [8].

Recent work by Camburn *et al.* [2] reviewed the most common prototyping objectives through examination of literature. Four prototyping objectives were found to be commonly referred to. These were, in order of prevalence:

- Refinement: The use of prototypes to gradually improve a design.
- Communication: The use of prototypes to share information about the intended design or its use to stakeholders.
- Exploration: The use of prototypes to identify new design ideas, supporting ideation.

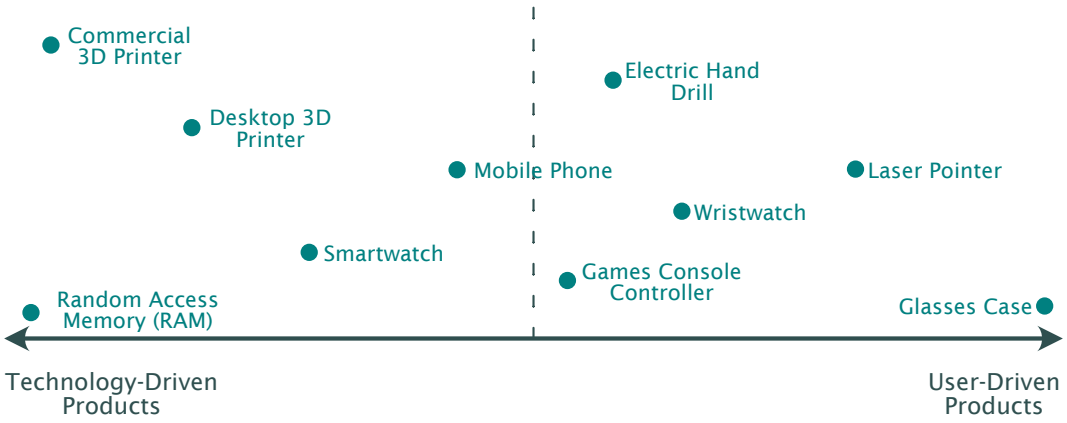

Figure 2.2: The continuum defined by technology-driven and user-driven products, adapted from Product Design and Development [8] figs. 11–8

- Active Learning: The use of prototypes to develop new understanding of the design space or relevant phenomena.

Of these four objectives, refinement was the aim of approximately two thirds of all prototyping activities. The use of discrete prototyping objectives allows for easier classification of prototypes. This allows designers to more clearly observe trends in prototyping across a project.

2.3.2 Prototype Classification by Design Stage

Ullman moves away from the classification of prototypes by purpose, moving instead toward a definition by prototyping stage [3]. In their work, four classifications are proposed:

- Proof-Of-Concept; intended as a learning device.
- Proof-Of-Product; intended to refine a design.
- Proof-Of-Process; intended to verify the design and the fabrication process to be used.
- Proof-Of-Production; intended to verify the final-production process for near-final stage prototyping.

Similar work is presented as part of the framework by Blomkvist and Holmlid [6], who state that there is a connection between prototype purpose and position in process. This is founded on work by Voss and Zomerdijk [44]. Several authors therefore feel the design stage is an important consideration in classification of prototypes. However, every definition referring to position in process relates back to the prototype purpose (which is closely aligned with the design stage). As such, it is thought that prototype purpose is the more appropriate classification method.

2.3.3 Prototype Classification by Precision

Another characteristic for classification often used is the fidelity of a prototype, with this often having an important role in how a design is perceived [2, 6, 10–15]. Merriam-Webster defines the term fidelity as “accuracy in details” or “the quality or state of being faithful” [45]. This is regularly applied to prototyping as the accuracy of representation a prototype provides relative to the intended (or final) design [1, 2, 29, 35, 46]. Additionally, the terms low- and high-fidelity are regularly used; with low-fidelity implying poor representation and high-fidelity a closely matched prototype and final design. Benefits of low-fidelity prototypes include:

- Being low cost,
- Allowing non-experts to better integrate into the design process, and
- Encouraging learning through failure [46–48].

Conversely, high-fidelity prototypes are more costly and take longer to construct, but provide a greater level of information [46, 48, 49]. Therefore, it is likely that a level of fidelity should be targeted with the prototype purpose and/or prototyping objective in mind [50].

An example in literature comes from Jensen *et al.* , who used four levels of fidelity in a case study design problem. Four prototype construction methods were studied (cardboard, laser cut plywood, 3D printed and machined aluminium) to allow for construction of a mechatronic padlock. These prototypes were considered low-fidelity (cardboard) to high-fidelity (machined aluminium) [10]. The paper demonstrated differences in the way users reacted to the prototypes, and attributes this to fidelity. The work assumes a final production method and/or

material akin to the machining of aluminium, with the machined aluminium prototype credited as being the highest-fidelity prototype. However, the 3D printed prototype was received well by the users. It is therefore possible that, in a real-world design task, the designer(s) may move to a plastic casing and/or additive fabrication method. If this were to happen, there is an argument that the 3D printed prototype now has the highest fidelity, though it is recognised this is unlikely given the product application.

Beaudouin-Lafon and Mackay proposed the term precision in place of fidelity [29] for reasons associated with undefined final systems. In this work, the authors used the precision term to refer to the representation of the prototype relative to the prototype's purpose. This is preferred for three reasons:

1. The use of a term relative to the prototype purpose allows distinctions to be made regarding prototype construction methodologies, without consideration of the final design.
2. The prototype purpose is often easier to define and will not change retrospectively (unlike the final design which commonly undergoes updates based on learning).
3. The construction of exploratory prototypes can be undertaken with high-precision, whilst this is much harder to achieve and/or define when using fidelity.

However, issues remain. Principally, the use of a relative term without quantitative justification causes abstraction between low- and high-precision characteristics. For certain applications, suitable qualification may be achievable. The usefulness in this separation is discussed by McCurdy *et al.* , who highlight five dimensions within which a prototype can be characterised [14]. However, these dimensions remain broad (for example, "Level of Visual Refinement" can be interpreted in several ways) and quantification is therefore challenging. Additionally, user driven design complicates this with many factors affecting a prototype's accurate representation [10]. For this reason, precision (or fidelity) was not thought a useful definition to classify by. Instead, the term will be referred to and discussed to provide additional context, as necessary, on a qualitative basis.

Other classification methods are reviewed and discussed in literature that consider:

- The audience the prototype is intended for.
  - Prototypes intended for internal use often have different forms to those for external use [1, 6, 9].
- The method and materials of construction employed [6, 9, 13].
  - One of the easiest ways of categorising prototypes. Often broken down in virtual and physical methods [3], other authors have proposed four categories: paper-based, computer-based, constrained physical and free-form physical [41].

For the purposes of this work, a singular definition of the prototype classification framework has not been identified. Instead, the discussion around classification is important for determining which characteristics are often considered critical to the prototype definition and understanding how the remaining work may apply to each of these frameworks. For this reason, future chapters will refer to classifications commenting on prototype purpose and design stage. Manufacturing method, material, interaction, precision and audience will be discussed as needed for context.

2.4 Methods of Constructing Prototypes

Once a prototype purpose and/or prototyping objective is decided upon, it is important to consider the method of construction (or fabrication). Separate to the limitations singular prototyping methods may present, it is recognised that other tangential factors should be considered. For example, several researchers have found that design fixation can be affected by the construction time a prototype requires [2, 51–53]. As such, an efficient, objective construction method should be identified for every prototype.

Hallgrimsson [9] proposed that prototype construction methods (referred to as model-making) are elected based on four guidelines:

1. Health and Safety
   - Ensure that the maker is confident with the related health and safety implications of the construction method, tools and materials.
2. Purpose

- Ensure that the prototype is built to target the prototyping objective and prototype purpose outlined as part of the prototyping activity. In practice, this means that looks-like, behaves-like and works-like models are built to the standard required. The temptation to over-engineer the prototype should be avoided.

3. Effectiveness
   - Ensure that the method of construction will allow the prototype purpose to be achieved and uses resources efficiently. This guideline should push the model-maker to reflect on the prototype purpose and consider the level of precision the model requires.
4. Appropriateness
   - Ensure that the method will be appropriate for the model to be made, and that the model is appropriate for the audience, tooling, materials, and design intent. This guideline should push the modelmaker to consider aspects such as level of required finish with respect to the portrayed message.

The use of these guidelines should allow the prototype construction to be directed such that the process is efficient. Through doing this, more prototypes may be fabricated and explored more efficiently – shown to be beneficial to designers [11].

Although many authors still state that prototypes are tangible assets (e.g. [3, 33]), it is more commonly agreed that prototypes may be virtual or physical representations of a design [1, 2, 7–9, 31, 34, 41, 43, 54]. Additionally, mixed virtual-physical prototyping methods (mixed methods) have started to be developed and used (for example, [55–59]). Hence, the methods used to construct prototypes have been divided into these three sub-categories for discussion.

2.4.1 Virtual Prototyping Methods

Originally used by the automotive and aerospace industries, virtual prototypes are considered non-tangible representations of a physical product [60]. Wang proposed a formalised definition for virtual prototypes and virtual prototyping as:

> *"[A] virtual prototype, or digital mock-up, is a computer simulation of a physical product that can be presented, analyzed, and tested from concerned product life-cycle aspects such as design/ engineering, manufacturing, service, and recycling as if on a real physical model. The construction and testing of a virtual prototype is called virtual prototyping (VP)." [43]*

One aspect not considered within this definition, however, is the use of sketches and other non-digital prototype construction methods that would not be considered physical prototypes. Work by Macomber and Yang [61] considered this in more-depth, explicitly looking at the use of sketches within prototyping.

Virtual prototypes can be constructed with a wide variety of methods and tools, such as geometric modelling (e.g., Computer Aided Design (CAD)), system modelling (e.g. agent-based) or other Computer Aided Engineering (CAE) methods [57]. These CAE methods may include structural, fluidic, thermal and/or manufacturing simulation. The results from these results may then be presented on paper, a 2-D screen or using Virtual Reality (VR). Examples of a selection of virtual prototyping methods are presented in Figure 2.3. The use of virtual prototype construction methods provides designers with increased flexibility, allowing for rapid exploration, knowledge development and transfer within the solution space [2, 20, 50].

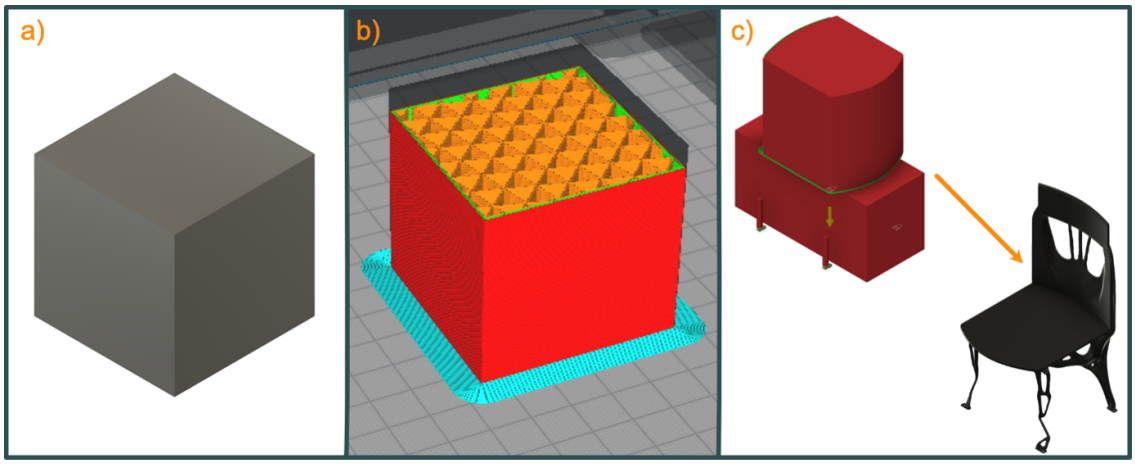

Figure 2.3: Virtual prototyping method examples. a) CAD geometric representation of a cube. b) simulation of manufacturing tool paths for a 3D printed cube. c) generative design set-up and output for a chair design.

One of the main issues associated with virtual prototype construction is that associated with integration of the design, analysis and simulation tools available [43]. Although tools are starting to allow this seamless transition – for example, Autodesk Fusion – and standards are being developed for files (for example, the ISO STEP standard ([62]) there remains opportunity for improvement. Furthermore, issues persist around the learning associated with the use of increasingly capable – but complex – software packages. This increases prototype complexity and thereby realisation time [57, 63].

2.4.2 Mixed Prototyping Methods

Over the past 20 years, there has been increased interested in the use of Mixed Reality (MR) – the term given to synchronous work in both the virtual and physical domains [57]. These methods include examples where physical artefacts may be tracked [55, 56, 59] and human behaviour is interpreted [58, 64]. The virtual element is then displayed on a computer [58, 59], overlayed using headwear [64] or directly projected onto the physical object [65–67] - with this often referred to as Augmented Reality (AR). Examples of mixed methods are presented in Figures 2.4 and 2.5.

Figure 2.4 shows a system intended for deskilling the design of cities by allowing users to interact with Lego blocks that cause a virtual city representation to be manipulated. Kent *et al.* [59, 68] discuss how a tangibility using a well known system (Lego) enables rapid design changes from a wide audience whilst simultaneously providing a higher level of detail in the virtual representation for improved feedback. This virtual representation additionally presents key metrics - such as the number of certain building types, distances from locations etc. - which the physical alone would not be able to provide without further analysis. A key advantage for MR systems.

Figure 2.5 similarly shows how combining the two domains allows for increased knowledge development. In this example, the use of a games controller with movable buttons - here defined using the location of QR code buttons - enables a designer to receive immediate feed-

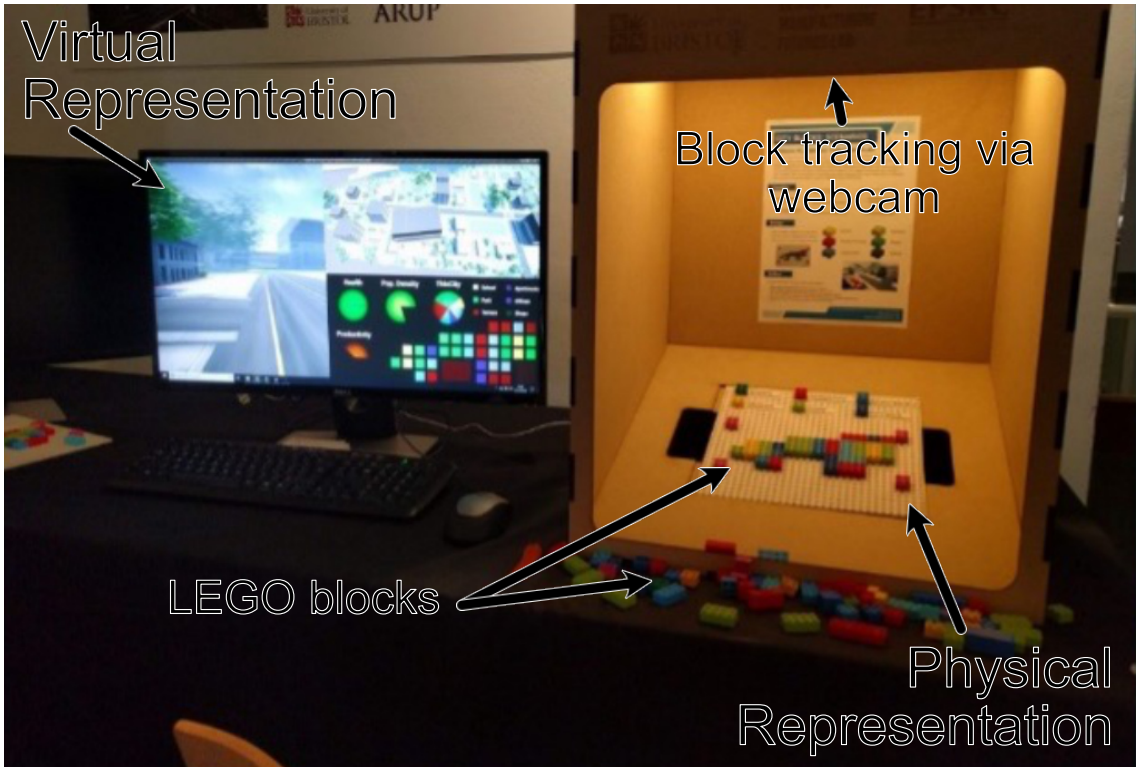

Figure 2.4: Virtual representation of physical blocks via a game engine for city design [59, 68]

back on the location of said buttons and controller geometry. This offers the ability to rapidly learn about user preferences and interface development whilst reducing the required physical fabrication.

In a similar period to that of MR, the concept of the digital twin has been developed and gathered interest. The digital twin is typically described as a physical entity with a virtual counterpart and data connection between [69], and is therefore similar to the notion of mixed reality. Kent *et al.* discuss this, with focus on the ability to leverage the synchronicity between the virtual and physical domains when using MR [58].

It is thought likely that the development of MR technologies will continue at pace due to the affordances in process streamlining, cost reduction and product performance improvement [57]. However, for this to continue it is thought by the author that physical methods of construction will need to keep pace. This is needed with regards to both the information pro-

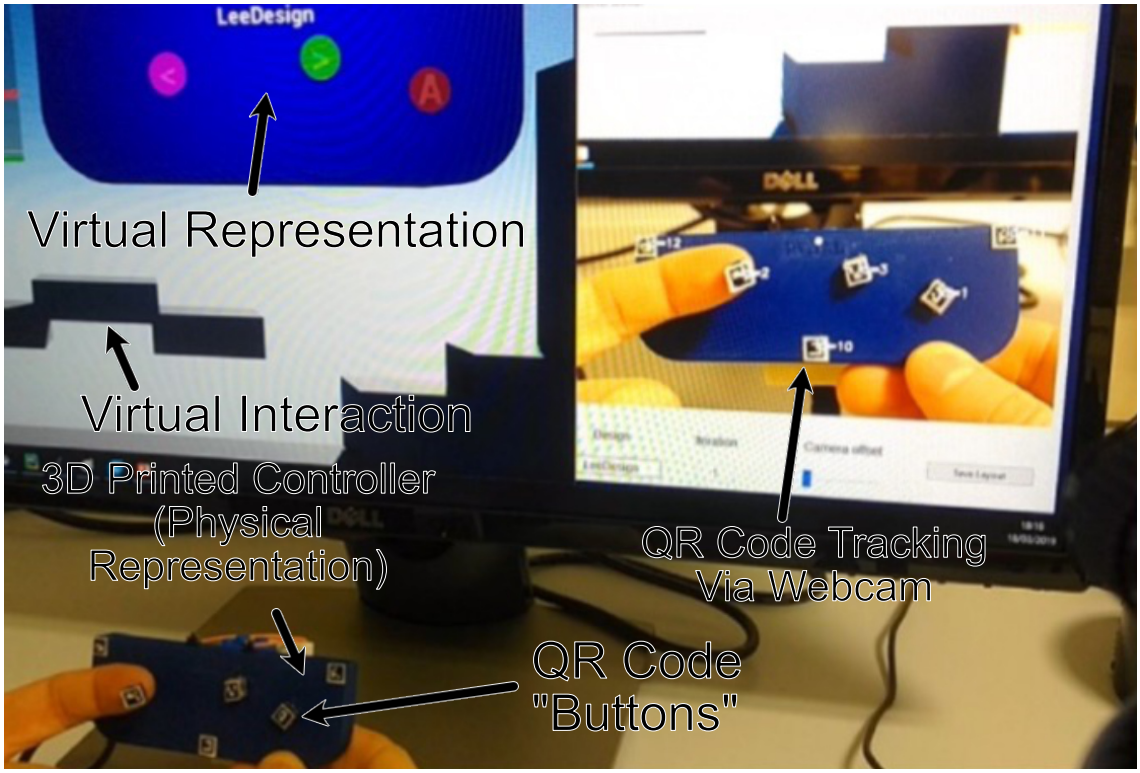

Figure 2.5: Virtual representation and simulation of an interactive and reconfigurable AM games controller [58].

vided by a prototype and the rate at which prototypes can be constructed, to support MR. In addition, increased automation is desirable to allow non-experts to fabricate models more readily. Appropriate methods are discussed in the following section.

2.4.3 Physical Prototyping Methods

Physical prototypes offer tangibility [16–18] inherently missing from virtual prototypes [19] - though this may be improved through the use of haptic gloves or similar [70]. The benefits of this tangibility are the ability to more efficiently understand the aesthetics, ergonomics and behaviour of prototypes [17, 29, 50, 65]. However, this comes with increased cost and fabrication time [20]. Several techniques are available to the designer, including the use of modelling materials (such as cardboard and foam), construction kit modelling, classical manufacture, and AM [41]. Each of these have their own benefits.

The use of cardboard and foam for prototype construction allow artefacts to be generated quickly, from low-cost materials. As such, the materials are regularly used in early-stages of prototyping [4, 9]. Although it may take skill to produce a well-finished prototype, the skill-level for fabricating simple geometric forms is low [9]. An example of a foam prototype is provided in Figure 2.6, showing an early mock-up of the first iPod (courtesy of Apple, from [65]). A similar cardboard prototype is also presented in Figure 2.6, showing a prototype from Dyson [4]. One disadvantage of these prototypes is the effect on user perception. In literature, users have demonstrated their view of a design is diminished when working with cardboard prototypes [71].

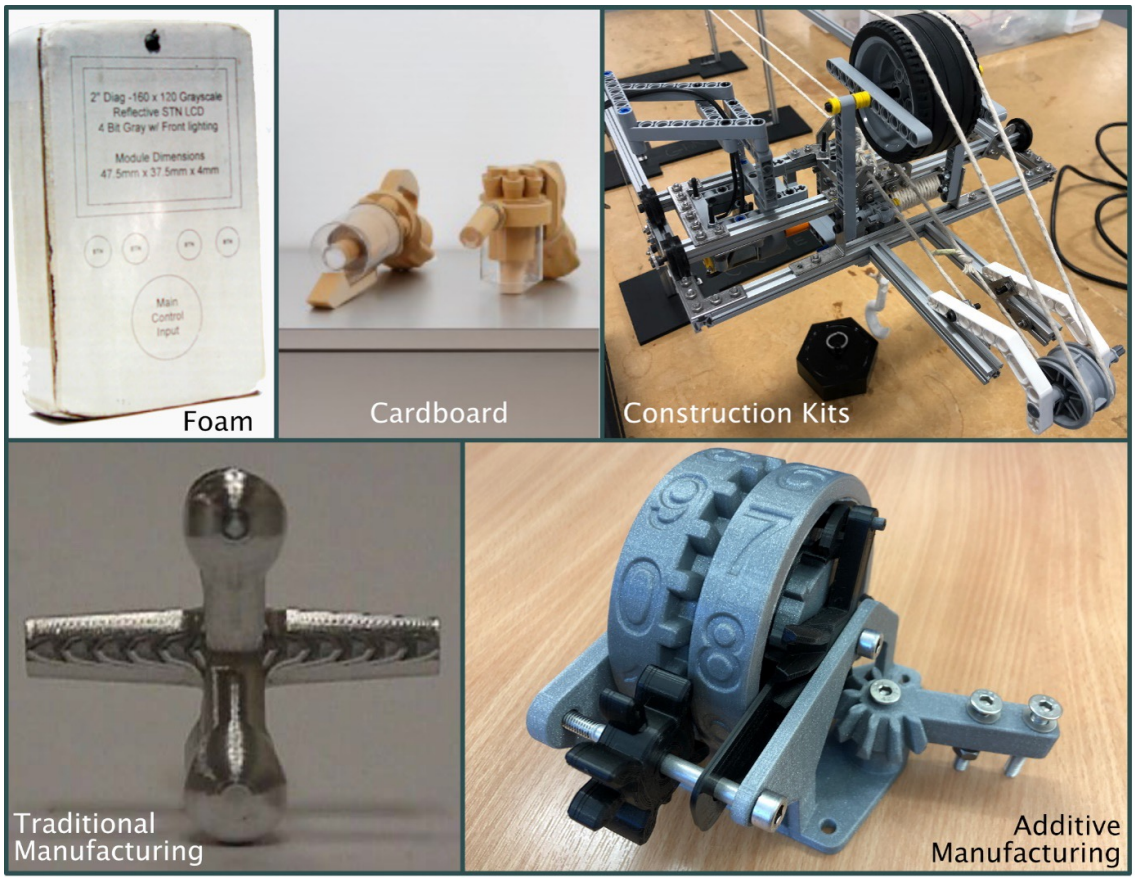

Figure 2.6: Example physical prototyping methods. The foam model is an early iPod prototype, courtesy of Apple [65]. The cardboard models are of Dyson vacuum cleaners, courtesy of the James Dyson foundation [4]. The construction kit model (Makerbeam and LEGO Technic) is of a crane mechanism from teaching at the University of Bristol. The traditional manufacturing example is a CNC milled example from the work by Frank *et al.* [72]. The additive manufacturing example is a functional prototype for a capacity counter, fabricated using MEX.

Construction kit prototype fabrication has started to be more commonly used in the engineering design process. The most well-known example of this method is LEGO [73], with several examples of use in literature [9, 13, 41, 68]. The main benefits of kit construction are:

1. Low barriers to entry with regards to technical skill,
2. Quick construction and easily modifiable,
3. Low cost deconstruction for reuse or disposal.

With the development of the Lego Technic/Mindstorms platform, construction kit prototype fabrication can now be integrated with control electronics and basic mechanical components (gears, belt drives etc.) [74]. An example LEGO prototype construction is shown in Figure 2.6. The detriments of construction kit prototype fabrication are the low-accuracy representation of form (when using LEGO, the minimum feature size is the size of the smallest block) and constraints around the possible construction combinations [75, 76]. Further, the prototype embodiment is often limited to plastics, though metal kits exist [77].

Towards the opposite end of the spectrum, traditional machining methods and their more modern equivalents exist. These include the use of hand tools, machining, turning and 2D cutting [20]. These processes may be manual, automated or a mixture of both. Often, techniques requiring significant tooling are neglected in prototyping due to the investment (economic and otherwise) necessary [9]. These manufacturing operations are normally well understood, and allow the fabrication of high-precision prototypes using a wide range of fully-dense materials [78]. Although the technologies have previously been considered slow and labour intensive, literature has shown that they can be considered alternatives to Rapid Prototyping (RP) technologies [72, 79–82]. An example of a prototype made using CNC milling is shown in Figure 2.6, originally from [72].

The primary disadvantage of traditional manufacturing techniques is the requirement for specialist knowledge (for the process to be safe and effective) [9], though others exist around tooling, tool wear, path planning and costs (for entry and use) [72]. Although recent developments in the control and costs associated with CNC machines have started to improve this, desktop AM technologies remain competitive.

A more modern technology that has seen significant uptake within the design community is AM, considered to have “come of age” over the last 10-20 years [24]. This technology allows material to be additively constructed to form a given geometry in a highly automated fashion [9, 83]. Originally developed in 1984 [84] to allow the rapid production of prototypes (hence the designation RP) [83], the technology has developed significantly over the last 40 years. Goudswaard *et al.* investigate this, confirming that AM has matured into an office-friendly technology for prototype fabrication (in 2020) [24]. This is particularly important for prototype fabrication, as it allows designers and researchers (the largest user base for AM) to fabricate prototypes in their office [85–87].

Further evidence that AM’s use in prototyping is widespread comes from the yearly Sculpteo “The State of the Industry” reports. In the last 5 issues (2017 – 2021), fabrication of prototypes and proof-of-concept/test models the most cited purpose of AM [21, 85–88]. If 2021’s report is looked at specifically, it is clear the use of AM for prototype fabrication remains substantial, with 82% of all respondents indicating that they used the technology for this purpose [21]. Comparatively, only 8% indicated they used the technology for mass-production.

Ullman *et al.* [3] state “3D CAD modelling and 3D printing technologies have reduced the relative cost and time required to create and analyze prototypes”. This ties into work by Viswanathan & Linsey [52] and Youmans [53], who investigated the effect of fabrication time on design fixation. Through reducing the fabrication time and effort, design fixation is reduced. As such, there are benefits of AM that relate to direct improvements in the prototyping process. These prototypes can then be used for a range of learning - from functional parts, through "looks-like" models, assembly testing and behavioural assessment [89]. This is enabled by the range of AM technologies and processable materials that exist. Further discussion around AM’s affordances, challenges and constituent technologies are discussed in more detail in Chapter 3.

When deciding on the construction method to be used, a designer should thoroughly understand the prototype purpose, the prototyping objective methodology, the tools that are available and the surrounding restraints of the design project. Additionally, this process should be closed loop, with knowledge of the tools and techniques available for prototype construction feeding into decision around the prototype purpose.

2.5 Chapter Summary

This chapter has answered the two RQs posed for this chapter. It has been shown that a variety of characteristics are important for prototypes, depending on use and product type. Generally, these can be classified as the look and feel of the prototype, how the prototype works, and how the prototype is expected to behave. Although other classification methods are used in literature, the overall characteristics often refer back to these groupings. Additionally, it has been found that AM is a favourable fabrication method due to it being highly automated and able to fabricate accurate geometric forms. However, there are several AM methods that may be used, all with individual advantages and disadvantages. It is important, therefore, to review the AM landscape.

Chapter 3
A Review of Additive Manufacturing

3.1 Chapter Overview

This chapter summarises AM and its sub-methods, recognising how they are used to manufacture products and prototypes. Focus is given to MEX as a method of interest due to its wide use, with the associated workflow and typical fabrication described.

3.2 Introduction to Additive Manufacturing

AM is a term given to manufacturing methods that, in layman's terms, add material to a substrate to form a part (or parts). The technique is also referred to as Additive Layer Manufacturing (ALM)) [90] and, more colloquially, 3D printing [84, 87]. However, the use of the term ALM in reference to additive, though often acceptable, can be a little misleading. This is due to the inference that any AM technique is inherently a layered process. With current technology this is usually true [90–92] and is therefore used in literature interchangeably. However, methods exist that overcome the normal layering in parts [91, 93]. 3D printing, though easy for a large proportion of the population to immediately understand, is not representative of all AM processes.

AM is also commonly referred to as RP as this was its original purpose [90]. However, the technologies associated with the term have been developed beyond the point of exclusive use of prototyping [87]. Jean-Claude André discusses this, with direct manufacture and home manufacture becoming accessible since the turn of the century [84].

The rest of this text will use AM exclusively to define the group of manufacturing methods that allow the fabrication of parts through addition of material, though literature may refer to ALM, 3D printing, RP or other similar terms.

AM is used for a variety of applications in aerospace [94–97], automotive [98–101], electric machines [102, 103], consumer goods [4, 104], healthcare [105, 106] and other sectors [107–110]. This is for several advantages that offer unique capability over alternative manufacturing methods such as high level of automation, low level of expertise and the ability to produce complex geometries. This is discussed further in the following section.

3.3 Affordances of Additive Manufacturing

Authors have previously discussed AM as a technology with the potential to revolutionise the way products are made [90]. To understand why this may be so, some of the key benefits of various AM technologies are considered.

One of the most cited benefits of AM is the ability to manufacture increasingly complex parts [86, 87, 111]. This complexity is broken down by Gibson *et al.* as:

- Shape Complexity – virtually any shape can be fabricated;
- Hierarchical Complexity – shapes of different scales can be fabricated together, allowing millimetre scale structures to be incorporated into macro-scale, part-size structures;
- Material Complexity – materials can be processed at individual points within the fabrication independently from the rest of the part; and
- Functional Complexity – fully functional assemblies can be manufactured in-place [112].

Through developing this complexity into products through DfAM, it is possible to elevate performance. This is leveraged further when combined with technologies such as shape topology and generative design. Examples are provided in literature, such as [113–115].

It is well understood that AM provides a highly automated form of manufacture, as discussed previously. This allows costs to be reduced by reducing the skilled labour required [90]. Further, distributed manufacture is made more accessible [116], allowing for more responsive and efficient manufacturing. A prime example of this is the use of an AM system on the International Space Station (ISS) by NASA since 2014 [117]. This initiative has allowed spares and tools to be designed on earth or the spacecraft, uploaded to the ISS and printed (replacing the need for a supply mission). As on earth, the hope is for this to provide greater autonomy and flexibility [118].

Advantages around the speed of manufacture are also derived from the reduction of process steps [90]. Regardless of complexity, the steps involved with AM are generally limited to AM fabrication and post-process finishing (with some existing systems integrating this functionality [119]). In addition, the manufacture of additional tooling is not needed in AM

fabrication, with the parts being built directly onto a build plate or other substrate (support material can be used if needed). This makes changes to product form easier (and thereby enables mass customisation - the high-volume manufacture of personalised products), reduces overall production time when making small volumes, and increases flexibility for machines to manufacture a wider range of products.

Finally, the process is generally considered safer than CNC machining. For both methods, the program sequence for tool operations needs to be generated by a user. For AM, incorrect values for the controlling parameters may lead to poor fabrication quality but are unlikely to damage the machine or cause a user harm. On the other hand, poor control of CNC machines may damage the machine or harm a user [90]. However, AM is not without safety implications. The use of high-power lasers (or electron beams), high temperatures and potentially dangerous materials each have their own risks [120]. Even consumer MEX technology poses risks around particulate emissions [121]. This said, these risks are generally controllable and predictable, posing a lower risk to human life or of serious injury.

3.4 Limitations and Challenges of Additive Manufacturing

As with the affordances already discussed, each AM technology has individual limitations and challenges. However, there are a range of issues that are common between most of the processes.

With very few exceptions, AM processes rely on the availability of a virtual representation of a design [9] (e.g. a CAD definition). Although this drives one of the core benefits of AM (automation of manufacture), there is an inherent overhead in developing a virtual representation of a design. This said, most design processes regularly use virtual representations of design [50]. The development of the “Digital Twin” in early-stage design is likely to improve this availability further [122]. Therefore, this limitation is likely to only be applicable to the very early stages of design.

More applicable to AM throughout the design process are the difficulties in material processing. Although the range of additive manufacturing methods are able to process a variety of materials [123], no one method is able to process the full spectrum. Further, the mechanical properties of the fabricated materials can vary between manufacturing techniques, with this recognised in literature (e.g., [124–126]). As such, the fabrication method used should be chosen within the context of the design problem, with DfAM principles considered during the design stages [112, 127, 128]. Similarly, process planning and prediction has started to be integrated into the design stages to overcome issues with residual stress and anisotropy in mechanical properties [111, 129–132].

One of the most recognised and well cited drawbacks of AM is the increased cost and reduced speed of fabrication (compared to casting or machining) for simple parts [90, 111]. Although the increase in fabrication time is somewhat offset by AM's ability to reduce tooling lead time and costs, this is generally compensated for in large-volume production of simple parts. Additionally, many AM parts will need to be post-processed (often using subtractive methods) to improve part quality, increasing costs and production time [133]. The use of pre-processed materials – such as powders, filaments, or wire – also increase the production costs associated with AM [134].

AM also demonstrates specific issues associated with the fabrication directly. These include delamination, where the layers of the AM fabrication peel apart. Other issues exist around bridging and unsupported regions, with this needing to be considered in how parts are designed for this fabrication method or as a pre-process modification. Further challenges also exist (for example, around the repeatability of the AM process), though these are less relevant to the work detailed within this study.

However, despite these evident challenges to the wide-spread adoption of AM technologies, interest in the methods continues to increase, with the sector experiencing average growth of 27.4 % over the last decade [135, 136]. This is assisted by careful design of AM products able to overcome many of the associated challenges, and reignite the case for mass production (for example, GE aviation making several parts for aerospace turbine engines from AM at scale [137]).

3.5 Additive Manufacturing Methods

AM is a term that encompasses several technologies that each provide a method (or methods) for fabrication. The appropriate technologies have been identified and categorised by ASTM and ISO [22, 92]. Figure 3.1 summarises these categories and methods, adapted from similar diagrams and work [23, 123, 138]. Overall, there are 7 high-level categories and 18 methods identified. However, due to the speed of development currently observable within AM there are several other methods that have shown promise [93, 139].

Of the current AM methods, MEX is the most widely used. Recent studies have shown 95 % of AM users use MEX printing [21]. In comparison, Selective Laser Sintering (SLS)) – a powder bed method – is the next most popular technology, but with only 68 % of survey respondents using the technology. In addition, 80 % of respondents had some form of in-house MEX capability, whereas only 26 % had in-house SLS capability. Alternative work has shown that MEX accounts for roughly two thirds of overall demand [141] and is the most installed AM technology [140, 142]. Hence, it can be seen that MEX is an important technique in the AM community and (due to AMs use) within the prototyping/design community. The next section examines the MEX method in more detail to better understand the unique technical capabilities and challenges.

3.6 Material Extrusion

The ISO definition for MEX is, simply:

> *"Process in which material is selectively dispensed through a nozzle or orifice" [92].*

At its core, this is all the MEX process requires, building materials up using depositions, layer-by-layer. Although normally automated, manual examples exist with consumer success (e.g. the Doodle Pen [143]). In most modern MEX machines, however, the material deposition

Figure 3.1: Additive technology categories, as specified by ASTM F2792 [22]. Adapted from information in “Overview on Additive Manufacturing” ([123, 138], with supporting information from [140].

is automated, with the use of pre-processing software to plan tool paths and generate machine code. Although some machine manufacturers use proprietary software, some of the most popular examples are open-source (e.g. Ultimaker Cura [144], Prusa Slicer [145]).

As discussed, AMs use in prototyping is widespread, with fabrication of prototypes and proof-of-concept/test models the most cited purpose of AM over several years [21, 85–88]. Of the AM technologies, MEX is the most commonly used by industry, and has been since 2017 [21, 85–88] , though it has not bee possible to conclusively identify what the applications generally are. Further, plastics remain the most used material, though it is not possible to conclude if the use of plastics is driven using MEX or vice versa with the available evidence.

3.6.1 Material Extrusion Pre-Processing

Programs such as Ultimaker Cura (used throughout this study), allow users to import geometry files. These files can be meshes (e.g. .stl or .obj) or AM specialist file types (e.g. .3MF or .AMF). Classically .stl files are used, though the .3MF file type is growing in popularity as it can store geometry, textures, colours and other model data based on the XML standard [146]. These programs are known as slicers. This is because they slice the imported geometry into many layers, based on the printer parameters the user has set (or using default values). As part of this slicing, parameters can be set around the shell quality, layer height, infill density, material, and many others. From here, machine code can be exported for fabrication. Figure 1.3 shows a sample fabrication and the primary constituents (of the fabrication and machine).

3.6.2 Constituents of Material Extrusion Fabrication

A MEX fabrication is principally formed of four constituent elements; a shell, an infill pattern, a support structure and build plate adhesion.

A shell normally consists of top and bottom surfaces, exterior walls, and interior walls. The shell defines the fabricated parts external geometry. Inner walls are required to ensure the part is sufficiently rigid, that there are no gaps in the external surface and to allow infill to be deposited without causing seams on the external surface [142].

An infill pattern that is deposited within the volume contained by the shell. This infill pattern normally has a relative density of 10-20%. By using a lower infill density, the volume of material that must be deposited to fabricate a part decreases, improving fabrication speed and cost [23]. Relative densities (compared to solid deposition) lower than 10% would improve these metrics further but are often found to inadequately support upper print surfaces. Literature has discussed the effect of infill patination and density widely (for example, [100, 126, 147, 148]). Examples of standard infill patterns are shown in Figure 3.2. Although there are a wide array of infill patterns intended for different applications, literature has previously found that the effect of infill patination on mechanical properties is limited (< 5% change) [147].

Figure 3.2: Different infill designs that can be printed. From left-right, top-to-bottom: Lines (0 degrees), concentric, octet, gyroid, lightning, cubic, triangles (20%), triangles (50%) and triangles (80%). Printed using an Ultimaker S3, sliced using Cura 4.12.1.

A support structure may also be deposited that allows for the fabrication of geometry that is not supported by the substrate or previous deposition. Structures that generally require support are overhangs (above 60 degrees) and bridging (over 20 mm). The support structures may take one of many forms, and are often printed in a soluble or easily breakable material (though aren't required to be) [23].

Build plate adhesion remains a common feature of MEX parts, with the sole purpose of improving adhesion between the part and substrate (nominally the build plate). The build plate adhesion methods available will vary depending on the application used. However, they normally refer to a single layer of material that increases the contact surface between the part and substrate, whilst also priming the deposition head.

3.6.3 Material Extrusion Hardware

MEX print hardware generally consist of three main parts; the feeder, the deposition head and the build plate (also referred to as the build platform) [23]. Each of these parts function to deliver, melt and deposit material in a controlled manner.

The feeders in MEX move material – as filament – into the deposition head using a sprung-gear system. The force that is applied to the filament must be closely controlled to ensure accurate delivery of material without damaging the filament. In higher-end printers, dual-geared systems have started to be used to improve this process. For the remainder of this work the feeder system is assumed to be functional for normal MEX applications, and will not be considered further.

The deposition head clearly is an important consideration when judging the capability of a MEX machine. Further to the discussion around the feeder mechanism, a user should also consider other elements when choosing a machine. One such consideration is around the number of materials that can automatically be used within a single print. Many mid- to high-end printers now come equipped to handle multiple materials as standard or with first-part upgrades (for instance, the Ultimaker S3/5 [149], Prusa i3 [150], Flashforge Creator Pro [151]). Other upgrade options include devices such as the Mosaic Palette that allows filament to automatically be changed mid-print [152]. Dual material printing allows for the combination of materials for aesthetic, functional and or mechanical design changes [153, 154] . Thus, parts can be more readily integrated into a single fabrication and post-processing steps can be reduced [155].

A further advantage of printing with several extruders is the ability to print with a range of nozzle sizes. Nozzle size refers to the diameter of the outlet of the nozzle(s) through which the melted filament will pass through during deposition. Inherently, the deposition rate is directly proportional to the nozzle size (all other parameters being equal) and it is therefore quicker to print with a larger nozzle. For printing finer details, however, smaller nozzles are preferred [140]. As a compromise, most desktop-size printers are fitted with a 0.4 mm nozzle [149, 156, 157]. As such, the minimum deposition line width is roughly 0.4 mm, though work has shown this can be consistently reduced by ~10% [108]. Nozzle size reductions are the most straightforward method to reduce minimum print size. In some instances, this can be achieved through changing print cores (removable Ultimaker assemblies that make up the print head), though most instances require the manual changing of the nozzle itself using hand tools.

Another important consideration when choosing a nozzle concerns the material that depositions will use. If using abrasive materials – that are able to quickly wear the soft brass nozzles normally used – hardened nozzles should be used [158]. Abrasive materials include metal-fill, composites and ceramics.

A user may also consider the mechanism through which the deposition head translates in space relative to the build plate. The main method used in desktop printers (at the time of writing) is a cartesian style, where the deposition head translates relative to the build plate in x, y and z. The specifics of the process are not discussed here as the effects are limited in the scope of this study, but further information is available in [159–162].

Finally, the build plate must be considered. The two primary considerations around this part of the machine (assuming mechanisms for relative movement have been decided) relate to temperature and material. Although early printers commonly used unheated plastic build plates (also referred to as print beds), there has been a trend towards heated, tempered glass beds. This is primarily to allow the use of higher-performance thermoplastics on desktop printers that require a more controlled fabrication environment. The use of a heated bed also improves print quality and consistency [23, 163]. No single build plate material is agreed to be the best solution, and the choice will depend on the materials to be printed. As with the feeder mechanism, the build plate will not be considered explicitly in the rest of this work, and is instead assumed to be satisfactory for MEX application for standard print materials.

3.6.4 Material Extrusion Materials

The MEX fabrication process generally uses thermoplastic filament on spools, usually of 1.75 mm or 2.85 mm diameter. These filaments are often priced favourably compared to other AM methods, with prices (at the time of writing) around £30/kg [164]. High performance or functional materials are often priced higher than this, as would be expected. The range of processable MEX materials does, however, include examples that aren't thermoplastics. MarkForged, for instance, provide continuous carbon fibre that allows for much stronger parts to be manufactured than would otherwise be expected [165]. MarkForged also, as well as Desktop Metal, provide MEX machines that allow the fabrication of metal parts [166, 167].

Of the processable MEX materials, Polylactic Acid (PLA) remains the most widely used according to industry survey [168].

3.6.5 Advantages for Prototype Fabrication Using Material Extrusion

The primary advantage of desktop MEX machines is their relatively low-cost and low-barrier to entry [23, 126, 140, 142]. For this reason, they have become particularly popular with hobbyists and designers. Although industrial machines exist that can cost significantly more, desktop machines normally allow for greater control of individual print parameters and are therefore more appropriate for prototype fabrication [23].

In addition, the use of MEX machines is normally considered safe relative to other AM technologies [142]. Although certain materials have been shown to release unhealthy levels of particulates, the most common print material (PLA) is generally safe to use in well ventilated rooms without added safety precautions [121, 142]. This extends to the general use of nontoxic and durable materials that can be safely stored and printed with, whilst allowing colour accurate models to be fabricated [142].

The speed of manufacture and material usage may be improved through the use of internal infill patterns [23, 140, 142]. In prototyping, this reduces sunk costs, and thus design fixation [52, 53, 169]. Furthermore, the ability to fabricate mechanisms in-place is also advan-

tageous as manual handling can be reduced, further reducing sunk costs. To maximise these benefits, print parameters can be adjusted to balance print quality and speed. Fundamentally, this means controlling the feed rate (and thereby the melt rate) and plotting speed [140], whilst reducing the volume of material that must be deposited.

Finally, the ability to post-process the fabricated parts means that layer-stepping may be smoothed, colours may be changed and geometry modified using subtractive methods (if needed) [142]. This allows a wider range of properties to be achieved than would otherwise be possible.

3.6.6 Disadvantages for Prototype Fabrication Using Material Extrusion

One of the main disadvantages of MEX is the need for support structures to support overhangs and large bridges – increasing the volume of material deposited [23, 140, 142]. This requires post-processing of the part and increases the sunk costs. The use of DfAM techniques may mean this can be minimised [127]. However, the temporary application of MEX for prototype fabrication for designs intended for alternative manufacturing methods may make this impossible.

Similarly, the use of MEX for prototype fabrication may mean other properties differ between the intended design and prototype configuration. In literature, this is recognised for sharp corners [140], the anisotropy of mechanical properties and layer “stepping” [142]. As such, prototype fabrication should be completed with understanding of the discrepancies between the prototype fabrication and intended fabrication.

Finally, the use of thermoplastics may also cause issues when prototyping designs intended for fabrication in metals, composites, or other materials. Although generally acceptable for “looks-like” prototypes (especially when metal-fill filaments can be used to emulate the aesthetic [170], functional and role prototypes may exhibit unexpected behaviour. Fabrication of other materials is possible, but generally more expensive and complicated [23, 140].

Interaction With Material Extrusion Prototypes

It was shown in Chapter 2 that interaction with prototypes is an important part of the design process for a large variety of goods. This is often referred to as, at least part of, the feel of prototypes, and so this is considered in MEX fabricated prototypes.

Part of interaction associated with geometric form is understood to be an accurate representation of the intended product, so that the physical form one must take to pick up, move, or otherwise engage with a product is consistent. Although small discrepancies may be apparent due to processing artefacts, the macro-scale form is often accurate to within fractions of a millimetre. However, the feel associated with the prototype mass properties - mass, mass balance and RI - would be poorly portrayed for three reasons.

The first of these reasons relates to the fabrication material. In MEX, this is often a thermoplastic, which may have a different density to the intended material. For reference, PLA has a density of 1.24 g/cc, whilst aluminium has a density of 2.7 g/cc and EN24 steel density is 7.84 g/cc at room temperature. For products intended to be made using a single material, the mass balance will be unaffected, as the Centre of Mass (CoM) will remain at the Geometric Centre (GC) of the volume. For products intended to be made of multiple materials, the mass balance will be affected, with the distribution of mass changing. In all instances where the fabrication material is different to the intended material, mass and RI will be affected.

The second reason relates to the use of low-density infill patterns. As previously discussed, infill patterns are commonly used in MEX manufacture to reduce the time and cost of manufacture. Although this influences the product mechanical properties, this effect is small. Conversely, the effect on mass is often significant, with a reduction in infill density having a direct reduction in mass of the fabricated artefact. Further, mass balance and RI are affected, with the distribution and magnitude of mass now different to the intended design.

The final reason relates to the absence of internal components, geometry, and additional assembly. In early stage prototyping especially, simplification of components, geometry and assembly is often performed to reduce cost and time overheads (and thus fixation) associated with fabrication of the prototype. This normally affects each of the mass properties in all

instances. This happens with prototypes made using other manufacturing methods too, such as the example of the pizza box resembling an architect's laptop in the work by Houde and Hill [1]. As mentioned, a pizza box with a brick in it was used to resemble the geometry and weight of a laptop.

For the purposes of demonstration, a Bosch electric hand drill was considered. The nominal mass of the as-built, final design is 1459 g. This compares to an estimate from Ultimaker Cura (the pre-processer) of 331 g, 22.7 % of the intended mass, and as-printed mass of 300.71g (20.6% of the intended mass). Similar analysis for a Nintendo Switch JoyCon shows comparable results, with the printed mass 42.3% of the intended. As such, it is clear that the mass properties are not properly represented in MEX fabricated prototypes with the effect of this requiring further investigation.

3.7 Chapter Summary

A review of AM and MEX has been carried out that identified the important characteristics of the processes. Through this review, it is clear why MEX is commonly used for prototype fabrication (e.g. high level of automation, good geometric accuracy and low cost). However, it is recognised that properties - especially the mass properties - may not be accurately mapped between the product design and prototype fabrication.

Chapter 4
Perceptions of Mass Properties

4.1 Chapter Overview

This chapter aims to assesses how users perceive mass properties when interacting with prototypes. Initially, the chapter aims to clarify the type of product for which interactivity is important and constrains the study accordingly. From here, five main areas are presented to understand the perception of mass properties:

1. A review of the definition of mass properties;
2. An identification of the applicable products for which mass properties may be emulated for;
3. A review of thoughts from industry on the value of emulating mass properties, and their value in prototyping;
4. A user study that investigated how mass properties were identified when using an AM electric hand drill; and
5. An analysis of the biomechanics governing how a user would perceive RI when interacting with applicable products.

To conclude the chapter, a discussion around the objective function that would be used to govern how mass properties should be emulated is presented.

This chapter aims to answer RQ 1 - "How important are mass properties of MEX prototypes?". This is done through review of sub-RQs :

1. How are mass properties defined? What needs to be controlled for mass property emulation?
2. What products would benefit from mass property emulation in prototypes?
3. Can mass properties be identified by users within relevant products?
4. What are the relative importance of mass properties in relevant products?

Parts of this chapter are presented in the author's conference paper "Looks Like But Does It Feel Like? Investigating The Influence Of Mass Properties On User Perceptions Of Rapid Prototypes" [25] and will be referenced as such.

4.2 Mass Properties

The mass properties of a product are defined as the mass, mass balance and RI of the prototype. These properties are each defined mathematically within this section and in MEX is discussed.

4.2.1 Mass

Mass can be defined in two principal ways. The first is by considering it a measure of how much matter is contained within an object [171]. This is thought to be the term most people would give when discussing the perception of an object and is most synonymous with how mass is interpreted by people – as weight. However, it is an ambiguous way of defining the mass of an object, as there are many ways to measure how much matter forms an object. More accurately, mass is better considered to be the resistance to acceleration of an object when an external force is applied - easily derived from F = ma. It is this resistance to acceleration that users interacting with an object are normally perceiving and relate to the mass of an object.

In this context, the term inertia is also regularly used, though it is avoided here to provide greater clarity between the properties defined by an object's mass and RI. For all purposes currently of concern in engineering, mass is a positive, real quantity with the Système Internationale (SI) units of kg.

4.2.2 Mass Balance (Centre of Mass)

The mass balance of an artefact is normally provided as a CoM point. The CoM point is a singular position contained within the bounding box of an object. It is where the weighted average position of the mass of the object sums to zero. It is commonly used - in many sectors - as a singularity where the entire mass of an object can be considered as acting, with varying

levels of applicability depending on context. For the cases considered within this work (rigid, solid bodies) the CoM can be considered a static point relative to the object's co-ordinate system.

Mathematically there are several ways of defining the CoM position [172]. The first is to find the weighted mean position of the mass that forms an object. For an artefact with uniform mass density, this would be at the artefact's centroid. Otherwise, for objects with continuous volume, the CoM position can be found using Equation 4.1.

$$P = \frac{1}{M} \iiint p(\bar{r}) dV \tag{4.1}$$

Where P represents the co-ordinates of the CoM, M is the total mass of the object, ρ is the density of the system as a function of r, the vector position of mass relative to the reference position, and V is the volume of the object. This does, therefore, require knowledge of how the mass, or density, is distributed throughout an object. If this is not possible - as is often the case for complex shapes and organic geometry - a discrete approach is often adopted. This method splits the volume into many discrete cells using a mesh and then uses these cells as point masses to calculate the CoM position. This is done using Equation 4.2.

$$P = \frac{1}{M} \sum_{i=1}^{N} m_i \bar{r}_i \tag{4.2}$$

Here, P and M remain unchanged, i is the particle number, N the total number of particles, m_i the mass of particle, i, and r_i the position of the mass with respect to a reference position. It is assumed throughout the rest of this work that a combination of discrete point masses will be used.

4.2.3 Rotational Inertia

RI is the resistance of an object to angular acceleration when an external torque is applied to the object about a given axis. In its simplest definition, the resistance is equal to the sum of the products of each element of a body's mass and the square of the element's distance from the axis [25]. It is commonly referred to as (Mass) Moment of Inertia and angular mass, but RI will be used throughout this work to avoid confusion with terms in the inertia tensor.

The effect of any given particle of mass, m, on a system's RI can be shown to be equivalent to mr^2, where r is the perpendicular distance of the particle from the axis of rotation. As such, the RI of a rigid body represented by many particles around a known axis can be found by using Equation 4.3 [172].

$$I = \sum_{i=1}^{N} m_i r_i^2 \tag{4.3}$$

Where I is the RI of the body around the axis, i is the particle number, m_i is the mass of the particle, i, r_i is the perpendicular distance of the particle, i, from the axis and N is the number of particles. For objects rotating freely in three-dimensional space, the problem is a little more complex.

Inertia Tensor

For bodies free to rotate in three-dimensional systems, as will be discussed within this work, the RI around three mutually perpendicular axes can be represented in a diagonally symmetric 3x3 matrix. This matrix is often referred to as the inertia tensor.

To derive and understand the inertia tensor of a body, the angular momentum of a body should be considered – as in Equation 4.4.

$$\bar{L} = \sum_{i=1}^{N} \bar{r}_i \times \bar{P}_i \tag{4.4}$$

Where $\bar{L}$ is the angular momentum of the system, $\bar{r}_i$ the position vector of each particle, and $\bar{P}_i$ the angular momentum vector of each particle. This can be rearranged as:

$$\bar{L} = \sum_{i=1}^{N} m_i (\bar{r}_i (\bar{r}_i \times \bar{w}_i)) \tag{4.5}$$

Where $\bar{w}_i$ is the angular velocity of a particle. This can then be expanded in each axis to give:

$$L_x = m\left[\left(y^2 + z^2\right) w_x - xyw_y - xzw_z\right] \tag{4.6}$$

$$L_y = m\left[\left(x^2 + z^2\right) w_y - xyw_x - yzw_z\right] \tag{4.7}$$

$$L_z = m\left[\left(x^2 + y^2\right) w_z - yzw_y - xzw_x\right] \tag{4.8}$$

It is then possible to construct a 3x3 matrix, known as the Inertia Tensor, that contains the definition for rotational inertia (from $L = Iw$). This looks like:

$$I = \begin{bmatrix} I_{xx} & I_{xy} & I_{xz} \\ I_{xy} & I_{yy} & I_{yz} \\ I_{xz} & I_{yz} & I_{zz} \end{bmatrix} = \begin{bmatrix} \left(y^2 + z^2\right) & -xy & -xz \\ -xy & \left(x^2 + z^2\right) & -yz \\ -xz & -yz & \left(x^2 + y^2\right) \end{bmatrix} \tag{4.9}$$

As can be seen, the inertia tensor is a symmetric 3x3 matrix. The three diagonal terms are referred to as the principal RI terms, and the remaining terms are the products of inertia. The products of inertia represent the reaction of a product around a given axis in response to a torque applied to a mutually perpendicular axis.

For any given volume, it will be possible to find a co-ordinate system for which the products of inertia are zero. This is due to symmetry of mass distribution around at least one axis. In this instance, only the values on the diagonal are non-zero. For the work detailed within the thesis, it is assumed that only the principal moments of inertia are of concern. The reasons

for this are twofold. Firstly, the RI is considered around the product centre of mass and, due to small differences in the mass symmetry around this point, the products of inertia are likely to be small. Secondly, in most systems the principal moments of inertia dominate the product moments of inertia and, therefore, the products can be neglected.

4.3 Applicable Products

One of the most notable mentions of mass as an important property in prototyping is that in Houde and Hill [1], as previously mentioned in Chapter 2. In this example, a brick is placed in a pizza box to resemble an architect's laptop as part of an Apple design project. The prototype is used to understand the behaviour of the user and product in context using a form factor that is somewhat akin to the intended design. The authors categorise this prototype as "a rough look and feel prototype", with role also explored, according to their own classification model. The look of the product was assimilated to the pizza box, with feel apportioned to the weighting of the box.

In work investigating sporting performance, several authors have identified that the mass properties of sporting equipment affect the performance of athletes (for example, [26, 173, 174]). In these examples, the mass, mass balance and RI (referred to as swing-weight in many sports literature) are all recognised as factors that may affect performance. In each, RI becomes the focus. In the most recent work, that by Cross and Bower [26], two sets of three rods are considered with respect to their mass and RI, in conjunction with the mass of a single hand. The first of these sets was designed to have equal mass, with the second designed to have equal RI in a single axis around the end of the handle (including the hand). The work found that a decrease in swing weight (RI) led to an increase in swing speed, and therefore performance. In addition, system mass was not found to substantially affect performance. It is of note, however, that swing weight considered system RI, not just principal product RI. The effect of this is discussed later within this chapter (Section 4.6.3).

Not all products will undergo the same design and prototyping methodology, however. For instance, a games controller is likely to have successive prototyping iterations that target refinement around the ergonomics and feel. For such products, the mass properties are

thought important considerations. In contrast, a turbine blade in an aircraft gas turbine is likely to undergo prototyping to identify whether the performance of the part is satisfactory and that the anticipated manufacturing process is suitable. Even when fabricated using MEX technology, these turbine blades are unlikely to be used interactive assessment, but rather used for Design for Assembly (DfA) testing or similar (though exception may be made for assembly testing). As such, it is important to recognise product types that are likely to be affected by incorrect mass property representation in MEX prototypes.

If we return to the example from Houde and Hill, the product being considered is a portable computer [1] (generally now referred to as a laptop or tablet computer). In this instance, the ease of portability and interactivity were considered for a product intended to be used by a consumer (a consumer good).

It was hypothesised that for most instances where products were to be interacted with as part of their primary function, the mass properties would be important. It was assumed that consumer goods would be the most appropriate type of goods; these goods are tangible commodities produced and purchased to satisfy the current requirements of a buyer [174]. Although this grouping includes products such as cars, fridges, and furniture – which are out of scope – it also includes consumer electronics, tools, and many other handheld or portable products. These handheld and portable products' mass properties were thought important considerations based upon the study thus far. In addition, they are of a geometric scale that would allow their fabrication using desktop MEX machines as part of the prototyping process. Therefore, the remainder of the study will focus on these products.

It is recognised that other products not directly considered may benefit from having representative mass properties in prototypes. For example, a crane would normally require the CoM to be located above its base, or a boat require accurate mass and CoM representation. However, primarily due to the scale and complexity of these products, there were considered out of scope for investigation.

4.3.1 Case Study Products

Within this work, three case study products will be used. The case study products considered were high volume, handheld devices that require high levels of human motor control for interaction that are of a size suitable for fabrication on typical desktop MEX printers. Typical desktop machines include the Ultimaker and Prusa series of MEX printers, with these becoming increasingly common in hobbyist and industrial settings [149, 156]. These machines typically use 0.4 mm nozzles, matching the previous assumptions. The products are presented in Figure 4.1, with relevant mass and geometric properties. These geometric properties are derived from the virtual representation of form, whilst the mass properties were found as below.

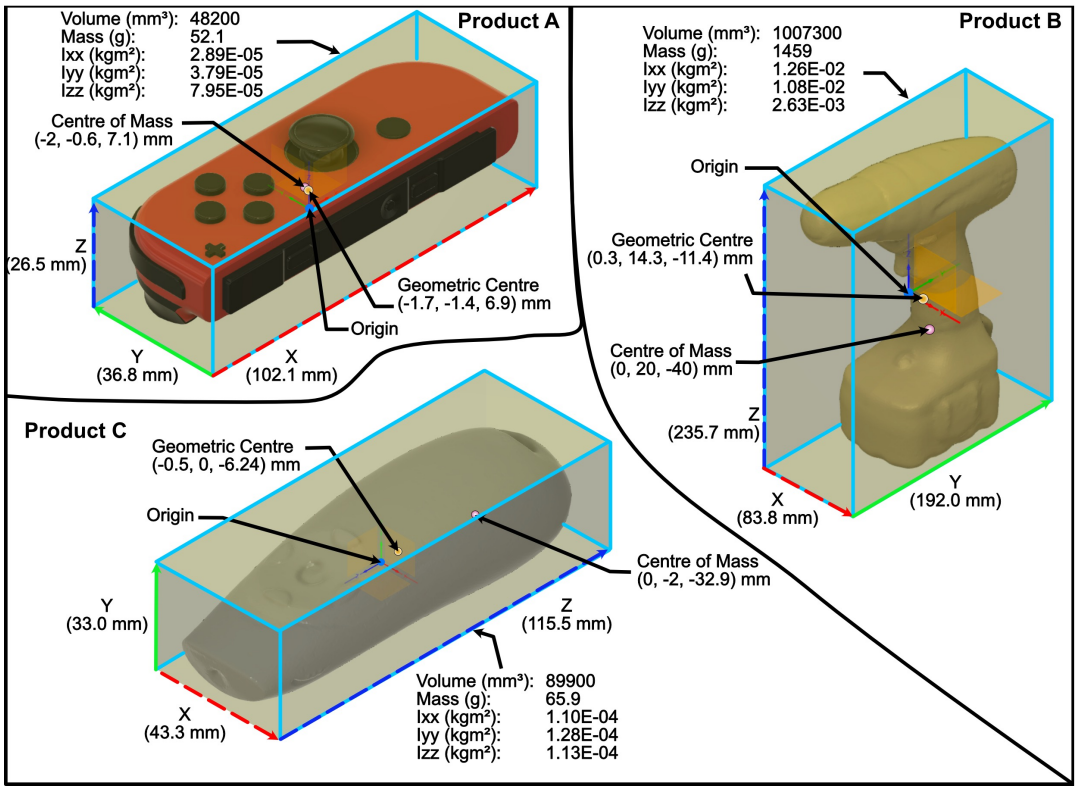

Figure 4.1: Case study products. Product A is a Nintendo Switch JoyCon. Product B is an electric hand drill. Product C is a laser pointer.

- Mass - Weighing scales were used directly to measure the mass of the case study products.

- CoM Position - 3D printed tooling was used to align the products across multiple weighing scales, with the product CoM position evaluated from these measurements.
- Principal RI - A trifilar suspension system was used (as in [175]) that uses the period of rotation to measure a product's principal RI around an individual axis. The same tooling was used as for evaluation of the product CoM positions. It is recognised that the error in case studies A and C RI may be large due to their low mass.

The y- and z-axes CoM positions of case study B were offset from the derived properties to represent an investigation into the use of alternate battery sizes. The values shown in Figure 4.1 represent the properties post-modification. The modification of these properties was thought a potential use case for emulation of mass properties in AM prototypes - where many mass properties for a geometric form could be tested without costly redesign. Table 4.1 present the evaluated properties, for reference.

Table 4.1: Mass properties for the three case study products.

Case Study Product	Mass/g	CoM/mm			RI/kgmm^2		
		x	y	z	xx	yy	zz
A	52.1	-2.0	-0.6	7.1	28.9	37.9	79.5
B	1459	0	20	-40	12600	10800	2630
C	65.9	0	-2	-32.9	110	128	113

Case study A, a Nintendo Switch controller, was chosen as it required both large-rapid movements as well as small, controlled movements. Further, the increase in required mass (between the as-designed and baseline 3D printed prototype) was found to be small, posing a challenge in offsetting the CoM. The laser pointer (Case Study C) was chosen as it would generally require stable control with relatively small movements, whilst demonstrating a large offset of the CoM from the geometric centre. Therefore, there was a hypothesised challenge in locating this mass. Finally, the electric hand drill in Case Study B was used as it had a larger mass and volume than either of the other case studies and required movement around the elbow (rather than wrist).

Other products, such as mobile phones, television remotes, other games controllers, were not considered due to similarity with the above, lack of access for review and simplicity in geometry.

4.4 Industry Review on the Effect of Mass Properties in Prototyping

Reported in previous work by the author, industry was consulted to understand their view on the importance of mass properties in prototyping [25]. Two companies were consulted to via email and their responses to a series of questions recorded.

The first of these companies was Amalgam model makers, based in Bristol, UK. As one of the world's leading modelmakers, Amalgam was well placed to discuss the fabrication and use of prototypes. The representative of Amalgam, Mike Harvey, was the company's Director for Prototyping.

The second of these companies was Moulton Bicycle Company, whose Technical Director (Dan Farrell) contributed to the study. Moulton Bicycle Company specialise in the design and manufacture of premier bicycles and are based in Bradford on Avon. In contrast to Amalgam, prototyping is a tool required for the design of a product (rather than the specialism of the company). Although the product range is not necessarily one with which AM prototypes would be associated, the general learning was beneficial.

Each company representative was asked the following questions, and have approved for their answers to be used within this work as partners to the EPSRC project EP/R032696/1:

Q1 Would you consider the incorporation of mass distribution into a prototyped artefact a useful feature?

Q2 Have you and/or your company previously completed any work into replicating the mass distribution of a part (or parts)? If yes, and you can, please provide an example of the part and how you replicated this distribution.

Q3 Do you have any suggestions on parts or assemblies that may be of interest to you and/or your company, or that may be good examples generally?

Both companies indicated that the incorporation of mass in a physical prototype would be useful in response to Q1, with Amalgam stating:

“Yes. While an early-stage prototype might not need to have realistic mass distribution, for many it would be a very useful, if not essential element."

Further supported by:

"It seems to me that the inclusion of realistic mass etc. is best suited to the mid-stages of a product development cycle. . . . late stages would usually include "Real" or bought-in components such as batteries, electronics, motors etc."

From these two quotes, the emulation of mass properties would be most appropriate for early- and mid-stage prototyping. Moulton Bicycle Company also cited the importance of mass on product prototypes and the associated perception:

"There is a thing about perception of mass going on, certainly with bicycles. A bike feels heavier if the mass is concentrated at one end rather than balanced. The momentum of an object is also something to consider."

It is highlighted how the feel of an object can be affected by the mass properties – more specifically mass balance – of the object. This is extended, with the company stating:

". . . a good example is the original Moulton bicycle, where the carrying handle is integral to the frame. For it to work properly the handle has to be at the centre of mass – if you get the mass distribution wrong it doesn’t work well or at all."

Here, functional aspects of the product are considered. For the example provided, the incorrect positioning of the handle (leading to poor or incorrect function) would negatively affect user perception of the product. As such, accurate representation of mass properties in prototyping is important to ensure functional components are designed correctly.

Through consultation with industry, further evidence has been collected that demonstrated mass properties are important considerations in prototypes. Further, in early- to mid-stage prototyping activities it has been confirmed that mass property emulation methods (in-lieu of final components) would be advantageous.

4.5 User Study on the Effect of Mass Properties in Prototyping

A study was conceived that aimed to investigate how students perceived mass properties. This involved interviewing participants at the University of Bristol following a short activity using similar – but non-identical – parts. Their responses were recorded and, along with a more detailed study design, are presented in this sub-section.

The work detailed within this section is expanded from the author's work in [25].

4.5.1 User Study Example Part

A drill model produced by Ultimaker was selected which, at the time of the study, was available to download from YouMagine under a creative commons licence (CC-BY-4.0) [176] (also in Figure 4.2). Minor edits were performed on the model within the CAD software Autodesk Fusion to add "mass pockets". These pockets were placed in the top of the drill (where the motor would normally be) and the base (where the batter would be attached). The modified model is available on YouMagine, also under the CC-BY-4.0 licence here [177].

The hand drill was used for several reasons:

1. The model could be printed at a suitable size in the Ultimaker 3 Extended build volume,
2. The product had measures of performance related to mass properties, and
3. The printed model was expected to have significantly different mass properties to a "normal" electric hand drill when fabricated with the recommended print settings (0.1 mm layer height, 20% infill).

Figure 4.2: The drill from Ultimaker [176].

Each drill was manufactured using the same split of black and pearl white Ultimaker PLA [178] and Ultimaker 3 Extended printers, at 105% of the original model scale to allow the drills to fit on the bed plate, whilst maximising the size of the notably small grip. The print method recommended by Ultimaker was followed, though the infill pattern was changed to a grid pattern to aid with the addition of mass. Several other settings were changed to improve print performance, such as the use of a brim and reduced retraction, but these were not thought to have affected the mass properties of the part produced. A 8.5 mm High Speed Steel (HSS) drill bit was placed in each drill, with a small adapter, for the purposes of the activity.

Three drills were fabricated and used within the study. These were:

1. A standard drill model, with mass pockets but with no added mass,
2. A drill with mass added to the base of the drill, to emulate the mass of a battery, and
3. A drill with mass added to the upper section of the drill to partially emulate the mass of a motor.

The intention was for the drills to look similar but feel different to a user. They were not modified such that they would represent any real-world design. Instead, they were modified purely so that the mass properties were different from each other. The mass of each design were 0.41, 0.47 and 1.01 kg, and the CoM positions are shown in Figure 4.3.

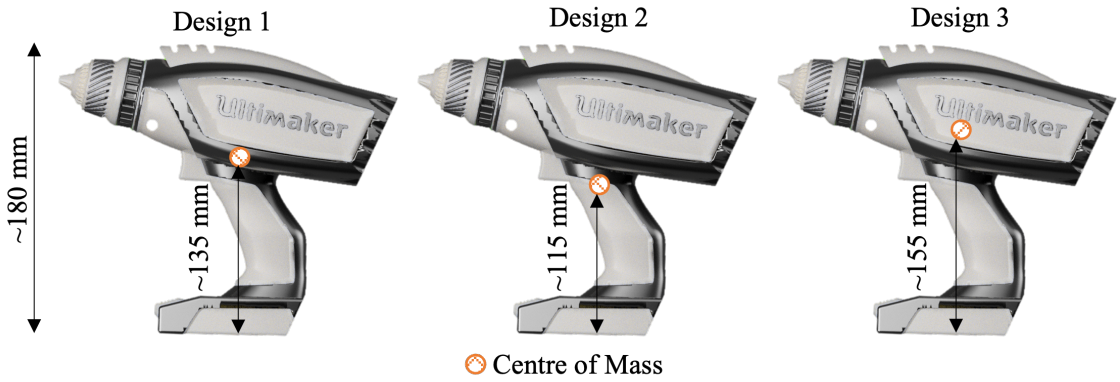

Figure 4.3: Centre of Mass (CoM) position for each drill design.

4.5.2 Study Mass Property Manipulation Method

The mass properties of designs 2 and 3 were altered by adding small lead masses and coarse iron filings into the mass pockets and infill structure. The lead pellets had a quoted, individual mass of 0.45 g, a diameter of 4.5 mm and a length of 5.42 mm. This sizing was driven by what was commercially available and the size of gaps within the infill. Masses were added to Design 3's infill by pausing the print and pouring the pellets, then iron filings into the structure. A small amount of adhesive was then used to hold the material in place. Figure 4.4 shows the drill with added mass during production.

4.5.3 Study Participants

The study was completed by 25 undergraduate Mechanical Engineering students from the University of Bristol. Of these students, 18 were from 1st year and the remaining 7 from 3rd and 4th year. The results from each of these groups were indistinguishable and are therefore reported together. The experiment was completed over a short timeframe (~2 days) to ensure participants did not divulge information to one another. The documents and setup used within this study were approved by the University of Bristol research ethics committee.

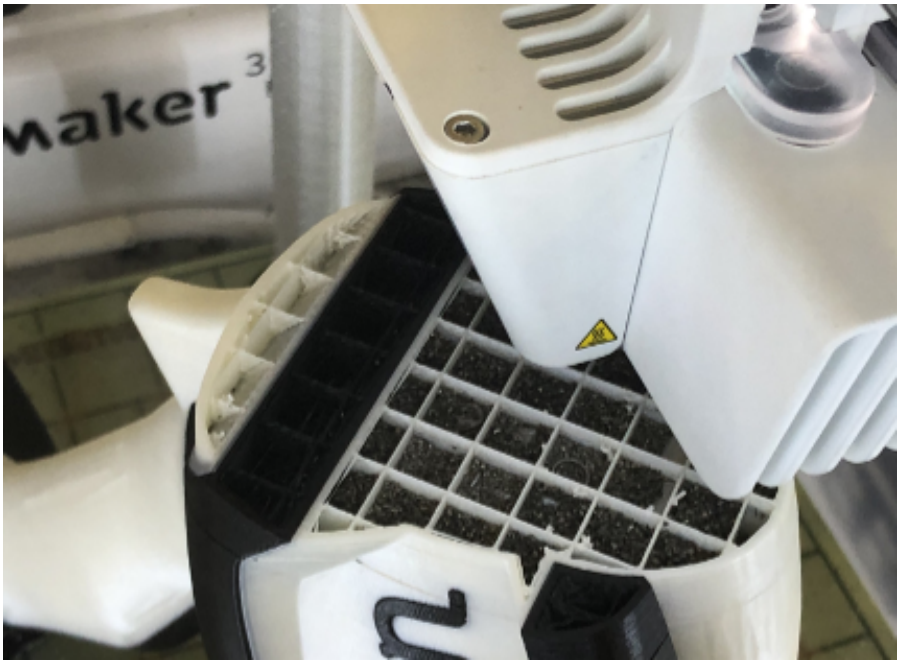

Figure 4.4: Design 3 being manufactured on an Ultimaker 3 Extended, with coarse iron filings and lead pellets contained within the infill.

4.5.4 Study Activity

The activity involved the use of each weighted drill before completing a short, three question survey. This was done away from other participants over a short-time frame to ensure independence of results.

The task involved using each drill individually, pushing the attached drill bit through a series of six holes in a 6 mm acrylic sheet. These holes were 10 mm in diameter (1.5 mm larger than the drill bit). The sheet, shown in Figure 4.5, was designed such that the drill had to be translated and rotated by the user to successfully protrude through each hole. This was done to emulate a realistic hand drill role. The acrylic sheet was attached to a standard desk using tape so that the position was standardised between participants.

A prize was promised and awarded for the fastest participant with a single and all three drills. This was done to ensure the task was performed with an unambiguous objective by every participant. The participants were asked to randomly select the order of the drills to be used, with this data presented in Table 4.2. Design 2 was used first more often than either of

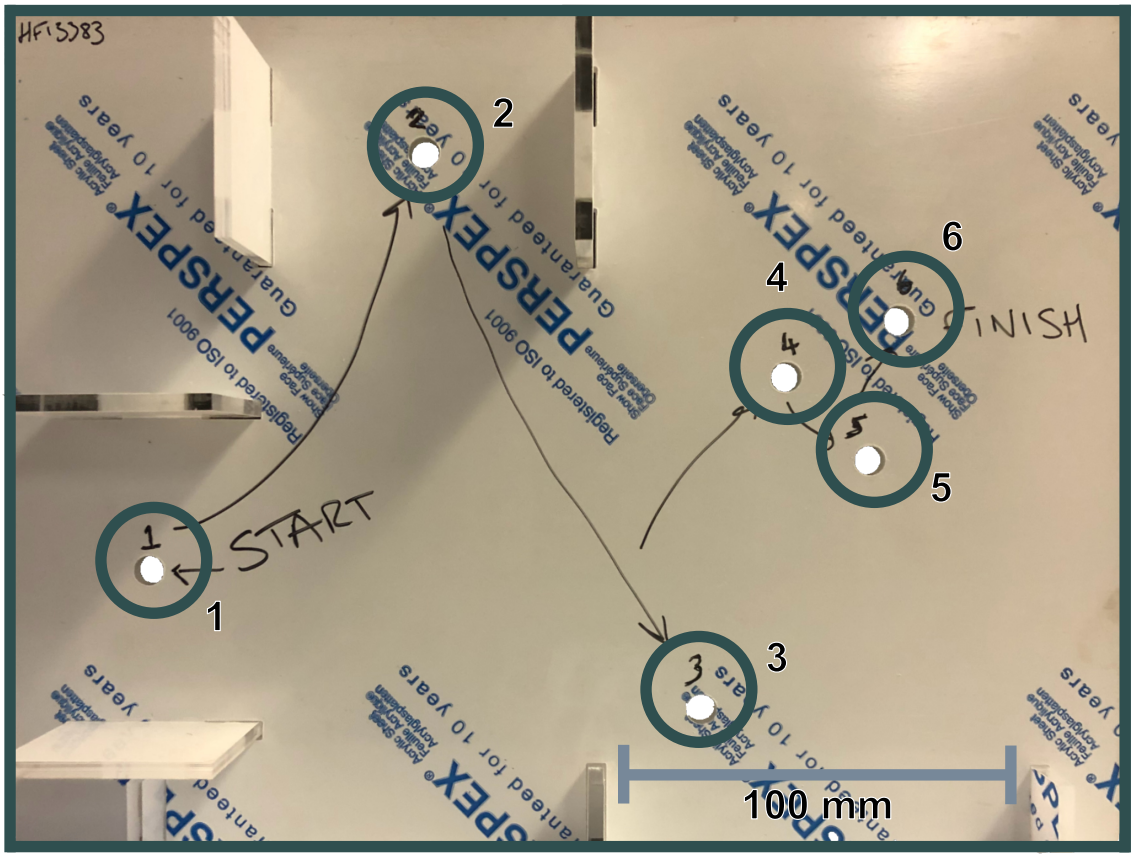

Figure 4.5: Acrylic activity sheet that was used by the participants. The holes were positioned such that the drills had to be translated and rotated.

the other two designs and was therefore used last less regularly. Otherwise, drill order was well dispersed. On reflection, the drill order should have been prescribed to ensure more even distribution.

Table 4.2: Breakdown of order of drill use selected by participants for the user study.

	1st	2nd	3rd
1	7	8	10
2	13	8	4
3	5	9	11

At the end of each recorded use of a drill, the participants were told the time it took for them to complete the activity (though they were not told other participant times). The survey, which was initially completed at the end of the task independently from the author (who oversaw the activity) consisted of three questions:

- Please score the three drills between 1 and 5 (1 being poor, 5 being good).
- What were your least favourite aspects of the lowest scored design(s) from question 1? There should cover all aspects of design.
- How would you improve the highest scoring design(s) from question 1? Please list your three main methods of improvement. These should cover all aspects of design.

After the survey was completed independently, the answers were reviewed, and a short interview clarified any areas of ambiguity. The supervisor attempted to not lead any responses, instead clarifying what was meant by the provided answers. Examples included clarification of “heavy, bulky” and “hard to move precisely”. The original answers and the clarifications were recorded.

4.5.5 Study Results

All 25 participants successfully completed the study with all three designs. Across all the participants, each design was scored both 1 and 5 by at least one participant. Further, in all instances a single design preference was indicated by the participants, with only three instances where the lowest scores were given to two drills by the same participant. However, it was later clarified that the participants disliked different aspects from each design, rather than not being able to tell them apart.

On average, Design 2 was the preferred design (with a mean score of 3.6), selected as the best drill 11 times. In comparison, designs 1 and 3 had mean scores of 3.16 and 2.88, respectively. This compared to median scores of 3, 4 and 2 (see Figure 4.6). From this figure, it is also clear that the variation in scores for Drill 2 were reduced, showing the drill was considered favourable more consistently. As Design 2 was used first by the participants more frequently than any other design, analysis was undertaken that observed whether a

relationship between drill order and score existed (as this was not randomised). This work - that considered the statistical variation between each drill used in each order - demonstrated that there was no clear correlation between order of design use and score, with scores and speed distributed throughout the order profiles. Further statistical analysis was not undertaken due to the limited number of participants within this study.

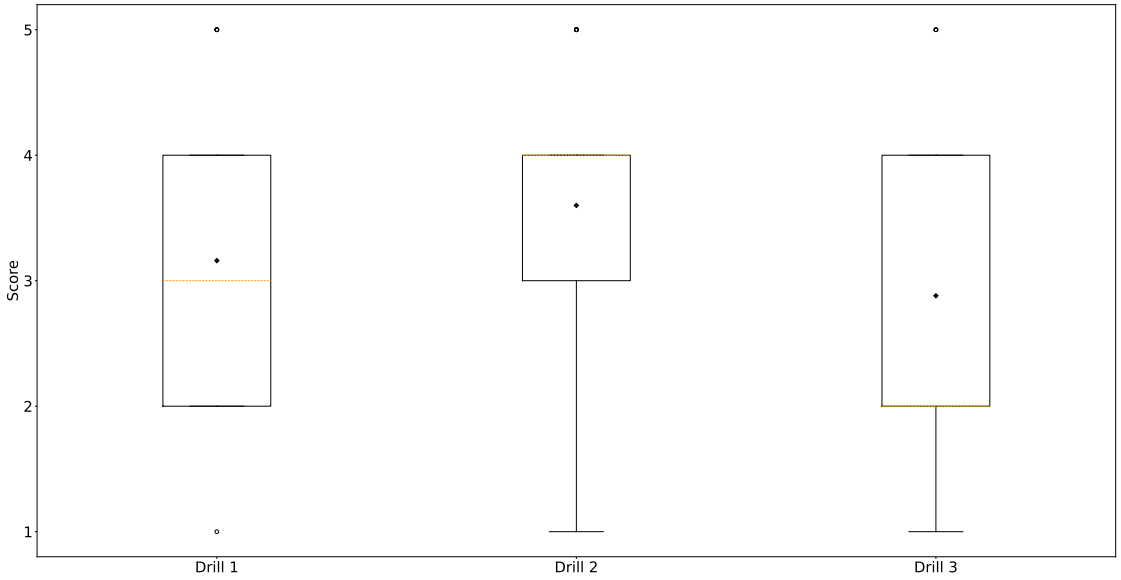

Figure 4.6: Box plot of participant scores for each drill in response to Question 1. The whiskers represent the central 80% of the data, the box the Interquartile Range (IQR) and the dashed line the median. The marker is the mean score.

The design most commonly fastest for the participants was Design 3 (11/25). Interestingly, this was the design that was scored the lowest by the participants. It had been hypothesised that the fastest design may be selected as the preferred design of the participants. This was predicted as the participants were aware there was a prize for the fastest participant and were informed of their times during the experiment. Instead, this relationship was not identified. The answers given to questions 2 and 3 were categorised into four groups; mass, balance, inertia and other. The first three of these groups related directly to the mass properties being investigated, with the fourth encompassing all other answers. The participants were not made purposefully aware of this categorisation during the experiment.

The participants used a range of language in their responses to the two questions. Phrases such as “heavy”, “unstable” and “light” were easier to interpret without further questioning, whilst “hard to move” and “hard to control” required clarification. Where required, ambiguous terms were ignored. The categorisation of answers for Questions 2 and 3 are shown in Figure 4.7, pre- and post- discussion. Each answer that had been given by the participants was questioned for further meaning, unless explicitly clear, to reduce bias in the interview stage. It is recognised, however, that some bias will have likely remained.

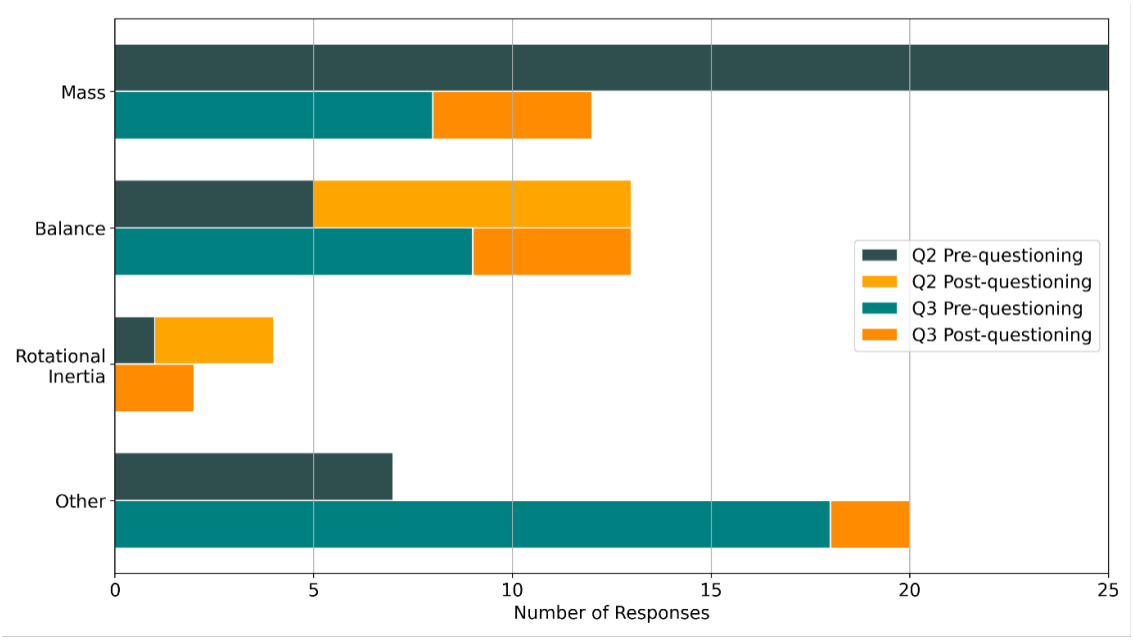

Figure 4.7: User responses to survey questions 2 and 3, categorised by mass property.

The results in Figure 4.7 demonstrate that the participants were able to identify that mass influenced their perception of the designs. All participants mentioned “mass”, “weight”, “heavy” or comparable terms. Mass was referenced more regularly when discussing participants’ least favourite design (rather than discussing improvements to their favourite). This may be because the participants had prioritised their choice of design using mass, and therefore they were already happy with the mass. However, this could not be confirmed with the information available from the study.

The CoM position, or mass balance, was clearly identified by less than half (36% for Q3) of the participants. When these answers were discussed, this was found to increase to around half of participants (52% for Q2 and 3). This suggested one of two things; the terms used to describe the mass balance of the designs were more ambiguous than for mass or the effect of mass balance was unclear to the participants without further discussion. This was true when discussing both the issues with designs and improvements – the most consistent property between Q2 and Q3.

RI was less well recognised in both Q2 and Q3. In both questions, less than 5 participants (20%) recognised RI, even after discussion around their answers. From the data available, it is unclear if this was because of a physical effect, greater abstraction of effect, or fundamental misunderstanding of the effect RI has. This is discussed further in the following section.

Finally, other properties were more often identified as methods for improvement in participants favourite designs than flaws in their least favourites. As every drill should have been the same (except for mass properties) this was expected. Principally, this was because in Q2 the participants were comparing products, where as Q3 required absolute considerations. As such, common properties were more likely to be considered in response to Q3.

4.5.6 Study Findings

It has been shown that the mass properties of the designs had a noticeable impact on the perception the participants had of the designs. This effect was more significant than the performance of the participant with the design(s). It is therefore clear that mass properties have an impact on user perception.

Every participant was able to recognise and communicate issues with mass, around half could do so with issues relating to balance, and few participants recognised RI. This was not a necessarily surprising result, with the level of abstraction increasing with the order of mass moment of inertia. However, clarification around whether the lack of perception of RI was physical or psychological was worthwhile.

The raw results for the study are available in Appendix D.

4.6 Biomechanical Analysis of Rotational Inertia Study

To better understand the physical perception of RI, simple biomechanical analysis study is undertaken looking at handheld goods. To do this, three example products are considered. As detailed in the applicable products section (Section 4.3.1) these were a Nintendo Switch JoyCon, a Bosch electric hand drill and a Kensington Laser Pointer.

4.6.1 Mechanisms of Interaction: Rotation Through the Wrist

For the average, able-bodied person, the wrist is capable of two distinct rotational movements: flexion/hyper extension and radial/ulnar deviation [179]. Flexion is motion in which the palm of a user's hand moves toward the user's lower forearm. In comparison, hyperextension is the opposite movement, where the dorsal surface of the hand moves toward the top of the forearm. Further, radial, and ulnar deviations occur when the hand is rotated towards the side of the forearm. Radial deviation being when the thumb side of the hand moves toward the arm, with the opposite motion being ulnar deviation. It is possible for the wrist to rotate around both axes simultaneously, with this referred to as circumduction, but for the purposes of this study the motion is ignored. Figure 4.8 shows the possible movements of the wrist, taken from [179].

If the product is handheld and used as such, it can be assumed the product CoM will lie at or close to the hand mid-point – and rotated about the wrist joint centre. In all instances of rotation around the wrist, there are four sources of RI that are perceived:

- the product about the principal axes;
- the offset of the product's geometric centre from the centre of rotation of the wrist joint;
- the hand around its own axis; and,
- the hand due to the offset of the hand's geometric centre from the centre of rotation of the wrist joint.

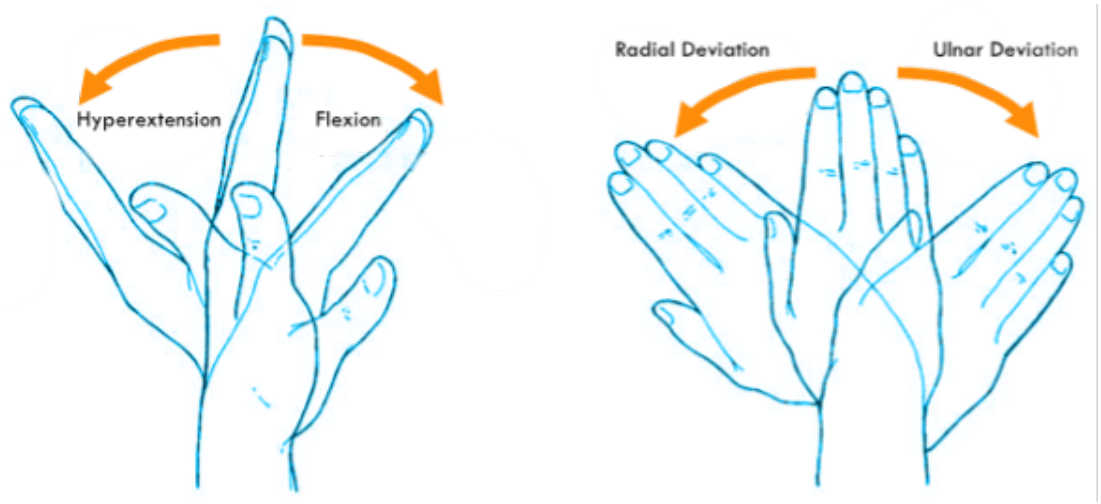

Figure 4.8: Movements of the wrist, adapted from [179].

Using data from Plagenhoef et al.'s work it is possible to estimate the RI from each of the sources, and allow the centre of mass, mass and RI to be calculated for body segments. When considering rotation around the wrist, it was assumed that only the hand and product would be relevant, with body measurements taken for an average person from [180]. This meant a mean mass and length of 416 g and 101 mm for the hand were used respectively (mean of men and women from the study).

The sources of RI associated with the hand were calculated as a lumped model, using the radius of gyration for rotation around the joint centre. For the product, the sources of RI were considered separately. The largest RI for each product was used to due to the idealised assumption of how the product will be held.

The determined RIs for each product are given in Table 4.3. This shows that for products A and C (the controller and laser pointer), the RI of the product about the product's principal axes is negligible compared to the RI of the system rotating around the wrist. For these products, the products RI accounted for less than 5% of the total RI of the system. For product B, the RI of the product around the principal axis accounts for ~20% of the RI of the system. Although this is significant, it was unlikely that fast movements of product B would be actuated by the wrist. Instead, it was anticipated that any such movements would be actuated by the elbow.

Table 4.3: RIs for the human-wrist system relative to the maximum RI of the product around its principal axes, found using data from [180]

Part	Sources of Rotational Inertia		
	Principal Axis (Product)	Hand Principal Axis	Parallel Axis of Product
Switch JoyCon	2.22%	34.65%	63.13%
Hand Drill	16.39%	1.61%	82.01%
Laser Pointer	3.02%	29.35%	67.62%

4.6.2 Mechanisms of Interaction: Rotation Through the Elbow

Rotations around the elbow are considered in a similar way to that previously presented for the wrist. This is necessary to account for rotation around a third axis, perpendicular to the wrist's two axes of rotation, as well as similar motions to the wrist that involve larger applied loads. Once again the data from Plagenhoef et al. was used [180], in this instance considering the data for both the hand and forearm. This meant that the reference mass and length were updated to 1658 g and 277.5 mm respectively. Table 4.4 presents the results from this analysis, demonstrating that the maximum effect of the principal axes RI for product B is less than 3%.

Table 4.4: RIs for the human-elbow system (considering the hand and forearm) relative to the maximum RI of the product around its principal axes, found using data from [180]

Part	Sources of Rotational Inertia		
	Principal Axis (Product)	Hand and Forearm Principal Axis	Parallel Axis of Product
Switch JoyCon	0.08%	87.68%	12.24%
Hand Drill	2.84%	19.79%	77.37%
Laser Pointer	0.12%	84.89%	14.99%

4.6.3 Comparison to Literature

As previously discussed, Cross and Bower presented work that demonstrated that swing weight (effectively RI) had an effect on sporting performance [26]. In this work, RI was calculated around the end of the handle (for rotation assumed around the wrist) with all system masses and lengths provided. Therefore, the proportion of RI is derived from rod RI can be calculated. Completing this analysis shows that, depending on the rod, between 20% and 25% of the system RI comes from the product principal RI.

The work demonstrates a deviation from the analysis presented throughout the rest of this section. However, this is principally due to the long, slender sections used that demonstrates a wide distribution of mass. Because of this form factor and the axis of rotation considered, the principal RI is much greater than you would nominally expect for the mass of the product. The case is therefore verging towards a worst-case scenario and one almost unique to sports equipment. If consumer goods are considered, similar shapes are normally avoided to keep the mass centralised. Therefore, finding that these scenarios' principal RI is still significantly less (~1/3) of the total system RI demonstrates that neglecting RI is likely to be acceptable.

4.6.4 Biomechanical Analysis Findings

It has been shown that the principal RI of a product around axes through the CoM are negligible in comparison to the system RI, at least in consumer goods. Instead, the other sources (the human body and parallel axis theorem) dominate the system. For this reason, it is thought acceptable to neglect to consider the principal RI when emulating mass properties.

4.7 Definition of Objective Function

To enable a methodology for emulating mass properties in MEX parts to be evaluated, it was necessary to form an objective function.

As has been demonstrated, it is important for the objective function to consider the mass and mass balance of objects, with the RI of the object itself of negligible importance. However, the way in which it considers these properties is unclear. This is because it has not been possible to accurately identify the relative significance of properties on user perception. Further, it is hypothesised that this assessment would change depending upon the application.

To demonstrate the expected variability in applied objective function, two models are considered – a putter head and a hand drill. In a prototype putter head, the position of the CoM is less likely to be of concern across its depth (the axis along the club). This is because

the CoM position relative to the user will be dominated by the length of the club. In contrast, the CoM position along the axis parallel to the grip axis of a drill will be important, with this dictating the rotational balance in the user's hand.

As a singular objective function is unlikely to be generally applicable to a range of products, a generalised objective function was generated. This function assumed that the product for mass and mass balance in each axis should be equal for proportional changes. In other words, a 1% change in any property would result in an equal change in the objective function. Its mathematical definition is provided in Equation 4.10.

$$min(Obj) = am + bC_x + dC_y + eC_z \tag{4.10}$$

Where m is the absolute mass error and C_i is the absolute CoM position error in each axis. a, b, d and e are set such that a 1% change in each mass property (relative to the maximum allowable) affects the objective function proportionally. As such, a is relative to the mass of the intended design and b, d and e are relative to the maximum length of the intended design in each axis.

As stated, it is recognised that the applicability of this function to specific products for specific applications is problematic. However, it will allow for a comparison of results, which was deemed the most important aspect for this work. Further, where necessary, the actual mass property values will be provided for comparison to provide further clarity.

4.8 Chapter Summary

Throughout this chapter, the answer to RQ 2 has been developed. An assessment of the absolute and relative importance of mass properties, with a focus on how these would be perceived by users in prototyping, has been presented through different workstreams. These answer the chapter RQs as below.

1. How are mass properties defined? What needs to be controlled for mass property emulation?

- Mathematical definitions of each of the mass properties - mass, mass balance and RI have been presented, showing that the amount and distribution of matter dictate the mass properties of a volume.

2. What products would benefit from mass property emulation in prototypes?
    - Applicable proucts were reviewed, with it thought that consumer products would benefit the most from the proposed mass property emulation in MEX prototypes. This is related to the high-levels of user-interaction of these prototypes, as well as them regularly being 3D printed within the design process.
3. Can mass properties be identified by users within relevant products?
    - Through user study and industry consulation, it has been found that mass properties can be identified by users as important characteristics in the assessment of product prototypes. Of these, mass is the most well recognised, followed by mass balance. RI was the least well recognised, though this may have been due to the demographic of participants.
4. What are the relative importance of mass properties in relevant products?
    - Biomechanical analysis of the hand and forearm have shown that, for most consumar products, it is likelt that the principal RI would not have a significant effect on the user-interaction with a prototype. Instead, the mass and mass balance dominate.

Additionally, the objective function should consider the context of the problem and what a prototype is intended to be used for. As this thesis aims to provide a solution for emulating mass properties independently from a specific problem, a generalised objective function is being used that considers the mass and CoM position in each axis equally.

Chapter 5
Methods for Emulating Mass Properties

5.1 Chapter Overview

The previous chapters showed that there is clear value in enabling the emulation of mass properties in MEX product prototypes. Doing so would allow increased value to be derived from these prototypes whilst improving the iteration speed, reducing costs, and improving end-use products. Methods to enable this emulation must be considered. To do this, an adapted version of Pahl and Beitz's design process is used [181], where requirements are captured in a Problem Definition Specification (PDS) and a Pugh matrix is used to compare concept methods of mass property emulation [182]. This is done to answer the RQ - what is the most appropriate method for emulating mass properties in MEX prototypes?

The best method is identified as the variable infill methodology; where material is deposited using the normal MEX deposition mechanism to position mass within the prototype. The main reasons for this were related to the ease of automation, ease of use and ease of retention of material. From there, review of initial set-up for the method is presented. It is recognised that, amongst other factors, the use of secondary, high-density print materials and discrete cell-density options would be beneficial.

5.2 Method Selection Process

Before careful consideration of the problem requirements and potential concepts, design drivers were considered. These are the principles that feed into the requirements outlined and are thought to improve the success of the proposed solution but may not be explicit from the problem definition. The design drivers used within this work are ease of use, cost, and emulation performance.

Ease of use is a primary consideration as it has previously been shown that a stakeholder's time investment required to fabricate a prototype is proportional to the level of design fixation [53]. The method should require minimal expertise and highly automated, to reduce the effect on stakeholder fabrication time. In addition, process uptake was hypothesised to

benefit from improved ease of use. To improve this metric, several methods are available. For example, increased automation, reduced post-processing and/or avoiding additional manufacturing operations.

Cost is another key concern. Although likely to be related to the ease of use, explicit consideration of cost (both economic and time) is important. Whilst ease of use reduces the burden on the stakeholder who fabricates the prototype, this may come at the expense of increased costs for others. For example, the purchase of a secondary fabrication unit may make the process very easy but come with high acquisition costs (similar to CNC vs manual machining). It is recognised that it is not possible to identify specific allowable costs for a generalised example. However, it was viable for the process to be limited to typical MEX hardware, not require bespoke materials and/or not increase the expertise required to fabricate a prototype.

Finally, emulation performance is a principal design driver. The process must allow for mass properties to be sufficiently well emulated. It is recognised that the emulation accuracy required is not well understood at this stage, nor is it necessarily appropriate to evaluate for every method of emulation. Instead, process parameters – principally material density – are considered. Other factors were also used and incorporated into the analysis. However, these were deemed secondary, with most represented, to some degree, within the main three design drivers.

To allow a suitable method to be identified and developed, a design process was undertaken that captures requirements from the problem and associated design drivers. From here, concepts were identified and assessed before being compared. The method could then be developed.

5.3 Method Requirements

The requirement capture process was undertaken so that the identified methods could be assessed against the problem. The formalisation of this has been shown to be a useful – in most instances necessary – part of the design process [181, 182]. For this work, the process

was not required to be as precise as would be expected in conventional application, with only a proof-of-concept solution desired. The focus was on capturing the over-arching requirements that were thought to be most challenging. The formal requirements capture is presented in Table 5.1.

Most of the requirements are functional and relate to the integration and use of the new method within the current MEX process. For each requirement, a validation statement and verification method are presented to ensure usefulness. Within the remainder of this chapter, the requirement IDs will be referenced for clarity on why decisions were undertaken.

5.4 Method Concept Generation and Selection

To address the problem specified in Section 5.3, three approaches were identified and considered. These were:

1. Incoroporation of lumped masses,
2. Addition of particulates and/or fluids, and
3. Printing of variable infill.

Each of the identified methods were assessed and compared. To do this a Pugh matrix was used [182] to allow for an analytical evaluation. As the precision of information available was not high, this was done simply to minimise judgement errors.

Table 5.1: PDS for the emulation of mass properties in MEX prototype products.

Req. ID	Requirement	Validation	Verification
		Performance	
P1	The method must allow common consumer product masses to be achieved.	Key performance indicator without requiring in-depth process analysis.	Consideration for a small selection of typical consumer goods.
		Functional	
F1	The method must be integrated into the MEX process.	The process is intended to function with the MEX process.	Qualitative assessment will be undertaken, along with process testing as appropriate.
F2	The method should not require additional hardware atypical of MEX machines.	Equipment purchase costs can be large and may limit useable machines.	Qualitative assessment will be undertaken, along with process testing as appropriate.
F3	The method should be automatable within the MEX process.	Manual intervention is often costly, prone to error and can increase design fixation.	Qualitative assessment will be undertaken, along with process testing as appropriate.
F4	The method should not require additional manufacturing processes (outside normal post-processing for MEX).	This would raise additional costs and time requirements and may increase design fixation.	Qualitative process assessment.
F5	The method should not require expertise above that of the normal MEX process.	One of the key draws of MEX is its simplicity, and this should not be lost with the target audience often non-expert users.	Qualitative process assessment and/or user study.
F6	The method should not require additional in-house or bespoke manufacturing operations.	This would increase required expertise and/or increase costs.	Qualitative assessment of process.
F7	The method should not require additional personnel to function.	This would increase costs.	Process prediction and assessment
F8	The method must retain mass properties throughout usable life.	The mass properties must not change between uses.	Qualitative assessment of retention methods.
		Safety	
S1	The method should not require materials that are hazardous, flammable, or otherwise harmful above that normally used within the MEX process.	It is recognised that the process is likely to be used in offices or other similar settings. Further, proper safety controls for material handling would increase required expertise and/or costs.	Assessment of proposed materials.
S2	The method should not present safety concerns above that of the nominal MEX process.	It is recognised that the process is likely to be used in offices or other similar settings, improving ease of use.	Qualitative assessment of process.

The Pugh matrix was formed to use a baseline and scores of +, 0 or -, to depict better than, same as, and worse than respectively. Scores were assigned to each method for seven factors: automation, ease of use, safety, cost/kg, hardware cost, emulation accuracy (considered as material density) and retention of mass. These were chosen based on the requirements from the requirements capture phase. Two baselines were considered, with the variable infill baseline presented in Table 5.2. A second example with a small, regular mass baseline is shown in Appendix B. The criteria used were: level of automation, ease of use, safety, cost/kg of material, hardware cost over and above that of conventional MEX, emulation accuracy (considered simply as maximum material density) and retention of material. These were each derived from the PDS previously shown in Table 5.1.

Table 5.2: Pugh matrix considering the identified methods for mass property emulation in MEX product prototypes. The matrix is baselined to the variable infill method.

	Variable infill	Small, regular masses	Large, bespoke masses	Standard parts	Particulates	Fluids
Automation	0	-	-	-	-	-
Ease of use	0	-	-	-	-	-
Safety	0	0	0	0	-	0
Cost/kg	0	-	-	+	0	+
Hardware cost	0	-	-	+	-	-
Emulation accuracy (Material Density)	0	+	+	0	+	-
Retention	0	-	-	0	-	-
Total	0	-4	-4	0	-4	-4

Level of automation referred to the ability of the process to act without outside influence or effort. Here, a high level of automation is preferred to reduce design fixation, as previously discussed. Subtly different, ease of use refers to the level of expertise and knowledge that a user must have to carry out the process successfully. Ensuring the method is easy to use will allow a wider range of audience to use the method. This also fits into the safety criteria, with high levels of automation and easy to use processes often lending themselves to improved safety. However, other effects - such as the safety of the material used and other required fabrication methods - will also be considered within this.

The hardware cost and cost of material per kg both factor into the viability of the method considered, with design fixation linked to the cost of fabrication. Emulation accuracy and retention are linked to the performance of the prototype (P1) and are directly linked to the performance of the method.

The scores presented in Table 5.2 were based on assessment presented throughout the proceeding sections.

5.4.1 Lumped Masses

The first identified concept was the use of lumped (i.e. as-one) masses that are contained within the MEX prototype. Within this, two sub-methods were further identified.

The first uses small, regular structures throughout a cell-based internal structure. To do this, the product prototype internal volume has a regular mesh generated over it that relate to the form of masses that have previously been manufactured (or must be manufactured before prototype fabrication). These masses may then be systematically placed within the internal volume, based on a pre-process optimisation, to emulate the required mass properties. This may be automated through a “pick-and-place” gantry or robot system.

Alternatively, fewer, larger structures may be used to fill voids within the internal structure. This is achieved through identification of a shape (or shapes) of a known material, such that mass properties may be emulated. The required shapes are then fabricated or supplied before being inserted within the part. This insertion may happen within the MEX process or as a post-processing step. Bespoke or standard parts may be used.

The application of lumped masses would theoretically allow the use of any material that is solid at room temperature (or the operational temperature of the prototype, if different). The density limit is the largest of the three concepts proposed and, therefore, the theoretical emulation accuracy is the best of the three approaches.

The use of many regular, small masses offers potential advantages over the use of larger masses, for example: regularity of mass reduces fabrication costs, automation may be easier to integrate and support generation is more straight-forward. However, several disadvantages also exist, including:

- The cell sizes that could be used may be limited by the form of the lumped masses
- The fabrication of masses may be expensive, especially if requiring tight tolerances
- The containment of the lumped masses may be challenging, requiring tight tolerances
- The placement of lumped masses in cells would require a significant alteration to the MEX process, with the use of a nozzle not possible and manual intervention likely to be time consuming.

To enable the use of this method, an automated solution is likely required – due to the number of masses that would need to be placed. To do this, gantry or robotic pick-and-place systems may be used. Ideally, the same movement system as the MEX process would be used – potentially using a second tool head. At the time of writing, the author was not aware of such a system existing (combining both MEX and pick-and-place capability) and so the hardware would therefore have to be developed. For potential users, this adds complication and expense.

The use of larger masses may alleviate the need for an automated system, as manual intervention should be less time consuming. However, if an automated solution were required it is likely to be more complex. Principally, this was because the masses would be of varying geometry. As such, it is unlikely that the MEX movement system could be used in this instance without significant modification. Alternatively, large, uniform masses may be used. This would reduce the overhead of manual placement - and make automated placement less time consuming - but would reduce the precision that could be achieved in some instances. In other instances, the masses may not fit within the prototype form. For this reason, this method was not considered in depth.

The lumped mass approach may also suffer from retention issues – where the inserted mass may move within the prototype volume. This is because of the tolerances involved within a nominal MEX process leading to small gaps being present around these masses. Further, in-

process insertion will mean that space must be left between the part and deposition head, to avoid collisions. Adhesive may be used to improve this, though this adds further complication and another failure point. This is a disadvantage of both lumped mass methods.

One option to overcome the retention issues, is to use standard parts, e.g. screws, nuts, washers, amongst others. This could be done in-process but would likely be easier to integrate as a post-process. Through fabricating threads as part of the MEX process, fasteners could then be incorporated, held in-place through the load applied to the thread. Although changes in assemblies could affect the emulation result, these were thought to be small. In addition, the use of standard parts would potentially save on the use of expensive, bespoke masses.

One of the key disadvantages of using fasteners is the reduction in potential emulation accuracy (relative to the use of free-form masses) due to limited form and material options. This is further complicated when accuracy of thread fabrication is considered, likely limiting users to larger fasteners.

Another is consideration of allowable orientations. An example is shown in Figure 5.1, where the orientation of a bolt would mean that post-process insertion is impossible and in-process insertion would lead to collisions with the deposition head. Instead, the mass is broken down into a nut and threaded bar, so that material may be deposited around the nut before the bar is inserted. This allows a similar assembly to be included but increases the complexity of fabrication. Further, tool clearances must be considered, which may impact the exterior of the prototype.

To summarise, the use of lumped masses, as small, regular masses, large bespoke masses or as standard parts, offers the potential for accurate mass property emulation. However, there are complications around fabrication and assembly that negatively impact ease of use and costs. Each of these methods will be considered as part of the concept selection.

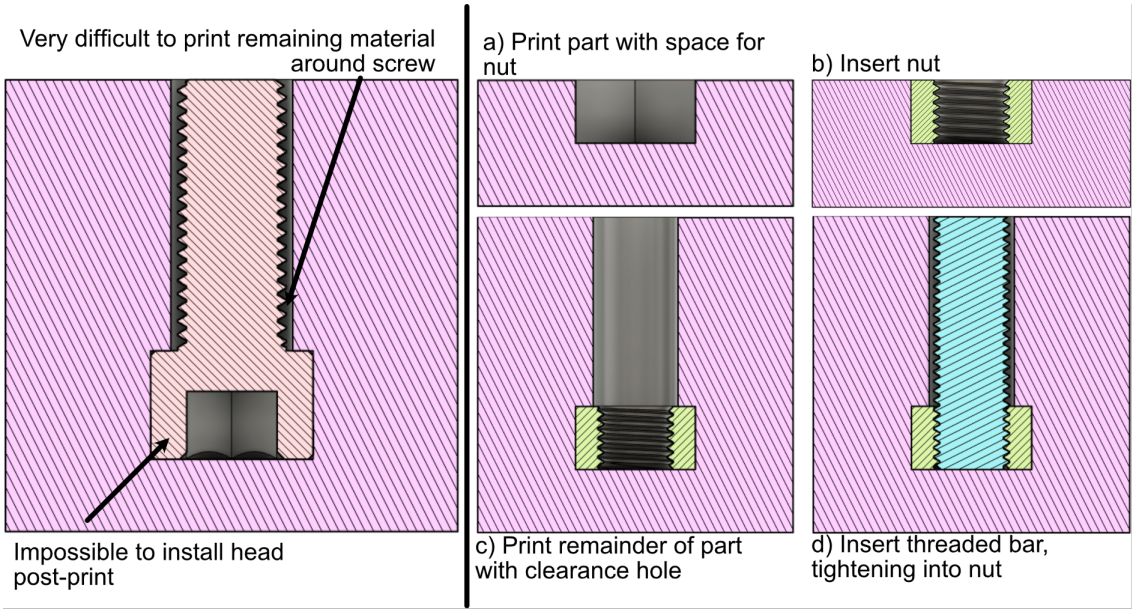

Figure 5.1: Demonstration of complications in integrating lumped masses showing how the lumped masses may need to be broken up. In the example, a bolt is split into a nut and threaded rod.

5.4.2 Particulates and Fluids

The use of particulates and fluids was the second concept approach to be considered. This method uses small pieces of solid material or fluids to fill voids within the prototype internal volume. For example, iron filings, pellets or water may be used.

It should be noted that a similar approach was used in the user study from Chapter 4 (and [25]). However, this was done to change mass properties, not target specific properties. As such, the accuracy of material insertion was less critical; changing the priorities of the process. Further, the addition of the particulates (iron filings and lead pellets) was completed manually. Although appropriate for the one-off study, this is not thought suitable for long-term use or industry uptake.

Further, retention of the medium within the internal volume is complex. For the work previously described [25], super glue was added to the top layer of the particulate and allowed to set before printing resumed. This was to ensure that the material would not move within the prototype post-fabrication, and therefore not change the mass properties that are experienced

by the user. Although this worked in some instances, in at least one example there is a clear audible rattling of material within the internal volume. For this reason, it is unlikely this could be relied upon for future work. Further, there were several examples where the MEX fabrication suffered from the inclusion of the particulates – Figure 5.2 shows an example of this. The use of fluids would, clearly, make retention more challenging still. Although the MEX fabrication should be watertight, the fluid would have to be under pressure to not shift within the sealed print. This would require the use of extra hardware, complicating the process and increase costs.

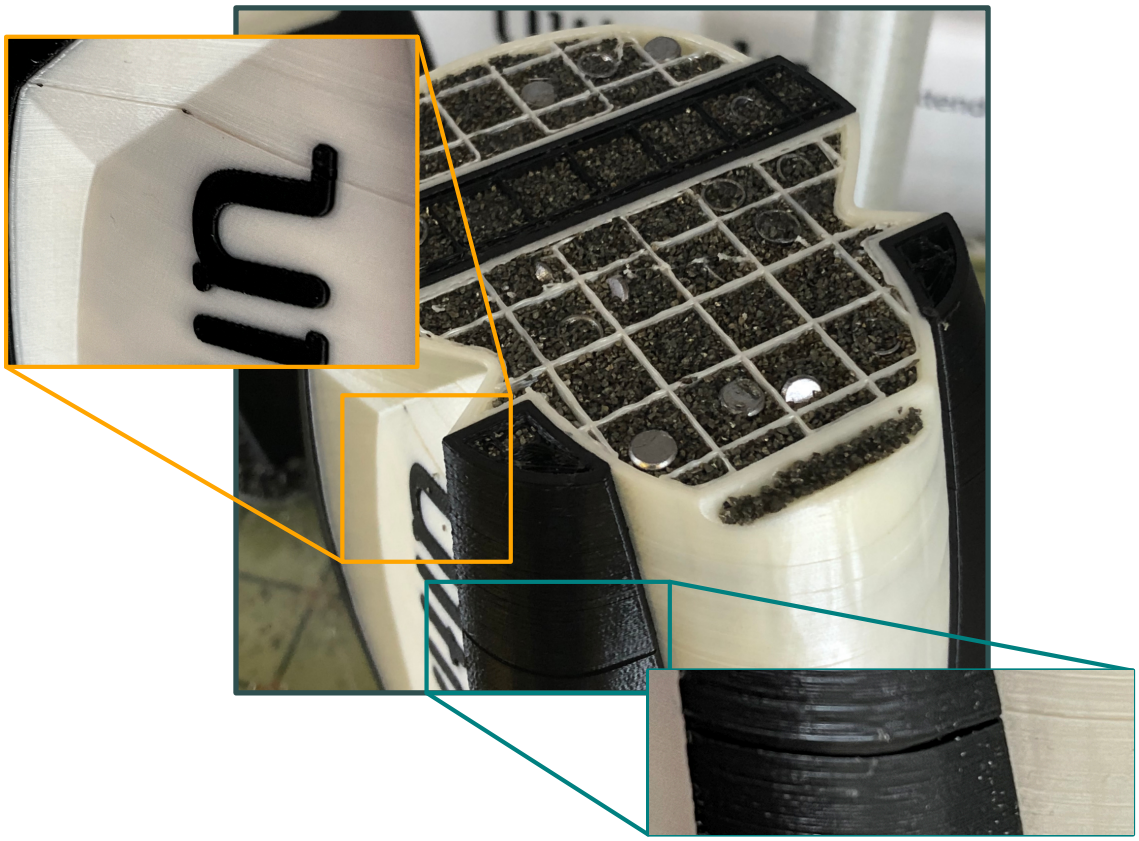

Figure 5.2: Example in-process fabrication using particulates. The highlighted regions exhibit MEX quality issues due to particulates getting trapped on the print path between layers.

The potential mass property emulation accuracy would likely be worse too, for commonly available particulates and fluids, than for lumped masses. This is because very high-density materials, such as Tungsten, would not be routinely available. However, for most consumer goods this was not thought to be an issue, with the mass envelope still being achievable.

There are aspects for which particulates and fluids offer a clear capability improvement over the use of lumped masses. Principally, they relate to the ability of medium to fill a provided volume without further design or modification. For the problem at hand, this means the internal volume voids and emulation material need not be the same shape. Therefore, costs can be reduced and the range of materials on hand can be reduced. Further, concern around inserted part orientation is no longer relevant.

5.4.3 Variable Infill

The variable infill approach uses the normal MEX deposition head and movement system to deposit material within the product's internal volume. This can be done using the normal print material or, for machines that support it, using a secondary print material. If a multi-material set up is used, a higher-density material may be used alongside the standard thermoplastic to improve emulation accuracy.

To enable the variable infill approach to work the product internal volume would need to be divided into cells, with each cell then having a definition. This was the preferred method of mass distribution as the underlying support structure may be simplified. From there, cells can be variably filled with material to suit.

The process will be fully automated – with sufficient modification to the pre-process computational workflow – and should require little to no further expertise from a user. Further, the post-processing should not change. There therefore appears to be several advantages to using the variable infill approach.

There are, however, downsides to the variable infill approach. The most significant is the maximum material density available for emulation. At the time the work was complete it was found that the most widely available high-density MEX filaments were metal-infused PLA, such as the RS Components copper-fill filament [183]. This filament contains ~80% copper and has a material density of 3.41 g/cc, compared to a density of roughly ~7.85 g/cc for steel [184]. As such, it was important to ensure that the mass of a range of consumer goods could be achieved.

If a hand drill, laser pointer and games controller are considered, the mass could be achieved without issue through the use of the copper fill PLA and PLA. For example, an electric hand drill's mass can be achieved using a PLA shell and any infill material with a density greater than 1.55 g/cc. The performance challenge will then be in emulating the CoM position. Further work would be needed to understand this in more depth.

Another concern is the cost – both economic and time – in printing the additional material. As discussed in Chapter 3, the fabrication time of a part in MEX is proportional to the volume of material being deposited (whilst keeping print parameters constant). For a given material set, the fabrication time can therefore be considered proportional to the mass of each material to be deposited. As it is hypothesised that most products will require an increased amount of material deposited – for the reasons given in Chapter 3 – the print time will therefore increase. Further, as more material is being used, print costs will also increase – with other operational costs also increasing. Without considering specific examples it is not possible to quantify the effect this would have. However, it is recognised that increases in time would be related specifically to the automated MEX process and the effect on design fixation would be small [53]. Therefore, the main issues with increasing cost and time relate to slower prototype iterations.

5.4.4 Selected Mass Property Emulation Concept

As was presented in Table 5.2, the variable infill and standard part methodologies were found to be the best, with scores of 0. All other methods scored -4 and were therefore disregarded. The differences between the two methods were that the variable infill methodology was better automated and easier to use, while the standard part method had lower associated costs. It may be possible to complete some level of controlled convergence at this stage to leverage the benefits of each and overcome the negatives. Although this was reviewed through a concept generation exercise, the generated concepts did not solve the issues around poor automation or ease of use and were therefore not considered further. The most promising of these was the use of lumped masses and variable infill, with this offering the potential of reducing fabri-

cation time whilst retaining the precision of emulation from a pure variable infill methodology. This was not taken further as this method still required the use of bespoke masses which were deemed outside of the scope of many prototyping workflows (and thereby this work).

Instead, the higher costs of the variable infill method were considered. The hardware costs were examined first. The main reason for the increase was because of the requirement for a MEX machine that could print in multiple materials – assuming the use of a secondary higher-density material. Although this was accurate, many modern machines are fitted with multiple nozzles as standard (e.g. Ultimaker S3 [149]). Further, for the volume of material likely to be used, the increase in material costs would likely be small. These negatives were deemed less significant than the challenges with automation and ease of use for the standard part method.

Overall, the variable infill was chosen for further development and will be the focus of the work presented herein.

5.5 Method Set-up

To understand how the variable infill method might be applied, the method set-up was developed. This primarily involved investigation of how products would be interpreted – i.e. how the product would be virtually represented – and what the internal volume would be composed of.

5.5.1 Virtual Product Represenation

There are many methods through which product forms may be represented virtually. In CAD, for example, the most common method is B-Rep (Boundary Representation). This is where the product boundary is defined explicitly through mathematical equations and limits. For this reason, it is possible to modify complex features with ease through parametric modelling. However, most 3D printing toolchains use mesh formats such as STL.

This section reviews the current meshing practice in 3D printing workflows in more depth, before discussing what is required for a mass property emulation workflow. In addition, the method and software used for the remainder of this work are described.

Product Representation Current Practice

The STL mesh format – the current de facto standard 3D model file type for 3D printing – defines geometric forms through triangulation of surfaces. This allows for efficient storage of a part's form, although circular/round features may suffer from a reduction in accuracy or use many more elements for definition. An example of this is shown in Figure 5.3a. The OBJ file format is also used regularly and often interchangeably with STL.

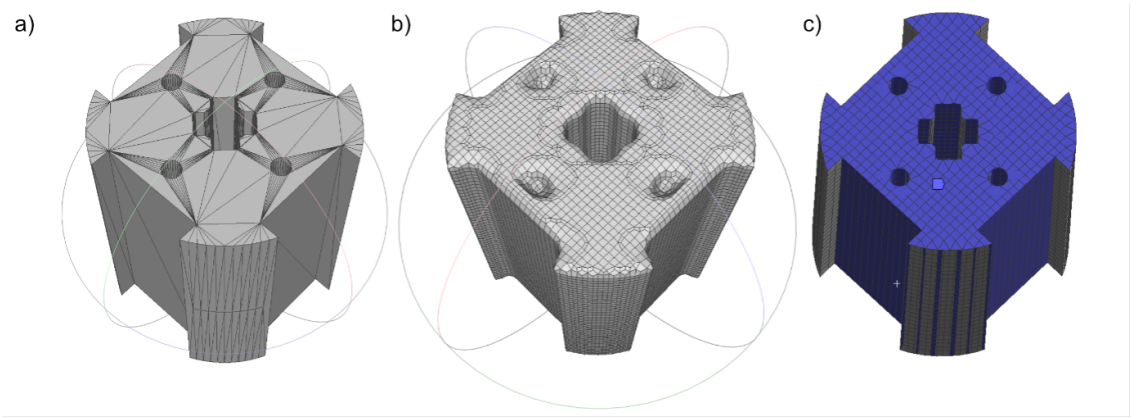

Figure 5.3: Different mesh representations for a motor rotor former. a) STL representation b) voxelised representation c) CHEXA representation. For reference, the distance across flats is 17 mm.

Two file formats that have seen more recent development are the Additive Manufacture Format (AMF) and 3D Manufacture Format (3MF). Both of these formats are based on XML and have been developed explicitly for additive manufacturing. Their main advantages over STL are their ability to store data on materials, colours and other related information [185]. The 3MF format is specified by the 3MF consortium, that includes members such as Autodesk, Microsoft, Prusa and 3D Systems [186].

It is viable for both the AMF and 3MF file formats to be used for the future methodology. This is because the XML format should allow information around the mass properties and cell-by-cell density data to be stored alongside the geometry.

Although the use of these file types would allow for an accurate representation of the geometric form, it is necessary to have a consistent, mesh-based definition of the volume - rather than just the surface. For this reason, finite volume meshing methods were considered (Voxelisation and Nastran standards).

Voxelisation

Voxelisation – the breaking up of a three-dimensional geometry into regular, cubic cells – may offer a solution to achieve a regular solid-body mesh that is required. This mesh style splits the body into equal volumes – generally cubic – that define the part form. An example is shown in Figure 5.3b.

Figure 5.3b shows that the definition of the holes and chamfers is significantly compromised. Although this was not thought likely to directly affect this work – as the shell could be defined separately using a separate mesh – it may make blending of the external shell with the interior volume more difficult. Finer meshes may be used to improve the geometric definition of the part and avoid this issue, but this comes at the expense of larger mesh file sizes and thereby increasing the computational overheads.

CHEXA Standard

The CHEXA standard defines finite volumes using 20 points and 6 sides. The standard allows a product form to be defined with improved accuracy over a voxelisation whilst ensuring cells have a near-equal volume (see Figure 5.3c). Further, it is possible to blend CHEXA elements with others (such as CTETRA that are defined with 4 triangular sides) for improved geometric accuracy. The regularity in cell definition is advantageous for the method as support structure generation is more consistent (and thereby efficient). In addition, slicing for AM is easier due to cells having regular cross-sections parallel to the slice planes.

Within this work, alternative elements are not used to improve geometric accuracy. This is because it was unnecessary for demonstrating method success. Physical fabrication and validation – seen in Chapter 8 – instead used STL files for the shell definitions (with required offsets to improve exterior, geometric accuracy). A future tool chain should be able to blend cell types or use an alternative mesh definition to improve this accuracy. More information is provided on this in Chapter 8.

To generate the CHEXA mesh, Ansys Mechanical Student 2020/21 was used. This meant that the mesh could not be exported directly due to limitations around the number of nodes that could be handled by this version of the software. To overcome this limitation, the mesh was written to a “Nastran input file” by Ansys that could be read as regular text (to aid import into Python). For future work, it may be possible to use alternative software packages, with CHEXA standards openly documented and used as part of the Nastran standard, or to use binary files that can be interpreted by a computer package to reduce file size.

5.5.2 Cell Composition

Once a finite volume mesh-based method had been decided upon, it was necessary to consider what compositions a cell may take. Principally, this was around whether this should be a continuous distribution or a number of discrete options.

Theoretically, it is possible for a cell to have a composition anywhere between and including 0% relative infill and 100% relative infill. Further, if multiple materials are used, the range can be extended (relative to the 100% infill baseline material) by depositing material in a higher density secondary material as previously discussed. However, there are several factors that may stop this from being achievable, including:

1. The existence of a minimum deposition volume, proportional to nozzle size,
2. The need to fully support cells with high-density, and
3. The large time investment needed to generate unique cell infill structures.

The use of fixed nozzle sizes means, in practice, a minimum deposition volume exists proportional to the nozzle size. When this is considered in conjunction with the cell size, it is possible to calculate the minimum relative deposition volume. This means that the space has changed to have a discrete 0% infill option and continuous composition option between the minimum and 100% infill for each material. Further limitations may be dictated by the use of a discrete step movement system (led by the use of stepper motors in most MEX control axes) but these are likely to be less significant than that associated with nozzle size.

It is important that each cell is supported such that deposition is retained in position during the fabrication process (and thereafter). Therefore, a secondary limitation is placed on the minimum deposition that is linked to the densest composition a cell may take, the cell size and the nozzle size. Keeping this support structure consistent throughout the volume should improve numerical emulation and slicing efficiency but may slow the fabrication process and reduce the emulation accuracy.

The generation of infill structures cell-by-cell would be time consuming and inefficient as part of the slicing process. This would be further complicated by the need to blend cells into one another to ensure material is properly deposited. For this reason, discrete composition options would be beneficial as look-up tables could instead be used, translating predefined Gcode for each cell rather than generating it from scratch.

For these reasons, a review of whether a discrete or continuous density distribution should be used was undertaken. It found that this should be limited to a binary selection of a minimum cell structure (to provide support) in the lower density material and a solid infill in the higher density material.

The first stage to identify this was to recognise that, at some stage in the optimisation process, it was likely that a non-deterministic generation of cellwise compositions would need to be completed. Due to the large number of cells required to accurately model a volume, it would be advantageous to adopt an approach that would allow the largest proportion of the solution space to be explored as possible. It was found that the most efficient approach was to use a binary cell composition system (see Appendix C). These binary cell compositions related to:

1. The minimum viable structure deposited in the lower density material that would enable support of the other cell structures.
2. A solid structure that completely fills the cell in the higher density material.

For the remainder of the work detailed within this thesis, these binary composition options will be used.

5.5.3 Hardware Changes

As discussed previously, to enable the success of the variable infill method, a secondary, higher-density material should be used. This would allow larger masses to be achieved within the same volume and should allow for a larger CoM envelope. The MEX machine will therefore need to be capable of printing two-materials, or regular material changes will be required. As the latter would be time consuming for a user, a multi-material printer is recommended. As these are reasonably common with modern hardware, it was not considered a limiting factor.

Secondary material options were also considered, with it considered useful to use higher-density secondary materials. Along with the copper-fill PLA filament discussed earlier, other filaments were also found on the market. For example, iron-fill and stainless-steel fill PLA were available with densities of 1.85 and 2.3 g/cc [187, 188]. Additionally, BASF produce a stainless-steel filament, intended for the production of solid metal parts, after sintering [189]. Although this material has a higher-density than the alternatives – 4.99 g/cc – acquisition costs were significantly more. The use of the BASF material was therefore deemed unsuitable and use of copper-fill – that was available, affordable and had the highest material density of the other filaments – was assumed.

For all of the potential secondary materials identified, abrasion was recognised as a concern. This is because the metal particles in the filament are harder than the brass nozzles often employed on MEX machines. As such, the nozzle is worn down as filament passes through it, widening the outlet and causing the output stream to become less concentric and/or increase in size. To avoid this, hardened nozzles may be used such as the 3D Solex Hardcore

Everlast [190], which features a ruby tip. This reduces the severity of the abrasion and thus ensures a more consistent output. Although this comes at increased cost to a user, the use of hardened nozzles is not uncommon and the costs were not thought limiting.

5.6 Chapter Summary

The chapter has presented the selection process for a mass property emulation method to answer the RQ "what is the most appropriate method for emulating mass properties in MEX prototypes?".. This has highlighted that the use of a variable infill methodology is preferred. Early considerations have further taken place around the method, identifying that small hardware changes will be required, and initialisation of the software toolchain has been understood.

Chapter 6
Mass Property Emulation Methodology

6.1 Chapter Overview

Having identified a suitable method for mass property emulation, development work was undertaken to work towards developing an answer for RQs 2 and 3. These were; "How can mass properties be emulated in MEX prototypes?" and "How can mass property emulation be embedded into the MEX workflow?".

The work starts by identifying a suitable optimisation strategy for locating infill for mass property emulation in MEX parts. This is done through investigation of local and global methods, non-deterministic optimisation and direct evaluation, before settling on a directed optimisation method. This method uses solution space knowledge – principally how internal volume CoM will likely move – to target the optimisation process whilst being relatively unaffected by the input geometry.

From here, the chapter applies the developed process to a primitive form to assess applicability. By doing this, a set of values for the controlling parameters is found. Further, their individual effects are investigated to allow for application to more realistic example forms. The chapter concludes with presentation of these parameter values in Table 6.2.

Parts of the work detailed within this chapter are published in the author's paper "Improving Feel in 3D Printed Prototypes: A Numeric Methodology for Controlling Mass Properties Using Infill Structures" (in review) [191].

6.2 Optimisation Methods

Once the definition of geometric form and binary cell compositions were decided upon (see Section 5.5), it was necessary to consider methods for identifying where infill should be located. At its core, this required the use of an optimisation method, where minimisation of the difference between the as designed and MEX output mass properties is targeted (in accordance with Section 4.7 and Equation 4.10). A variety of methods were investigated – initially focussed on considering each cell as a variable before a volume-wide approach was adopted – and discussed within this section.

6.2.1 Local Cell Based Optimisation

Local optimisation methods considering cells as variables, although theoretically the most efficient at finding minima, were not investigated in great depth. Principally, this was because of the potential for geometry to cause the method to target localised minima, rather than the global minimum. An example of a form that may cause this is shown in Figure 6.1. Here, the method would likely find that the move along the X axis would cause the emulated CoM to move toward face A, away from the target CoM. This is because there is a region where the method would be unable to place as much material away from face A, whilst being positioned as directed along the X axis. The method would then stop searching along this axis, not discovering that if the axis is searched completely then geometry would be found that would allow the CoM to move away from face A, back towards the target. It may be possible to overcome this through careful control of the optimisation algorithm, but this would require expert knowledge from a potential user. Therefore, local optimisation was not deemed appropriate for the application.

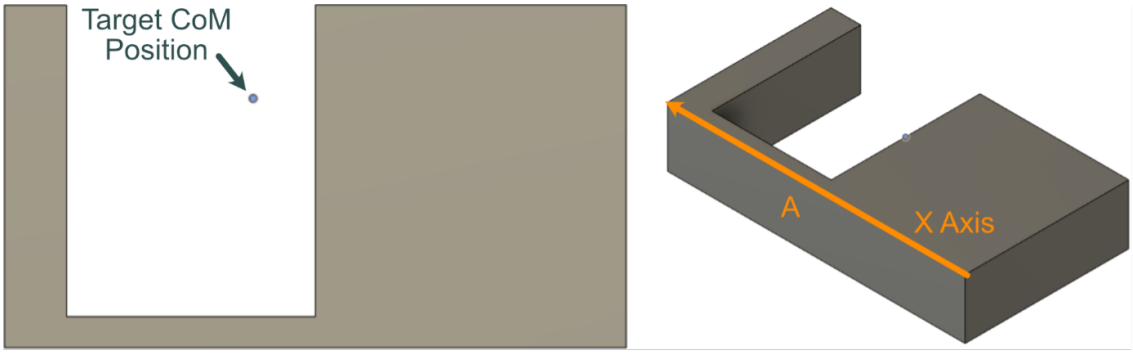

Figure 6.1: Example geometry which for local optimisation would struggle.

6.2.2 Global Cell Based Optimisation

Initial investigations used global optimisation methods (such as Monte Carlo Optimisation (MCO), particle swarm and genetic algorithm methods [192]) to overcome the issues associated with local methods. These methods considered individual cells as dimensions. Although

these methods could identify how the infill composition should change to target mass and CoM properties for simple problems with few cells, they quickly became inefficient for larger problems. This is a widely stated, proven and discussed in literature (for example [193, 194]).

These inefficiencies were exaggerated by the nature of the problem. For the emulation problem discussed here, each of these global optimisation methods are initiated by randomly generating a starting solution over the solution space (here, randomly generating a cellwise infill composition). Due to the large number of cells used to adequately define geometry and provide sufficient precision for a useful result to be generated, the calculated CoM will generally lie relatively near the GC. This is known as the central limit theorem, discussed in more detail in Appendix C. For many applications - especially those the method is likely most valuable for - it is unlikely the CoM will be relatively close to the GC. As such, a method is required that allows adequate exploration of the design space with a large number of cells (to ensure sufficient geometric accuracy is retained).

6.2.3 Direct Approach

To overcome the effects of the central limit theorem, a new approach was developed that uses knowledge of the required CoM position to target possible solutions. At its core, this method moved away from considering each cell as a variable. Instead, the problem was broken up and considered the three geometric axes and total mass as the four optimisation dimensions.

Direct Evaluation

To enable the desired CoM position to be achieved, the use of a point mass at a calculated distance from the GC would be preferable (in most instances). However, it is not possible to practically incorporate a point mass. Further, this method would not work if the point mass were to be needed outside of the contained volume of the part. Therefore, the investigation turned to a method that allocated the binary cell definitions around the required CoM target

position, providing the required volume for mass to be located. Figure 6.2 shows how this may be done for a two-dimensional analogue, with mass being placed symmetrically - when possible - around the target CoM position.

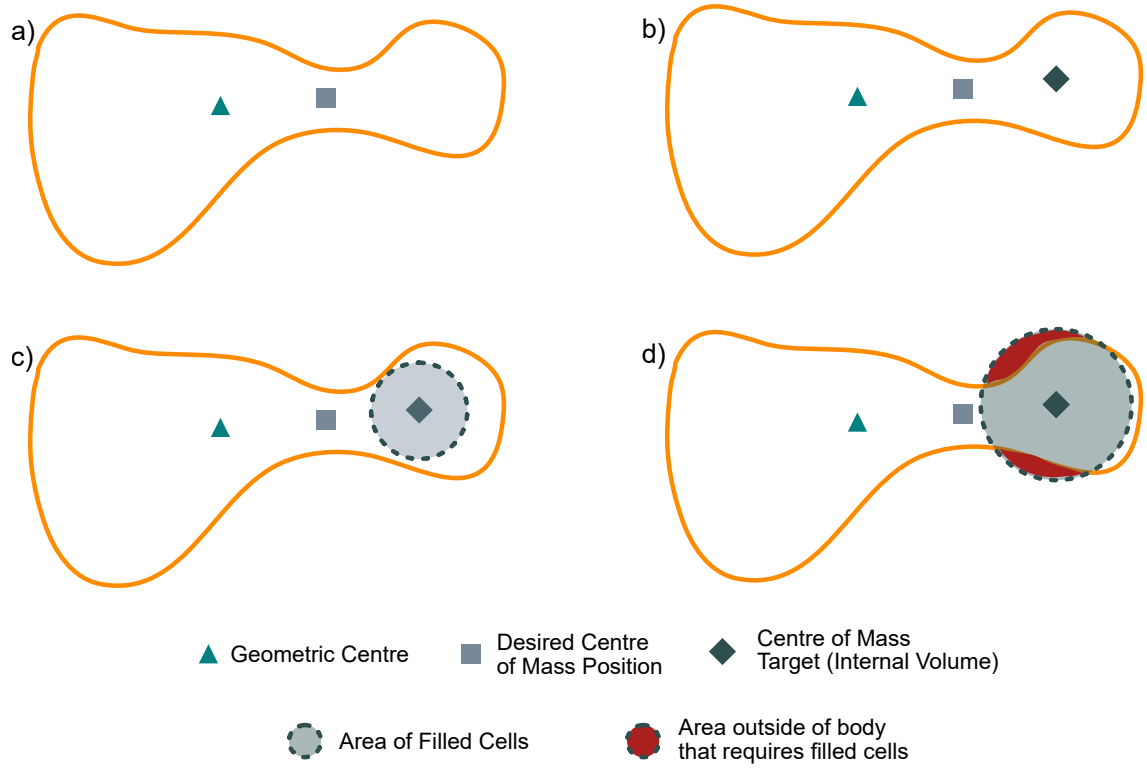

Figure 6.2: The directed evaluation process. a) The geometric centre and desired centre of mass position are identified. b) The internal volume centre of mass target is calculated based on the mass target and desired centre of mass offset from the geometric centre. c) High-density cells are placed around the internal volume center of mass target position to achieve the mass property targets. d) Issues arise when cells need to be placed outside of the internal volume geometry, causing assymetry and a reduction in contained mass. This can cause the evaluated mass properties to be incorrect.

Figure 6.2a identifies the location of the GC (▲) and desired CoM (■) position within the product volume. From this information, it is possible to identify where the internal volume CoM (◆) target should be (to balance the effective mass at the GC(▲)), as in Figure 6.2b. Cells adjacent may then be assigned a high-density composition around this target CoM (◆) (Figure 6.2c). Issues arise, however, when it is not possible to properly balance the number of high-density and low-density cells around this target CoM position (◆) to achieve the mass target (Figure 6.2d). This would cause the mass and/or CoM position (■), depending on how the issue was handled, to be generated incorrectly.

To overcome this issue, whilst retaining direct evaluation of the solution, the code would need to have an initial understanding of the geometry, likely creating a network that understood the effect of individual cells. However, for the scale of problem likely being considered, this was hypothesised to involve understanding the value of tens of thousands of cells with millions of potential combinations. As such, this is a computationally expensive approach and not appropriate for the problem.

Direct Optimisation

To overcome the computational expense of direct evaluation, an optimisation approach is proposed that is independent of the geometry being considered and computationally efficient (relative to direct evaluation). Figure 6.3 graphically shows how this method works using a two-dimensional analogue.

The directed optimisation method has six primary steps. The first is the initialisation phase where the desired CoM position (■) - e.g. of the as-designed product - and GC (▲) are identified (Figure 6.3a). This then allows an initial estimation for the internal volume CoM position (◆) to be found (Figure 6.3b) that would allow the desired CoM to be achieved. This is done using knowledge of the shell and potential cell composition – i.e. cell high and low densities.

Once the internal volume CoM target (◆) is found, an exponential probability distribution may be generated (◌), centred around this point (Figure 6.3c). An exponential probability distribution is used to try and concentrate the mass around the target point, whilst allowing the method to overcome irregularities in geometry. This exponential distribution is defined by:

$$P = e^{(-r/\beta)} \tag{6.1}$$

Where P is the probability of a cell having a high-density, r is the distance of the cell centre from the target internal volume and β is the scale parameter that defines the shape (or gradient) of the distribution. For this work, the value of β effectively determines the average

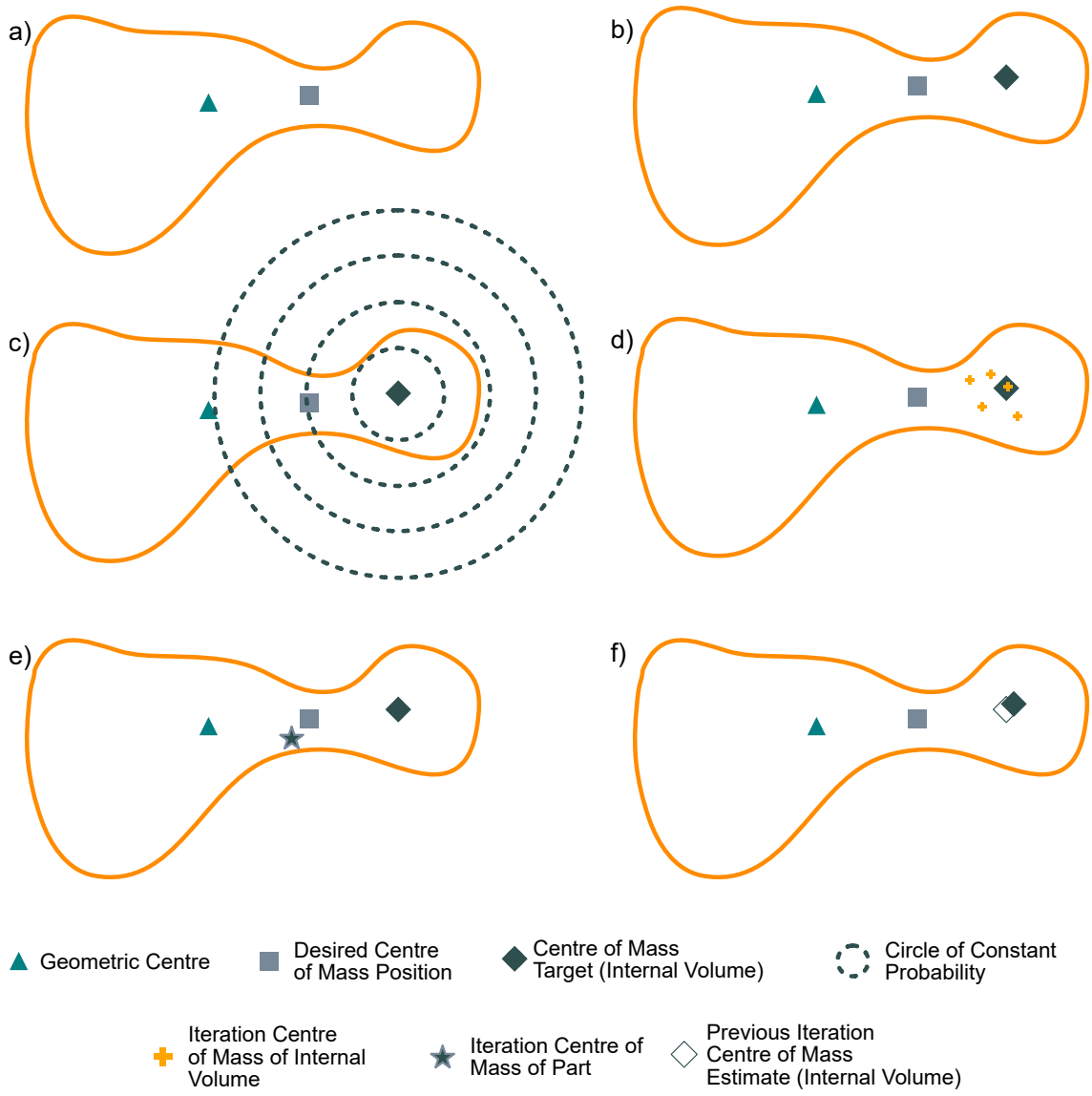

Figure 6.3: The directed optimisation process, showing each step. a) The geometric centre and desired centre of mass position. b) calculation of initial target centre of mass internal volume position, found through mass balance. c) generation of exponential probability distribution, with rings showing rings of constant probability. d) calculated potential centre of mass positions using the centre of mass estimate and exponential distribution. e) overall part centre of mass position found. f) target centre of mass position updated, repeat using new point (from c).

part mass returned by the method. The resulting probability distribution is a continuous, exponential probability distribution. There are three principal complications in the application of this (or any other probability function) to the problem:

- The binary nature of the cell compositions used.
- The use of discrete cells in a continuous geometric space.
- The application to potentially irregular forms.

As discussed in Section 5.5.2, it has been found that the most appropriate cell composition was binary. Cell compositions therefore refer to either the minimum cell structure to support the surrounding cells or a solid infill. As such, there is a step change in cell mass - and therefore effect on the evaluation - between the two compositions. This causes step changes in part mass with cells switching between compositions.

The effect of binary cell compositions is coupled with the use of discrete cells. The application of a continuous probability distribution with a discrete cell formulation causes the effect of changing β to have a discrete effect on the method evaluation. Additionally, for irregular forms where it is unlikely the geometry is perfectly concentric with the target CoM position, this is complicated by asymmetry in how the distribution is applied.

A bisection search method is used to find a suitable value of β such that the three complications are considered when shaping the distribution to find the desired mass. This search method identifies a β value for which the error in the number of high-density cells is less than a specified tolerance. This is discussed in greater depth in Section 6.3.2.

From here, it is possible to generate solutions using the target internal volume CoM (◆) and exponential probability distribution pairing (Figure 6.3d). This is done through the generation of random numbers for each cell (between 0 and 1, using a uniform distribution) and comparing this to the probability of each cell having a high-density. The cell is assumed to have a higher-density if the random number is smaller than the probability value for that cell (from Equation 6.1).

Due to the non-deterministic nature of this process, several iterations are undertaken (discussed in Section 6.3.1). Using these iterations (✚), an actual, equivalent internal volume CoM for the combination can be found through averaging these points. This information is then used to find a part-level CoM position (★) (Figure 6.3e) which is compared to the as-designed.

The target internal volume CoM is then updated (◇ -> ◆) (Figure 6.3f) – and the process repeats from the exponential distribution generation stage (Figure 6.3c) – or an exit condition is triggered.

The exit conditions for the method relate to absolute accuracy, number of iterations or change in CoM positional error between iterations. Once a target internal volume CoM is settled upon, a final set of results are iteratively generated using MCO. MCO was chosen as the optimisation method due to its robustness, simplicity and suitable computational performance. It is recognised that alternative methods (such as particle swarm optimisation) may provide scope for improvement in future work, but this was not thought necessary for the proof-of-concept solution as the hypothesised benefit related only to runtime.

The process has been developed using Python 3.9+ as a standalone function (please see: https://github.com/hjfelton/mpemulaton), requiring inputs of the geometric form (as a mesh from Section 5.5.1), the as-designed mass properties, and the objective function multipliers – though these may also be calculated from the mass property input. Figure 6.4 graphically shows the flow through the code.

6.3 Process Baselining

Following the creation of the pre-process methodology and code, process baselining - development of understanding - was deemed necessary. To do this, a simple, primitive form was used – a cube. This cube was 50x50x50 mm with a mass of 125 g and CoM position offset from the GC by 2.5mm in each axis. The representative mesh, shown in Figure 6.5, was generated in Ansys using 46656 cells based on learning from initial method trials. This equated to each cell having an edge length of ~1.4 mm.

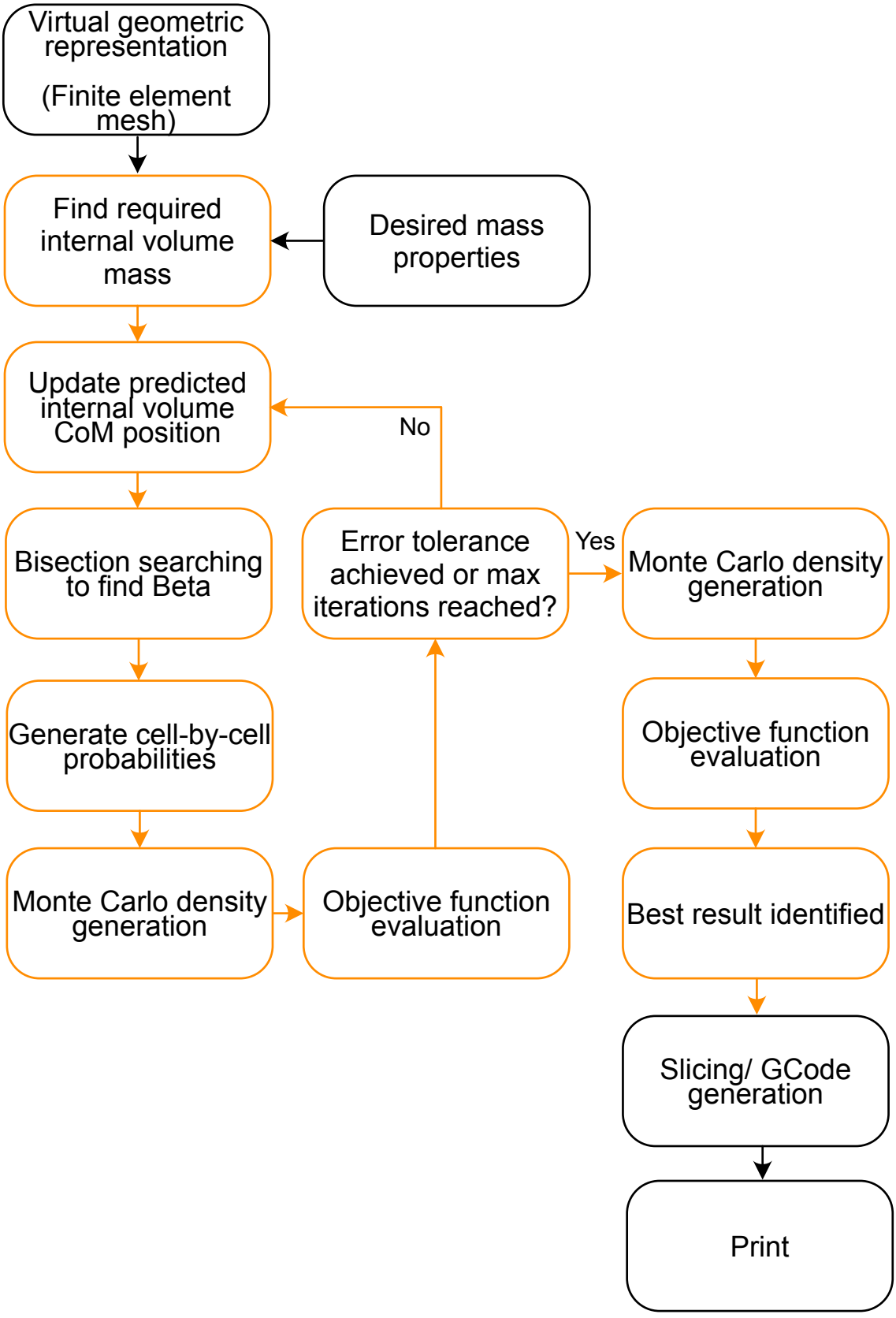

Figure 6.4: Flowchart for the code that completes the directed optimisation process.

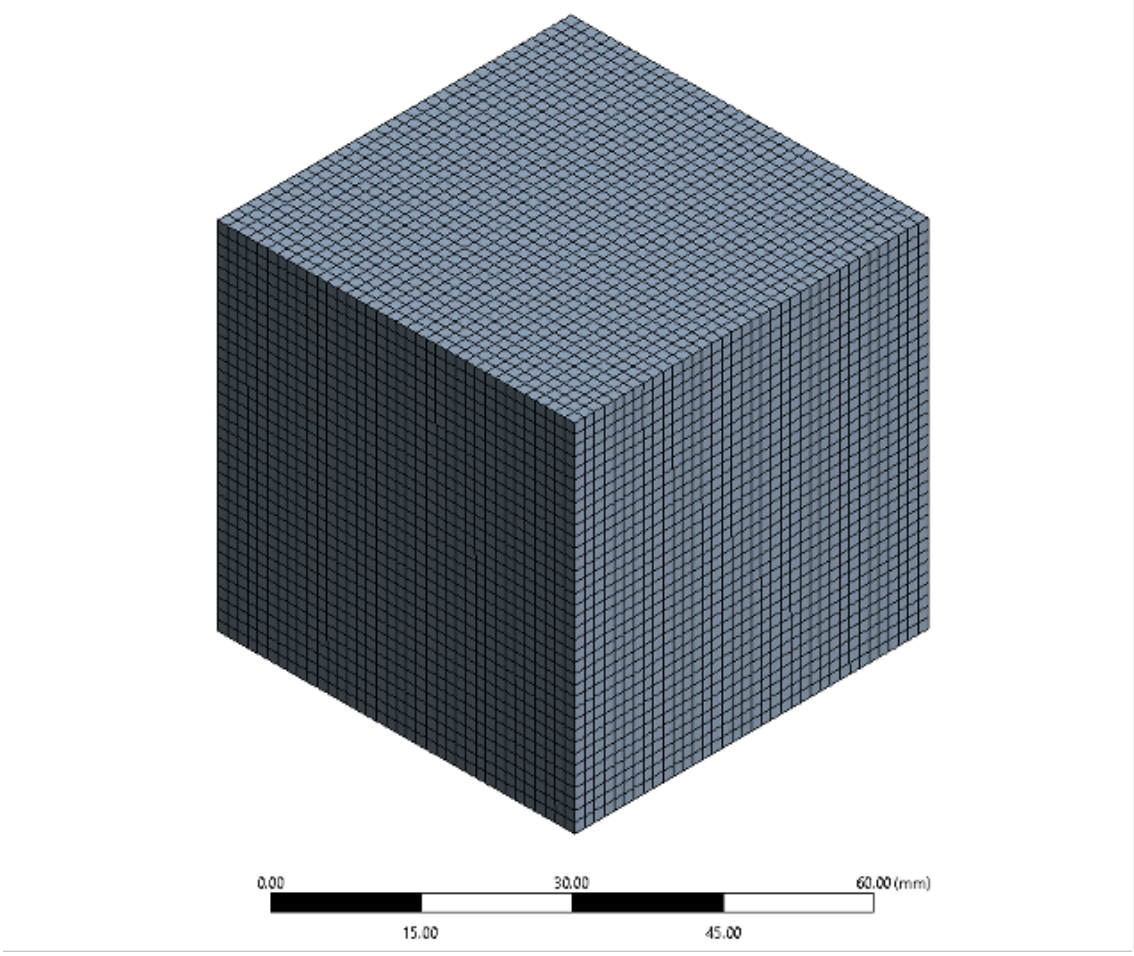

Figure 6.5: Meshed cube used for baselining the variable infill emulation method , with cell edge length of 1.4 mm.

It was recognised that the use of a primitive form may introduce errors that could not be identified during initial development. However, it was thought that the advantages the use of a primitive had outweighed these. Principally, the simplistic nature of the form and mass properties meant that errors in the underlying method and controlling mathematics could be identified and corrected at an early stage.

The aim of this work was to develop an initial set of baseline values for the controlling parameters that could then be applied to more specific problems. These parameters related to the control of the:

- Internal volume CoM searching,
- Probability distribution,
- Choice of materials,
- Internal structure,
- Cell size, and
- MCO.

It was recognised that each of these parameters effects were likely to be inter-related, with prior testing completed to develop an initial process understanding. In this work, although the absolute values where behaviour was observed changed, the individual parameter effects remained consistent over the design space. As such, the proceeding section discusses each control parameter individually.

6.3.1 Internal Volume Centre of Mass Searching

As previously discussed, find the internal volume CoM was an iterative process. This is controlled within the code with two key parameters. The first is the number of target internal volume CoM iterations are evaluated. The second is how many evaluations of these targets are completed within each evaluation - required due to the stochastic nature of the process.

Iterative searching was used to find the final internal volume CoM position that the probability distribution should be centered around. This has three independent exit conditions, any one of which would cause the method to end the search. These exit conditions related to when an acceptable CoM position error was achieved, when the maximum number of iterations was reached, and when the CoM position error between iterations was within an acceptable tolerance.

When the exit condition related to the number of allowable iterations, the parameter had a direct impact on the runtime – as expected. This can be seen in the right-hand axis of Figure 6.6. Analysis shows that the relationship is linear (as to be expected) with each iteration taking roughly 13.5 seconds.

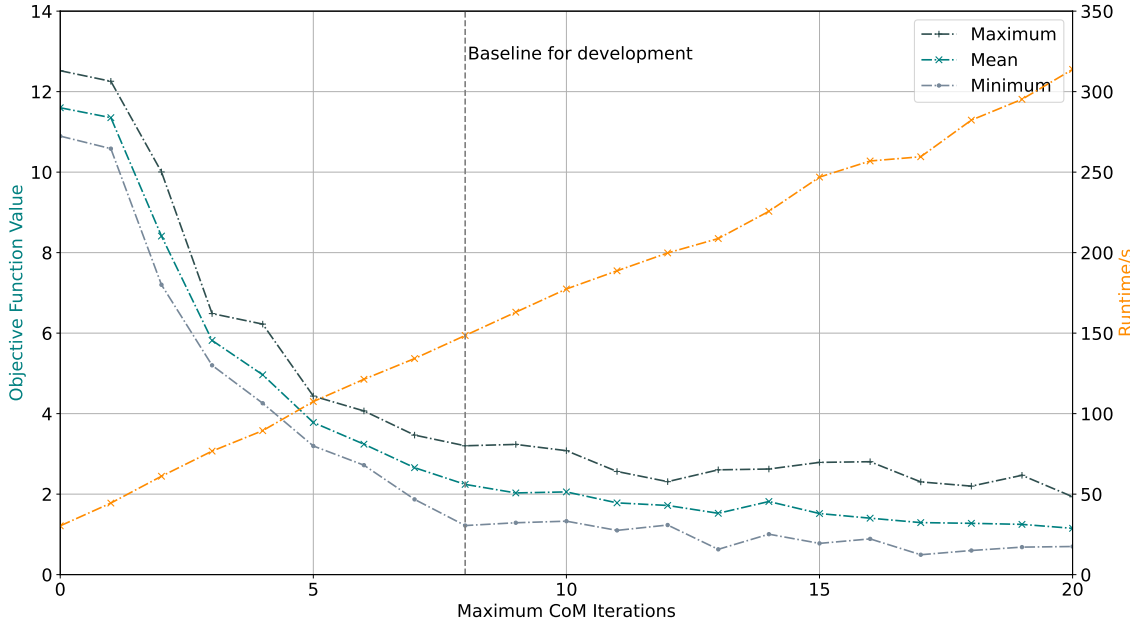

Figure 6.6: Relationship between the maximum number of CoM iterations, objective function value and runtime.

Figure 6.6 also demonstrates that the objective function (see Equation 4.10) value decreases (i.e. the error reduces) as the number of CoM search iterations increases. A compromise between runtime and model accuracy must therefore be found. It can be observed that the improvement per CoM search iteration reduces as the number of CoM iterations increases (i.e. there are diminishing returns). For this reason, it was decided that the compromise would be found as the improvement levels out (but runtime increases linearly). For the purposes of baselining the method, a maximum of 8 CoM iterations was decided upon as a baseline parameter value.

As the purposes of this work is to investigate the potential accuracy of the process, the allowable error (absolute and between iterations) is set to 0. In practice, this value would likely be increased depending on the desired performance.

For each CoM search iteration, the CoM was estimated through generation of cellwise probabilities. To do this, a probability distribution is applied over the volume (as presented in Section 6.2.3 and discussed further in Section 6.3.2). This allowed individual cell masses, and thereby volume wide mass properties, to be calculated. Due to the stochastic nature of the

process, it is possible for the result of the process to be variable. Multiple assessments are therefore completed and averaged. This allowed an actual internal volume CoM to be found before the target search CoM can be updated.

Figure 6.7 shows how the x-axis CoM position distribution (over 500 samples) changes with the number of iterations used to calculate the CoM. It can be seen that, at least for this example, the number of iterations is not clearly related to the distribution of CoM position. However, the author believed that this was likely affected by the primitive form used, with the symmetry allowing for more consistent results to be found. A compromise is found through using 5 generation iterations to provide a level of robustness that may be required for other geometries.

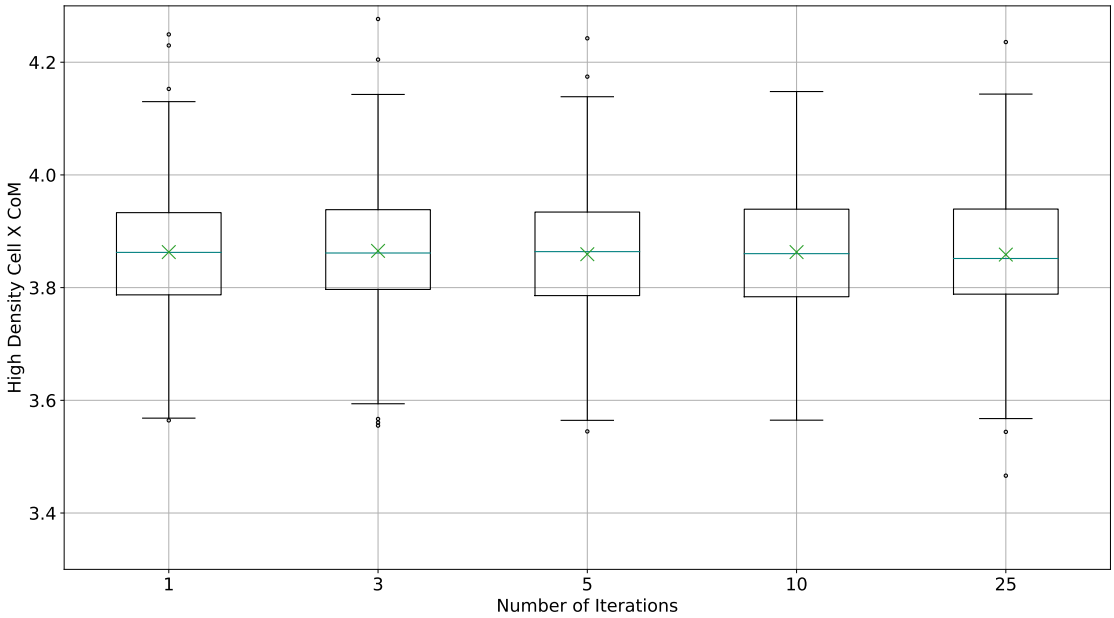

Figure 6.7: High density cell x-axis CoM position distribution for several iteration levels. The box represents the interquartile range (IQR), with the interior line the median. The whiskers represent 1.5 times the IQR, with the outliers marked. The means are shown as an “x”.

6.3.2 Probability Distribution

The cellwise densities are generated through the application of a probability distribution (see Equation 6.1) around the target CoM, as discussed previously. Using the scipy "minimize scalar" bounded (Brent) method, the solution space is explored as a tolerance to β. This method for root-finding uses inverse quadratic interpolation and secant and bisection methods to reliably but efficiently identify roots for a problem. The returned value for β evaluates a suitable approximation for the number of high-density cells within the internal volume that provides the required mass.

To control the search method, a β tolerance is specified. This is defined as the allowable difference (error) between the actual and required number of high-density cells, with this value used as the exit condition. As would be expected, the smaller the allowable tolerance, the longer the runtime of the method (as shown in Figure 6.8).

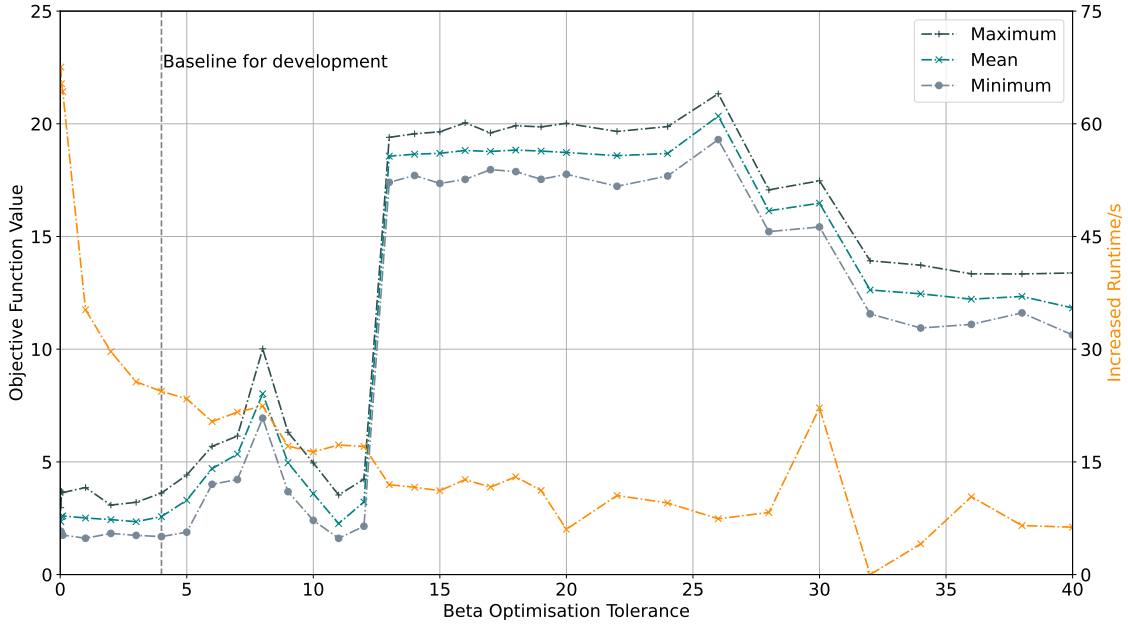

Figure 6.8: Beta tolerance against objective function value and runtime.

Figure 6.8 additionally demonstrates that the relationship between β and objective function value is less clear. Prior to considering the presented behaviours, the application of the probability function should be understood.

As a cell can be positioned at any distance from the target CoM (a function input), a continuous probability function is required. As such, the function provides probability values for a continuous distribution of inputs with no limit. In contrast (and as previously discussed), the process uses a discrete mesh. Changing β can therefore have a step-change on the objective function evaluation. Further, high-uniformity in meshes - such as in the cube - can mean that large clusters of cells are all affected simultaneously with changes in β. This exaggerates the observed stepping, with small differences in β potentially leading to large differences in the number of high-density cells generated. This is the direct cause of the step between β tolerance values of 12 and 13.

A further complication comes from the ability to return a β value that is associated with a smaller error between required and evaluated mass than limited by the β tolerance (as this is a limit not a target). This can therefore return better results at higher β tolerances than would otherwise be expected. This is the reason for the decrease in objective function value for β tolerances between 8 and 11 and the reduction in objective function value after β tolerances of 26.

The use of the primitive cubic form would exasperate the issues discussed. This is because of the regularity of form of the associated mesh, creating many clusters that cause significant changes in the number of cells affected in discrete steps. In contrast, a more complex shape may allow for smoother transitions due to irregularly spaced cells, caused by the mesh algorithm manipulating the mesh to suit the geometry. By doing this, each cell is affected by the function differently and, therefore, clusters are less likely to form from small input changes.

All this considered, it is possible to observe that the use of small β tolerances – in the presented data a tolerance of less than 5 – reduces the overall objective function value. For this reason, the baseline value for β tolerance is taken to be 4 for the remainder of this work. Smaller values of β were thought to more reliably control the emulation result, but came at significant runtime penalty.

It should be noted that for the purposes of the work, a range of β values between 1 and 1000 were investigated as bounds for the method. For edge case applications – particularly those where the internal CoM requires a large relative offset from the GC – the upper bound may need to be increased. Further, it may be possible to improve runtime by changing these bounds, but this will be dependent on application. Due to the efficiency of the Brent method for values relatively far from the root value, it was thought unlikely to have a significant effect. The range used was considered acceptable for the purposes of investigation.

6.3.3 Materials

Across all MEX fabrication, PLA is considered the defacto standard material for quality, cost, processing, and availability. For this reason, PLA is used throughout this work as the primary material considered. Within this section, work is completed that aims to understand how the material configuration used (i.e. PLA and a secondary print material) may affect the emulation result. To do this, secondary materials are considered according to the density of said material relative to PLA. Material Density Ratio (MDR) is used to refer to this metric.

It was generally considered feasible to print multiple materials due to the advent and wide availability of multi-material MEX machines. In many instances, these are now available at a consumer level – for example [149]. Therefore, it seemed reasonable that they would be available in a design office setting (as targeted by this work).

It was assumed that the majority of the applications for the method would require masses larger than that achieved by a nominal PLA only print (i.e. one with a thin shell and 20% infill). MDRs between 1 and 9 times that of PLA were considered. This range represented the use of PLA alone (1) and lead (9). MDRs less than 1 were not considered. There may be real world applications where this is not appropriate, but they were considered out of scope for this work. Extension to include these should be possible is appropriate materials are available, though it would also be possible to fill less of the internal volume to effectively decrease the average mass density across the volume.

The results of the study considering MDRs between 1 and 9 are shown in Figure 6.9. This shows that for MDRs up to ~2.75, the CoM components (averaged) dominate the mass result. This was expected, as mass cannot be localised effectively with lower density materials. The mass target can still be met as the total volume available is large enough to contain the required mass.

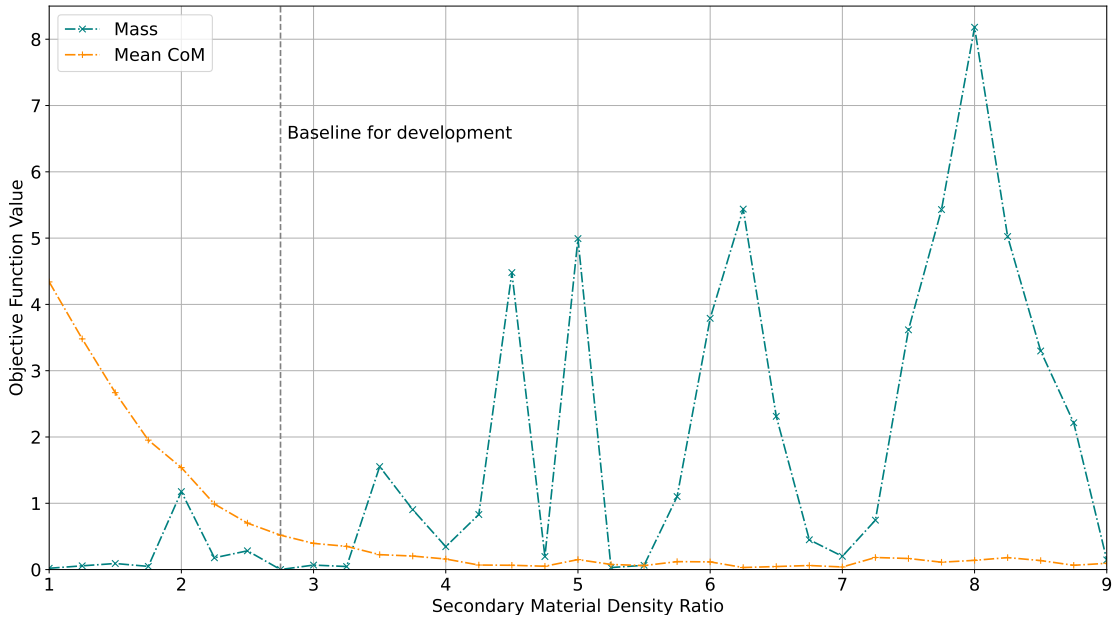

Figure 6.9: Objective function value, from mass and CoM error, for a range of material combinations. The secondary material density ratio is relative to PLA.

At an MDR of ~3, a consistent, minimum cost is reached. This minimum is achieved through a compromise being achieved between the maximum cell density and the number of high-density cells. Both factors have a direct impact on the emulation result. As previously stated, the maximum cell density must be large enough to allow mass to be centralised such that the volume-wide CoM can be moved from the GC. The number of high-density cells, however, is another important metric such that the stochastic nature of the process can be minimised (i.e. the effect of individual cells is small enough that variability from the stochastic process does not significantly affect the result). It should be noted that using a greater number of MCO iterations may also overcome some of these effects, but this comes with a runtime penalty.

For the remainder of this work, the secondary material is assumed to be a copper-fill PLA from RS Components [183]. This material was chosen as it provided an MDR close to the aforementioned optimum MDR of 3. Testing was completed to ensure that materials could be reliably printed together, with no issues observed. To reliably print metal-fill filaments, it is recommended that a hardened nozzle would be required. This was not thought to be a significant limitation, with many first- and third- party hardened nozzles available for printers such as the Prusa i3 and Ultimaker 3. Materials with a higher MDR may also be used, though there are generally less widely available.

6.3.4 Internal Structure

To ensure that the high-density cells are adequately supported, a supporting infill structure was needed. Although it may be possible for a simple homogenous infill composition to be used – as is already available in most commercial slicers – there are several potential issues. These are:

1. The infill pattern may not be evenly distributed throughout the cells within the product,
2. The infill density may need to be large to provide sufficient support to every cell, especially when using small cells, and
3. Print path planning complexity would increase when slicing, with variability in support causing differences in the starting point for a high-density cell, as well as the print directions, for each cell.

To understand what properties should be targeted when considering the minimum support structure, the effect of the relative minimum density of a cell on the emulation result were considered. The results from this consideration are presented in Figure 6.10. Within the figure, it is shown that objective function value increases with minimum relative cell density. It should be noted that, for the generation of this figure and for the remainder of this work, the relative minimum cell density was assumed to be directly related to the relative maximum cell density. This is because the high-density cell structure would be deposited around the minimum structure. This decision was taken to improve theoretical print times, slicing process efficiency and print quality by using a single material for the base deposition.

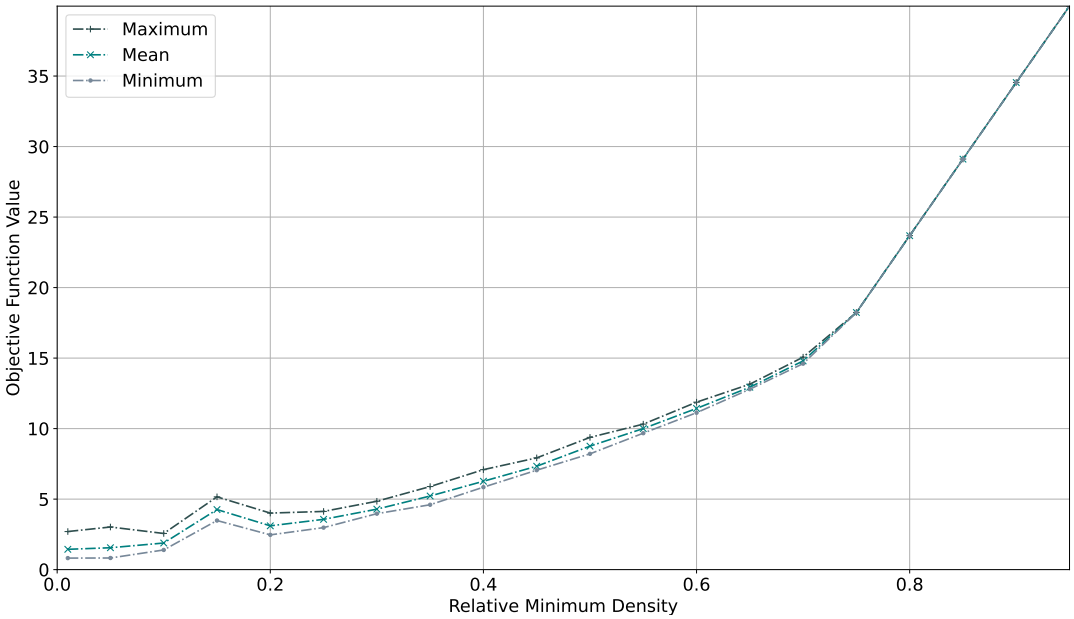

Figure 6.10: The effect of changing relative minimum density on objective function value.

As the relative volume of each cell that must be filled with the minimum structure increases, the minimum cell mass must also increase. Accordingly, the maximum cell density must therefore decrease. For this reason, the achievable mass envelope across the product volume shrinks. The CoM position envelope is similarly affected, due to a greater mass now effectively being located at the GC. Additionally, the number of high-density cells required to achieve the mass target also increases. As such, objective function value increases with relative minimum density (as presented in Figure 6.10). However, it is thought the variability between MCO results would reduce due to the reduced effect of individual cells on the emulation result.

It is therefore clear that the design of the internal structure was an important consideration to ensure that the minimum material could be deposited in each cell, whilst ensuring sufficient support. To do this, several infill designs were considered – presented in Figure 6.11c. Each of these structures was intended to provide a level of support that was proportional to the volume of material deposited.

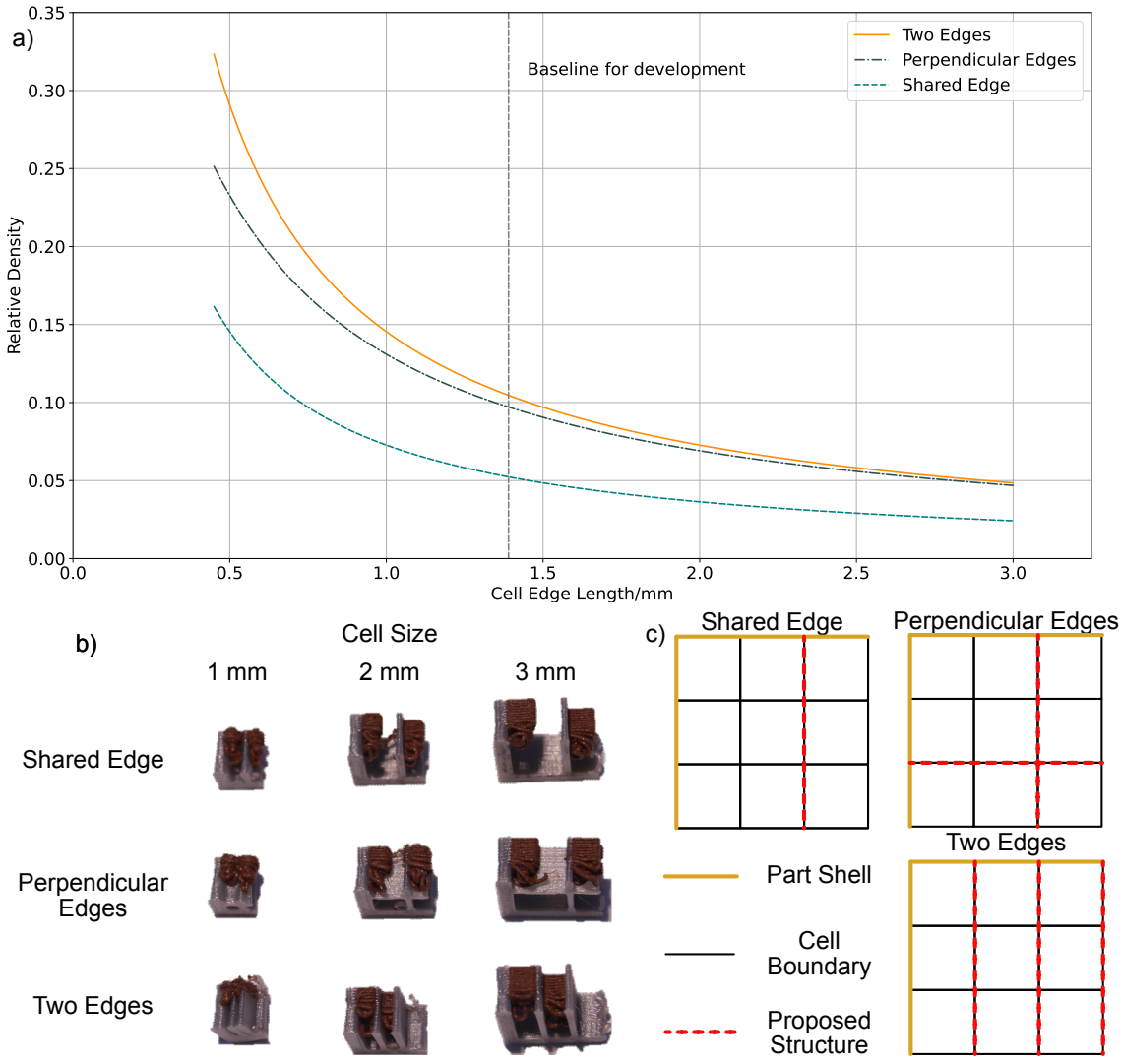

Figure 6.11: a) Relative minimum density for the proposed infill structure designs, b) Test prints showing the effect on overhangs when using the proposed infill structures for different cell sizes (printed with PLA and copper-infused PLA) c) Investigated infill structures to achieve minimum deposition volume and required support.

For each of the support structure designs, both the support provided, and deposited volume were dependent upon the cell and nozzle sizes used (discussed in Section 6.3.5 and Chapter 10 respectively). For this work, the cells were assumed to be perfect cubes with faces directly aligned to the global x-y-z axes. Additionally, the nozzle size was assumed to be 0.4 mm.

Figure 6.11a shows how the relative minimum cell density changes for each infill structure (across a range of cell sizes). From this work, it is clear that the shared edge design – where a single edge is shared between two cells – provides the lowest relative minimum density, as expected. However, it was recognised that this was almost the most challenging design to leverage for support of the high-density cells (as the provided support was minimal). To understand how this could be developed, small volumes of material were printed that investigated the level of support provided by each structure (for 1-, 2-, and 3-mm cells). This work is shown in Figure 6.11b as pictures of example prints.

The fabrications demonstrated that the first unsupported layer dropped by roughly one cell size (for all designs). The remaining layers appear, however, to then be recovered. It was therefore found that ~0.02 g of material would be incorrectly deposited, and it was thought that this would be further reduced when adjacent high-density cells were deposited. As such, the shared edge design was deemed acceptable and adopted for the rest of this process.

6.3.5 Cell Size

As with most computational methods, cell size affects result accuracy and runtime. To investigate and quantify the effect of cell size, the emulation method is applied to many mesh representations of the development model. The results from this study are presented in Figure 6.12.

Figure 6.12 demonstrates that the emulation result reaches an optimum when considering a mesh with cell sizes of ~2 mm^3. To properly understand this, two effects must be recognised:

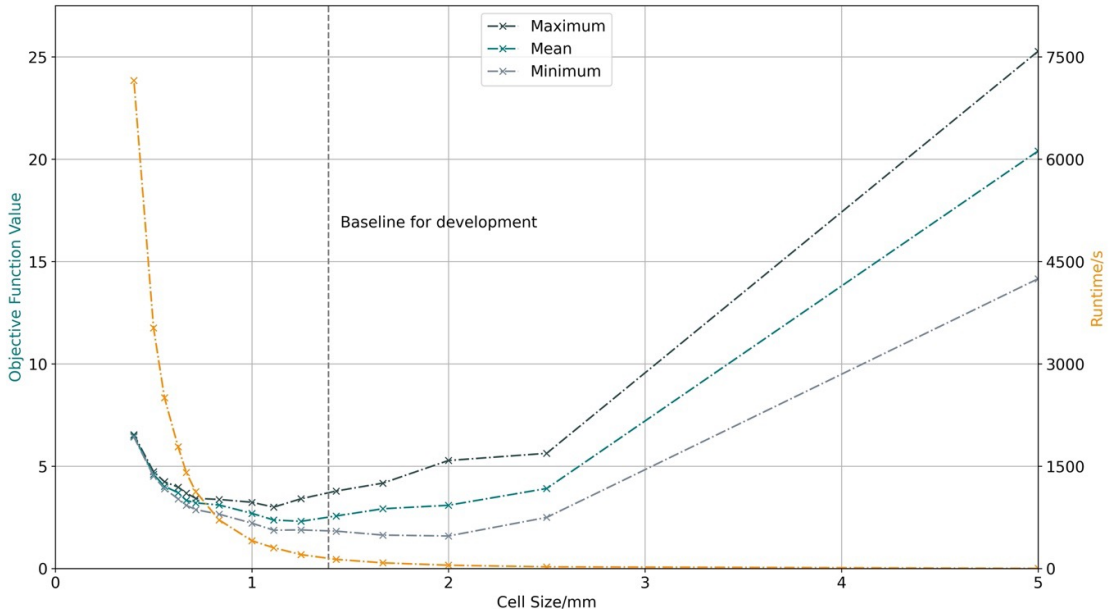

Figure 6.12: The effect of cell size on objective function value and runtime.

1. The increased variability of the process when using larger cells (as each cell affects the calculation more significantly),
2. The increase in relative minimum cell density when using smaller cells (as seen in Figure 6.11a).

Due to these effects, a compromise in cell size is required. Process runtime must also be considered, with a cubic relationship observable (where increasing cell size reduces the runtime). Although this may be somewhat offset through the ability to use less MCO iterations when using smaller cells (due to reduced variability), the savings are relatively small. It is therefore advantageous to use larger cells for process efficiency (as expected).

For process baselining, a cell size of ~1.4 mm was used, as this was a satisfactory compromise between runtime and process accuracy. For the cube, this translated to roughly 46,600 cells. It may have been possible to increase the cell size to ~2 mm to slightly improve the emulation result and runtime, but the reduced variability was thought preferable for development. For future applications, the use of cell sizes between ~1.2 and ~2 mm is recommended, depending on the part scale, nozzle size, materials, and available computational resource/runtime.

6.3.6 Monte Carlo Iterations

As a rule, the completion of a greater number of MCO iterations at the final stage of the process improves the result but is coupled with an increase in runtime. Figure 6.13 demonstrates this effect. The presented results used 10,000 samples for a range of iterations, from an overall sample of 50,000 results. Using the figure, it is possible to demonstrate that the median result (and associated distribution) improves with increasing MCO iterations. Interestingly, however, the IQR of the results remains relatively consistent – the IQRs for the results of 10, 25, 50 and 100 iterations all lie between 0.31 and 0.44.

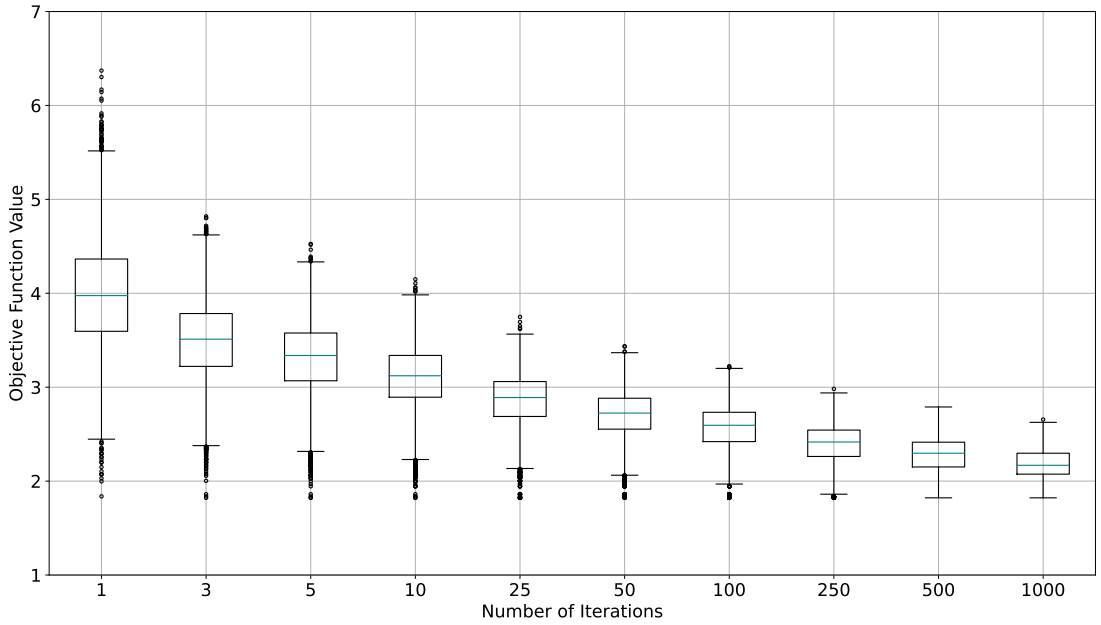

Figure 6.13: Effect of MCO iterations on objective function value. The box represents the IQR, with the inside line the median. The whiskers represent 1.5 times the IQR.

For the development of this work, the process used 25 iterations within the MCO. This was done to allow more data points could be investigated for the same computational time as running a larger number of MCO iterations. As trends were the focus of the development work, rather than absolute result values, this was deemed suitable. For final product emulation results, a larger number of iterations may be appropriate depending on the computation time available and the required accuracy of result.

6.4 Primitive Results

The baseline parameter values were used and the emulation method applied to the primitive, providing the results shown in Table 6.1.

Table 6.1: Primitive form results using baseline data. Percentage error is given relative to the cube bounding box length.

Property	**Target Value**	**Emulated Value**	**Absolute Error**	**Percentage Error/%**
Mass/g	120	120.07	0.07	0.06
CoMx/mm	2.5	2.38	-0.12	-0.24
CoMy/mm	2.5	2.46	-0.04	-0.08
CoMz/mm	27.5	27.43	-0.07	-0.14
Run-time/s		151.72		

6.5 Chapter Summary

The optimisation process used for locating the variable infill within the internal volume has been developed. This process uses solution space knowledge to direct the target, internal volume CoM before generating iterative solutions to understand how the result should be targeted, showing how mass properties can be emulated and how said method can be embedded into the MEX workflow.

A series of baseline parameter values was then developed to control this process, shown in Table 6.2. Additionally, improvement is demonstrated in the expected mass properties of the primitive relative to a nominal fabrication. Although this is encouraging, it is recognised that application to a primitive form may not be applicable and, as such, application to typical consumer products is recommended and conducted in the following chapter.

Table 6.2: Baseline parameters developed through the chapter.

Parameter	**Value**	**Parameter**	**Value**
Nozzle Size	0.4 mm	CoM Iterations	8
Infill Structure	Shared, single edge	MCO Iterations	25
Materials(s)	PLA and copper-infused PLA	CoM MCO Iterations	5
Material Density	1.24 and 3.41 g/cc^3 respectively	Beta Tolerance	4
Discrete Densities	Rel. Min, Rel. Max	Number of Cells	~45000

Chapter 7
Case Studies - Application

7.1 Chapter Overview

Following the evaluation of a baseline set of parameters that control the variable infill method, application to case studies was undertaken to further develop the answers for RQs 2 and 3. To do this, three example product case studies were reviewed – a Nintendo Switch JoyCon, a Bosch electric hand drill and a Kensington laser pointer - as previously discussed in Section 4.3.1. These products covered a range of interaction methods and product types. A sensitivity analysis was additionally undertaken to evaluate what was possible without consideration of current technological limitations. The chapter concludes by considering the results and their implications.

Parts of the work detailed within this chapter are published in the author's paper "Improving Feel in 3D Printed Prototypes: A Numeric Methodology for Controlling Mass Properties Using Infill Structures" (in review) [191].

7.2 Conventional Material Extrusion Comparison

A series of results were generated that used conventional MEX fabrication to allow for emulation result comparison for the products in Section 4.3.1. To do this, products were assumed to have a 1.2 mm shell and 20 % infill density – taken from the default settings in Ultimaker Cura at the time of research. The results for the anticipated conventional fabrication are presented in Table 7.1, with results for each mass value given with respect to the as-designed product mass properties. The CoM position errors are relative to the length of the product in the respective axis (as in the objective function terms).

Table 7.1: Mass property results for a conventional MEX fabrication of each case study.

Case Study Product	Objective Function Value	Mass Error	CoM Error			RI Error		
			x	y	z	xx	yy	zz
A	52.8	-49.6%	-0.3%	-2.7%	0.3%	-87.6%	-38.0%	-67.7%
B	92.9	-74.2%	0.2%	-3.7%	14.2%	-77.5%	-77.6%	-74.7%
C	65.4	-34.5%	-1.2%	5.7%	24.0%	-60.6%	-63.9%	-92.4%

As presented in Table 7.1, the mass is underrepresented in all case studies, in the worst instance by nearly 75% (1083 g). Similarly, the principal RI error is significant, with all RIs underrepresented. CoM position is generally better represented, though errors are significant in particular instances. For example, case study C has a Z-axis CoM error of 24% of the product length. As such, improvement in mass property representation may be possible.

7.3 Initial Results

A series of meshes were generated that aimed to have ~45,000 cells (as in the method baselining) to ensure appropriate runtime. The meshes for each case study product contained 45,328, 44,999, and 45,447 cells respectively. Results from the computational emulation method using these meshes, and the other baseline parameters, are presented in Table 7.2.

Table 7.2: Mass property results for the case study products following application of the emulation methodology.

Product	Objective Function Value	Mass Error	CoM Error			RI Error			Runtime/s	
			x	y	z	xx	yy	zz	Intel i5 9600	Apple M1
A	0.815	0.0%	-0.1%	-0.3%	-0.4%	-80.1%	-15.4%	-54.8%	227.23	194.44
B	2.487	-0.1%	0.1%	-1.2%	1.1%	-32.5%	-30.6%	-27.8%	209.05	163.64
C	28.943	-0.1%	-1.0%	6.1%	21.8%	-45.3%	-49.9%	-89.8%	222.36	186.46

It is clear that the application of the computational method can generate simulated depositions with significant improvements in the mass error and, in most cases, CoM position error. Further, the error in principal RI is also improved in every instance, even without direct consideration in the objective function. This was thought to be driven by the increase in mass, with principal RI previously underrepresented.

In addition to Table 7.2, a graphical representation of the cell composition can demonstrate how the emulation method worked. This is shown in Figure 7.1. It can be observed that, in case studies A and B, the position of high-density cells can be targeted such that the CoM position moves as required. This results in objective functional value improvements of 98.5% and 97.3% respectively.

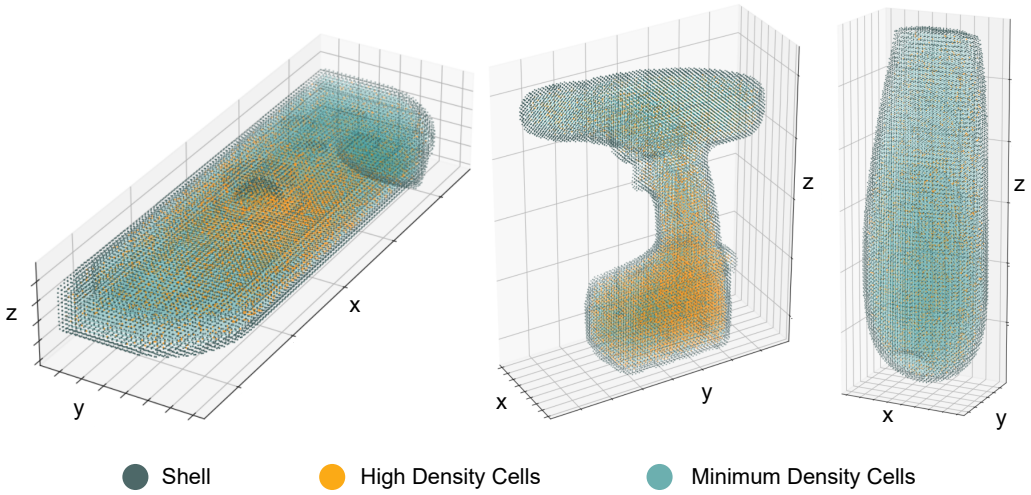

Figure 7.1: Graphical representation of cell composition spread in the three case study products.

In contrast, case study C did not undergo the same level of improvement, with the objective function improving by 55.7% - a relatively small increase compared to the other case studies. The two main drivers for this were related to the y- and z-axis CoM offset from the GC. Both of these axes required large deviations of mass from the GC, which were not possible within the allowable volume. As Figure 7.1 demonstrates, high-density cells could not form high concentrations as required for product C.

To understand the context of the results, 20 blocks with infill percentages of 0, 20, 50 and 100% infill were fabricated using otherwise consistent print settings. It was found that the standard deviation for the mass of each of these blocks was 1% around each of the respective block masses. Hence, it is recognised that the physical fabrication error is likely to dominate the numerical error in practice. This will be considered in more depth in the following chapter.

7.4 Sensitivity Analysis

To better understand what may be possible, within current practical limits and otherwise, a sensitivity study was undertaken. To do this, each case study is considered with the baseline parameter values modified and their effect reviewed. For the purposes of comparison a "Normalised Objective Function Value" is used in place of absolute objective function value.

This communicates the degree to which individual parameter changes affect the result for each case study, irrespective of the accuracy previously achievable. The normalised objective function value is calculated by dividing the results for each case study by the initial result for the respective case study. This means that normalised objective function values less than 1 demonstrate improvement in the emulation accuracy, values of 1 indicate identical performance, and values greater than 1 indicate a worse result. From the sensitivity review, a set of tuned parameter values are derived, and the new emulation result applied. The results are discussed and the implications assessed.

7.4.1 Nozzle Size

As discussed in the preceding chapter, the cellwise relative minimum density has a clear effect on the computational emulation result. Inherently, the nozzle size (previously assumed to be fixed at 0.4 mm) has a direct effect on this parameter. As such, it was thought important to consider nozzle size, as this was a viable practical parameter to change. To do this, 0.1, 0.25, 0.4, 0.6, and 0.8 mm nozzles are considered, as these are common for desktop MEX printers.

Figure 7.2 presents the effect of changing nozzle size, for each of the case study products, on the computational emulation result. The relationship between nozzle size and objective function value is as expected for each case study, showing good correlation with the baselining work. Generally, the use of a smaller nozzle generally improves the emulation result – at least theoretically. There are instances where this is found not to be the case - most apparent for case A. Here, the use of a 0.25 mm nozzle demonstrates improvement over using a 0.1 mm nozzle, and a 0.8 mm nozzle shows improvement over a 0.6 mm nozzle. These unexpected results were caused by a subtle effect, with the number of cells needed for the mass distribution and to achieve the mass being balanced. For different products and target mass properties there may be local minima that can only be achieved with a lower high-density cell mass. This is demonstrated in the data for case A. The other case studies considered, and future applications, could also experience this at specific nozzle sizes, but it is more pronounced for cases where few high-density cells are being used (such as case A). However, it remains that the use of a smaller nozzle generally improves the computed emulation accuracy.

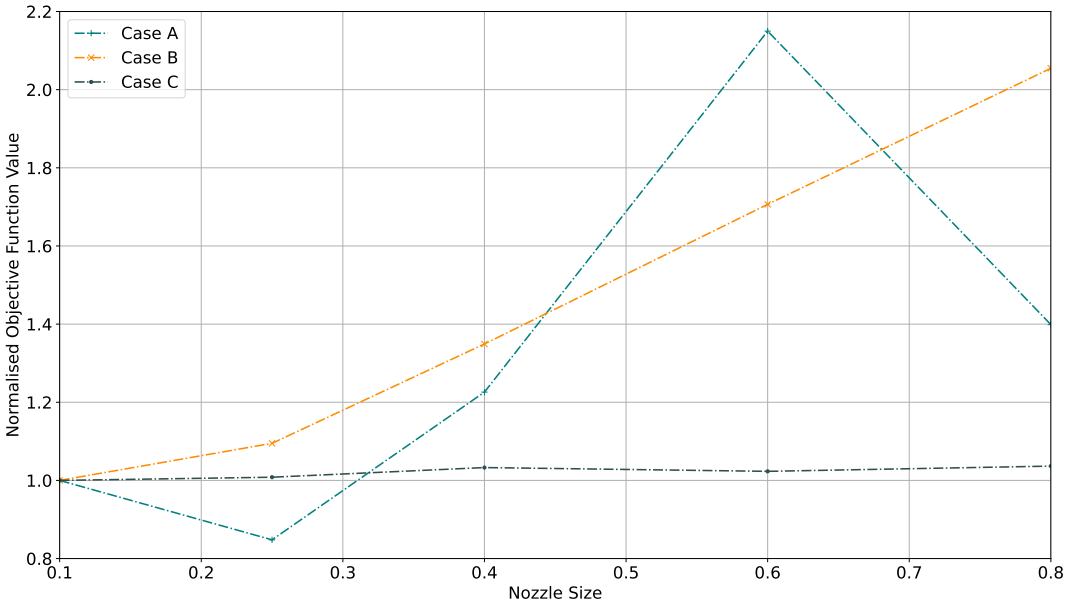

Figure 7.2: The computational emulation result for case studies A, B and C with changing nozzle size.

It is recommended that, if a smaller nozzle were used, some of the physical complications previously covered in literature are considered (for example, in the author's work on negligible cost microfluidics [108]). One such complication includes how reliability of deposition often deteriorates when using small nozzles due to nozzle blockages. Further, print time increases proportionally to the reduction in nozzle outlet area – though this effect may be lessened as the volume of printed material would also decrease.

From this work, the use of a smaller nozzle provides an improved result. Therefore, the tuned parameters will use a nozzle size of 0.1 mm for all case studies. This was thought to be the practical limit for desktop MEX machines with current, and near future, technology.

7.4.2 Materials

In the study thus far, PLA and copper-PLA have been considered, though there are alternatives commercially available. It is likely that the availability of alternative materials will also likely increase with time. This will likely be driven by the value in desktop MEX printers being able to print metal parts. This can currently be achieved using materials like RS Pro's copper-

fill PLA [183], but also with materials such as BASF Ultrafuse [189]. The Ultrafuse material can be leveraged to form printed parts with a material density of 7.85 g/cm^3. As such, as with baselining of the parameters, secondary MDRs (relative to PLA) between 1 and 9 (roughly equivalent to solid lead) are considered to investigate the effect. This is shown in Figure 7.3.

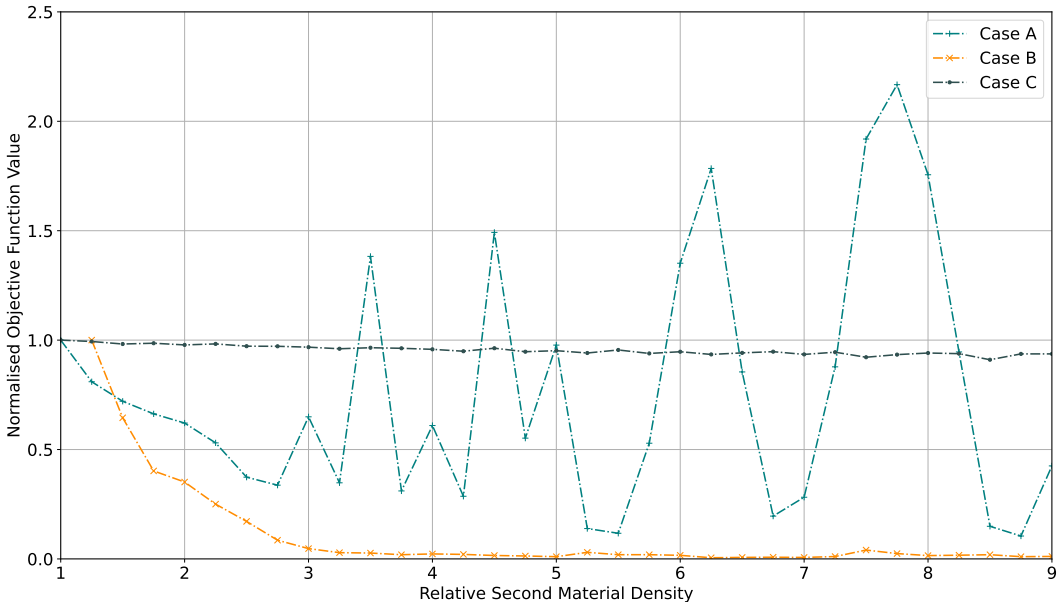

Figure 7.3: The computational emulation result for case studies A, B and C with changing secondary material density ratio.

Figure 7.3 demonstrate similar results to the baselining work, demonstrating that the relationship is consistent for different products. This relationship shows that the objective function result generally decreases with increasing MDR, though the variability also increases. In Figure 7.3, the variability is much larger for case study A relative to the initial result than for the other case studies. This is for two reasons:

1. The absolute improvement in result for cases B and C were much greater than for case A, so the variability is relatively small.
2. The number of high-density cells required to achieve the desired mass for case A was much smaller than for cases B and C. The effect of increasing the MDR has a larger effect and therefore, due to the discrete nature of the problem, larger variability is observed.

For tuning the parameters, it is shown that increasing MDR generally improves the emulation result. For this reason, a MDR of 9 is used as the tuned result for all products, with the understanding that a greater number of MCO iterations would be needed to overcome the increase in variability (see Section 9.6.6). At the time of writing, a filament with an MDR of 9 was not commercially available – at least to the author's awareness. As discussed, availability of higher density materials were expected to become more common.

7.4.3 β Tolerance

Figure 7.4 presents how changing the β tolerance (tolerance of β in Equation 6.1) impacts the objective function value for the three cases. As was evident in the previous baselining work, there are inconsistent changes in the computed emulation result. Principally, this was due to the use of a discrete mesh with a continuous probability distribution, as previously discussed in Section 6.3.2. These relate to the beta tolerance being a limit (not a target) and therefore allowing small errors to be acceptable, and the use of a continuous probability distribution for a discrete cell map. Both of these effects are shown in the plot for case A. The decrease between β tolerance of 8 and 12 is caused by lower β error being achieved, with the step after this point caused by the use of the discrete cell map.

For the reasons discussed, finely tuning β requires careful judgement when trying to balance runtime and accuracy. However, if absolute emulation accuracy is the important aspect – as in this work – it is reasonable to use a minimal β tolerance. The β tolerance is therefore set to 1 for all cases.

7.4.4 Cell Size

Figure 7.5 presents how changing cell size affects the emulation result for each case, when using a nozzle of 0.4 mm. Cases A and B demonstrate similar relationships. These cases demonstrate initial improvement in result before worsening; though the final point of each demonstrates improvement too. The initial improvement is due to the relative minimum density of the cells reducing, with the support structure taking up a smaller proportion of the cell

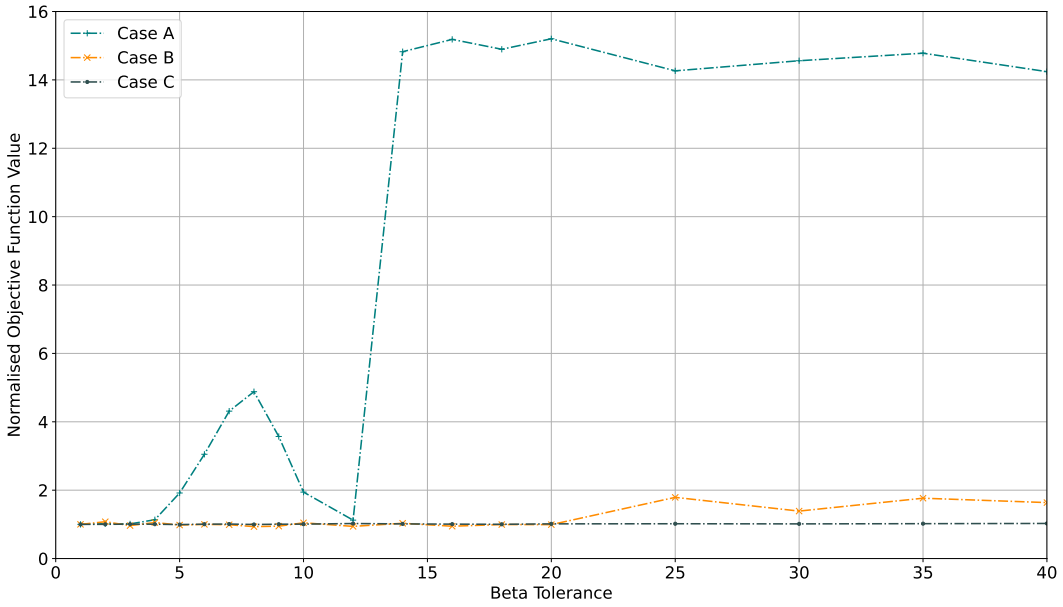

Figure 7.4: The computational emulation result for case studies A, B and C with changing β tolerance.

volume. The deterioration in result is then caused by each cell having a larger effect on the emulation accuracy. This means CoM position and mass cannot be achieved to the same accuracy or precision. This same effect causes the result for case C to consistently deteriorate.

The final improvement in result for cases A and B is from a local minima being found. Here, the reduction in relative minimum density combined with the target CoM position provides an improved solution. It is difficult to predict when this effect will occur, however, and so should not be relied upon. The tuned process has been chosen to use cell sizes of 1.25 mm, 1.5 mm, and 0.6 mm for each case respectively, based on data from Figure 7.5.

7.4.5 Internal Volume Centre of Mass Searching

The effect of changing the number of internal volume CoM searching iterations is shown in Figure 7.6. The figure demonstrates changing behaviour for each case, driven by the relative offset between the GC and the CoM position.

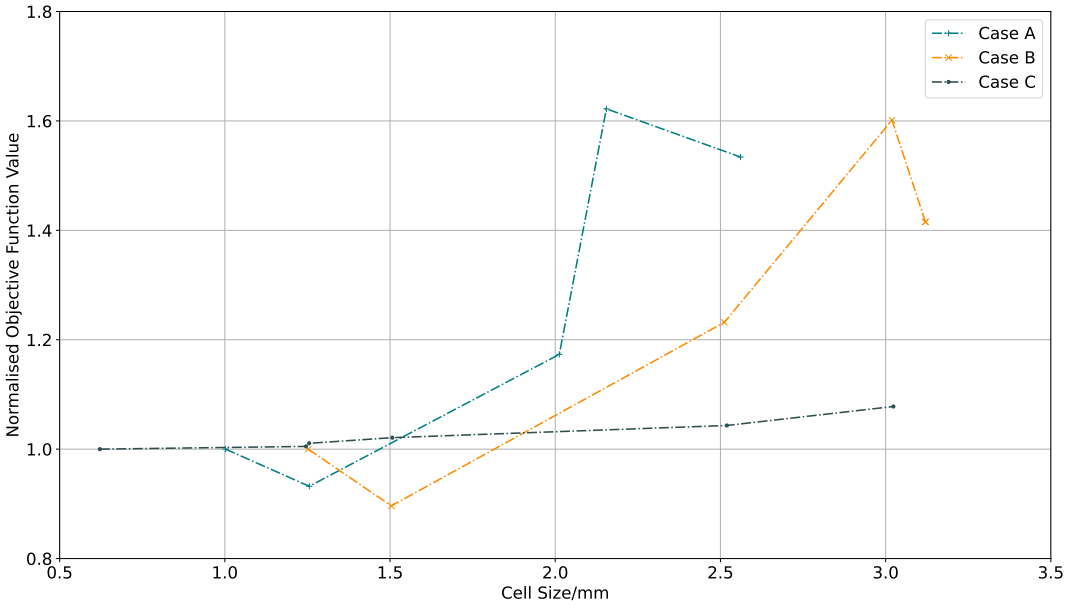

Figure 7.5: The computational emulation result for case studies A, B and C with changing cell size.

Case A demonstrates an improvement with increasing CoM iterations, albeit with this improvement reducing as the target and required internal volume CoM position converge. In comparison, case B demonstrates an initial improvement before the objective function value starts to increase (i.e. the error increases). This is caused by the same effect that causes case C's error to increase with increasing CoM search iterations. This is where the internal volume CoM target moves outside of the internal volume envelope. As the internal CoM target moves outside of the envelope, the applied probability distribution bias around the target CoM is lost. As the bias is lost, all cells within the volume have a near homogenous high-density composition probability. This reduces the accuracy of the emulation method, as previously discussed in this thesis. This is discussed further in Chapter 9.

For the purposes of tuning the current process, CoM search iterations are limited to 20, 6 and 0 for each respective case study.

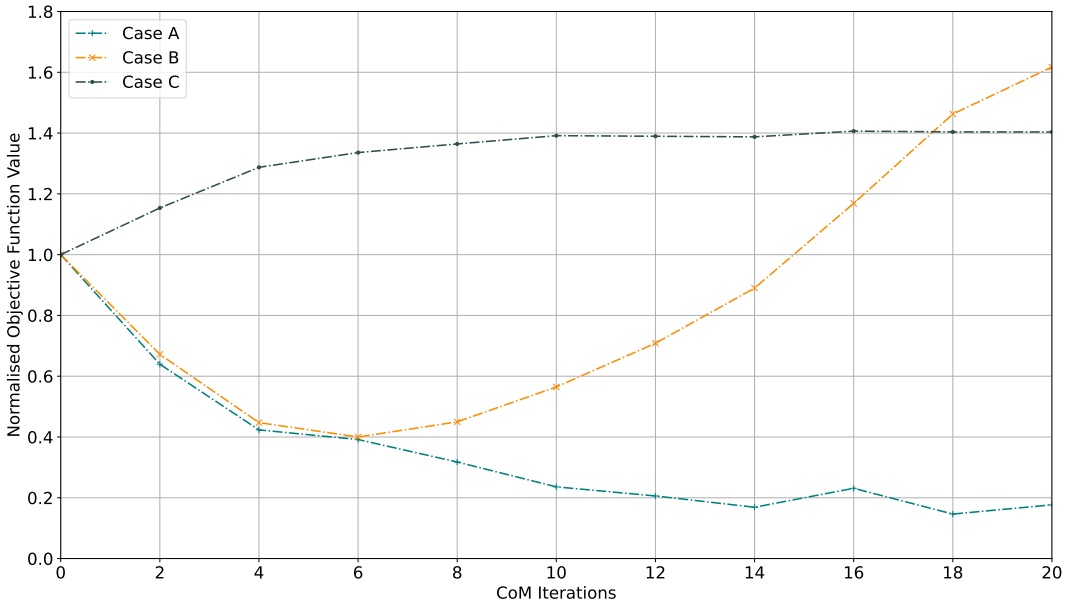

Figure 7.6: The computational emulation result for case studies A, B and C with changing CoM iterations.

7.4.6 MCO Iterations

Finally, as with baselining the parameter set, the number of MCO iterations used was investigated. It has previously been found that increasing the number of MCO iterations improves the result. To ensure this remained the case for the case study products, and to understand the level of improvement achievable, a study was completed. To do this, results were generated using MCO iterations up to 1000 for each product – presented in Figure 7.7.

As was expected, the computed emulation accuracy improves (generally) with increasing MCO iterations. This is clearer for cases A and B, whilst case C having a relatively flat relationship. Once again, this is caused by the large relative offset between the GC and target CoM position for case C. This caused the applied probability distribution to be flattened across the part. As such, the difference between MCO iterations is reduced.

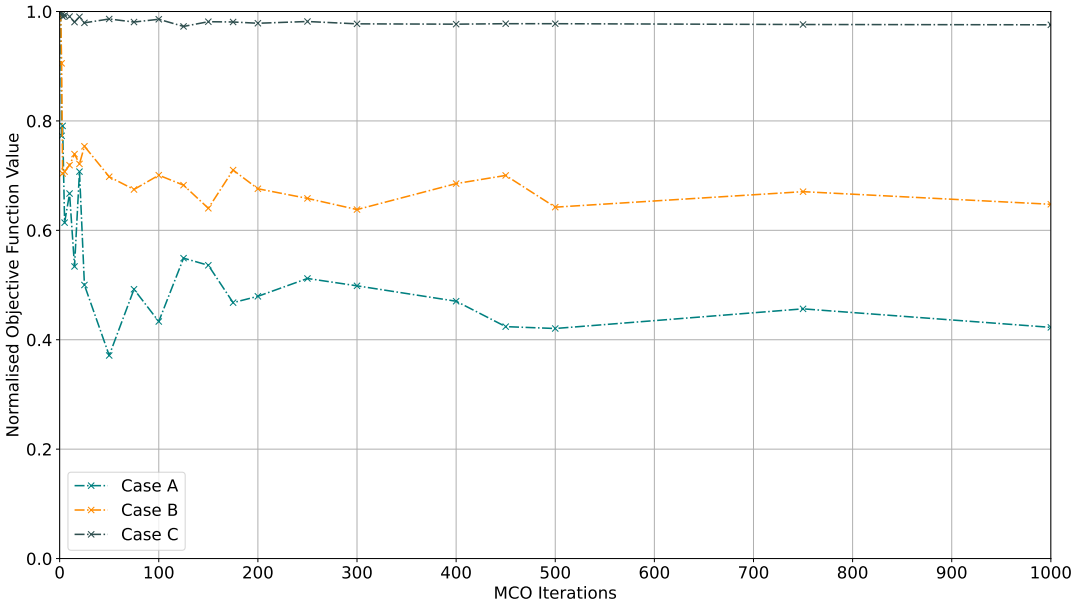

Figure 7.7: The computational emulation result for case studies A, B and C with changing number of MCO iterations.

The tuned process detailed herein was chosen to use the maximum number of MCO iterations, as this was inherently the most robust way to search the solution space. For this reason, MCO iterations were set at 1000 for each case. No higher limit was used as the improvement for each case was found to be reducing between 500 and 1000 iterations, and the increase in computational runtime was therefore deemed unnecessary.

7.4.7 Tuned Parameters

The parameters derived from the presented work are summarised within Table 7.4. However, it is recognised that there may be some interaction between parameters that has not yet been investigated. Hence, the parameters should be considered tuned, not optimal. Further, practical freedoms have been prescribed – principally around the use of a 0.1 mm nozzle and MDR of 9 – that are currently impossible and/or impractical. However, they were thought reasonable to investigate how the method may be improved with product specific parameters.

Table 7.3: Summary of tuned parameter values.

Product	Parameter					
	Nozzle Size/mm	Relative Secondary Material Density	Cell Size/mm	β Tolerance	CoM Iterations	MCO Iterations
A	0.1	9	1.25	1	20	1000
B	0.1	9	1.5	1	6	1000
C	0.1	9	0.6	1	0	1000

7.4.8 Tuned Results

The tuned parameters have been used with the emulation method and results computed for each case, as presented in Table 7.4. The results demonstrate a significant improvement over the baseline parameter results in the preceding chapter. Case specific improvements were 70.45%, 85.07% and 64.11% respectively. This reduced the individual property error, in the worst instance, to 5.5% (the z-axis CoM error in case C). This is equivalent to 6.35 mm in absolute terms.

Table 7.4: Summary of tuned, computed emulation results for cases A, B and C.

Product	Objective Function Value	Mass Error	CoM Error			RI Error			Runtime/s
			x	y	z	xx	yy	zz	Apple M1
A	0.24	0.1%	-0.1%	-0.1%	0.0%	-81.9%	-37.2%	-65.9%	239.28
B	0.37	-0.2%	-0.1%	0.1%	0.0%	-58.4%	-57.3%	-46.6%	2208.73
C	10.39	0.0%	-0.2%	4.6%	5.5%	-61.0%	-64.5%	-91.8%	2164.85

The runtime of the computational emulation process was increased for every case, by an average of 22.6 minutes (or 753%). It would be up to any potential user to decide whether the increase in compute time is warranted (in the context of the fabrication and application). As part of this, it should be understood that, although the relative improvements were large, the absolute improvements between parameter sets were small (fractions of a gram and/or millimetre in most instances). Further, fabrication time and cost would increase significantly. It is thought important to properly understand how the fabrication process – using either result set – would impact the emulation. This would provide an understanding of a suitable level of accuracy for the method.

7.5 Chapter Summary

The chapter has presented a set of example applications of the methodology. It is found that the computational method can emulate the mass properties of a Nintendo Switch JoyCon, electric hand drill and laser pointer to objective function values of 0.815, 2.487 and 28.943 respectively, demonstrating that mass properties can be - at least computationally - emulated within MEX prototypes. These represent respective improvements – relative to conventional fabrications – of 98.5%, 97.3% and 55.7%. The laser pointer demonstrated a poorer result, principally due to the relatively large displacement between the GC and product z-axis CoM. This is found to be a limitation of the emulation method, but should only affect edge case products.

A sensitivity study is further conducted that evaluated the potential benefits of moving away from the baseline values. It is demonstrated that improvements in result between 64.11% and 85.07 % are achievable (compared to the use of baseline parameters), however, this requires product specific investigation, increased process runtimes and currently impractical physical implications.

To understand what computed emulation accuracy would be reasonable, it is thought sensible to fabricate example products. This would allow comparison between the computed and fabricated mass properties and, therefore, what emulation accuracy may be achievable.

Chapter 8
Case Studies - Fabrication

8.1 Chapter Overview

Following the computational emulation of fabrications for the case studies proposed, investigation of how the result may be fabricated was completed. To do this, a slicing methodology was developed, and the products manufactured. The results are then analysed and discussed, to aid developing an answer for RQ 3.

8.2 Slicing

As outlined in Section 3.6.1, the pre-process machine code generation step is often referred to as “slicing” for MEX fabrications. This is because the part(s) is (are) broken up into layers, or slices, that can then be deposited – generally sequentially. This process allows machine code – Gcode – to be generated such that a machine can deposit material as required to build up a part.

Current slicing software was not able to process the output from the computational emulation stage of the proposed process. For this reason, a bespoke slicer was developed using Python. It is likely that this could be integrated into an existing software package to simplify the toolchain. The developed slicer required:

- A Cura [144] output for traditional fabrication (from which the shell, support and print bed adhesion code was taken).
- The computational emulation output presenting the cellwise cell compositions.
- The geometric product definition (as a mesh, currently using the Ansys output as used in the computational emulation).

The Cura output was used to provide the code for definition of the shell, support and print bed adhesion depositions. One of the over-arching reasons for this was to demonstrate compatibility with the basis of current techniques. This was done to highlight that it should be possible to integrate small additions to existing software packages. Otherwise, it was also

clear that it was unnecessary to develop alternative methodologies to those that already exist and are widely used. Further, the use of a surface defined shell over a cellwise had advantages with regards to surface quality, as demonstrated in Figure 8.1.

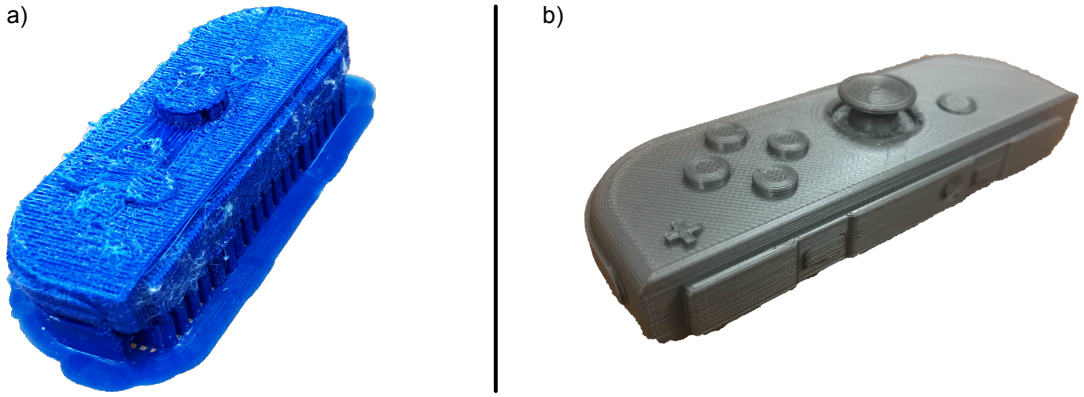

Figure 8.1: Comparison of shell fabrication between a cellwise definition and a surface-based definition.

The parameter values that control fundamental principles of deposition were also taken from Cura. For example, layer height, print speed and print temperature were copied. This was done to ensure consistency and reduce user workload. The material specific values were taken from the manufacturer's data sheets (e.g. print temperature, bed temperature).

The slicing process itself has several stages, as presented in Figure 8.2, with the order of code generation imitating that completed by Cura. As previously discussed, the minimum support structure deposited within the internal volume of the product is deposited in a single stage for each layer. All high-density cell depositions are then completed subsequently. This is done to improve the quality and speed of deposition (as individual depositions can be longer). To do this, cells are organised into layers and rows, with this process currently requiring most of the processing time. It is important to note that these depositions are not necessarily straight, instead following the path defined by the cell boundaries. It is therefore possible that the deposition may require deposition around tight radii and angles, which MEX often struggles with. However, this was unlikely based on the mesh checking and cell sizes used.

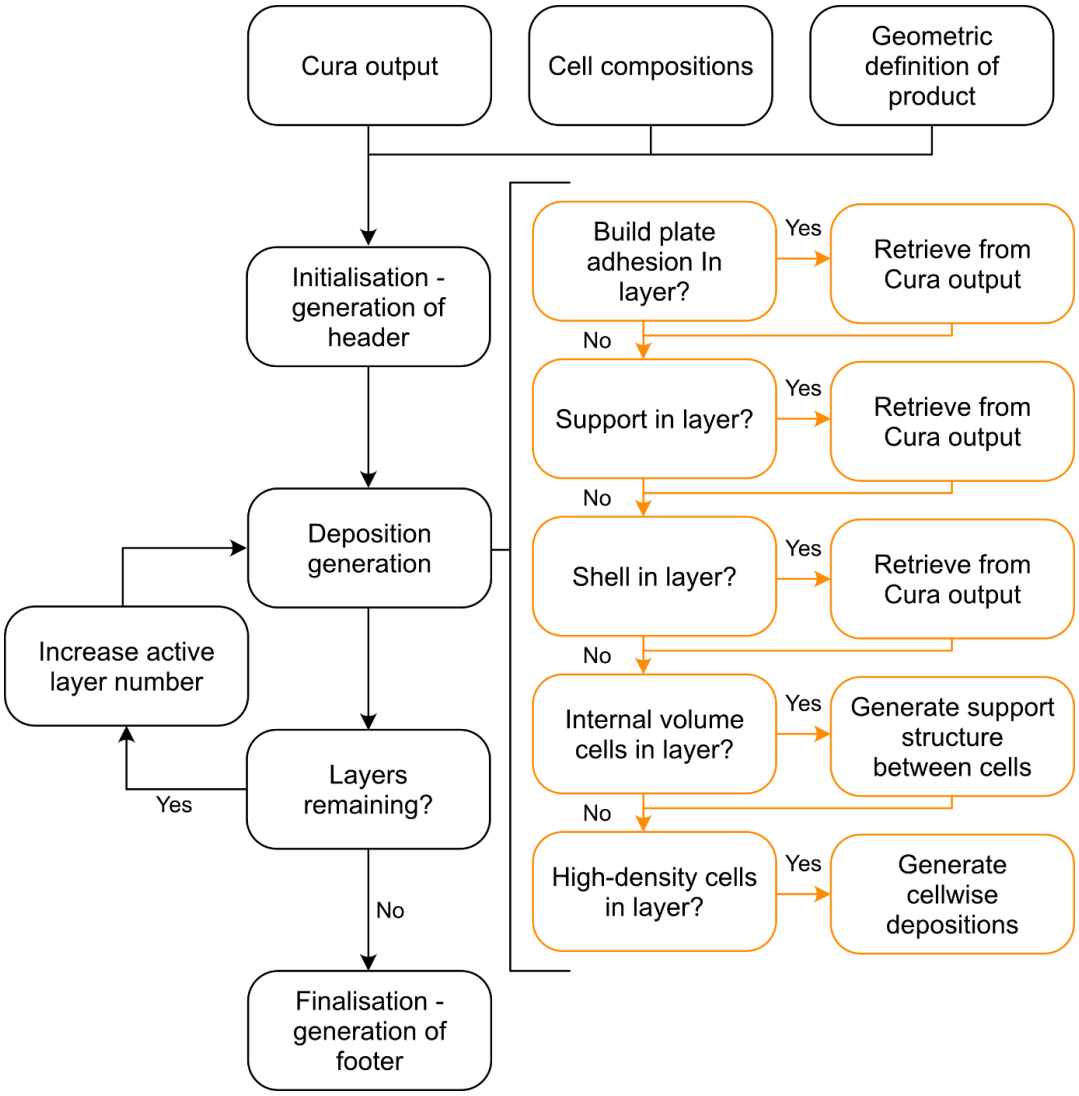

Figure 8.2: Slicing flowchart for the fabrication of product prototypes with emulated mass properties.

Following the generation of the in-layer minimum structure code, the code for high-density distribution is generated. For this work – as a proof-of-concept – this is done on a cell-by-cell basis. In other words, individual cells are deposited, without consideration of their surroundings. This improves the efficiency of the slicing process but has a negative impact on the deposition quality and processing time. Future work may look at improving this.

The slicing process, in its current form, takes ~665, ~3366, ~735 seconds for case studies A, B and C respectively. This is a significant increase over conventional slicing methods that take <30 seconds for most parts. This may be improved with better integration into traditional slicers, as this removes the need to post-process conventional gcode. In addition, it is hypothesised that the use of the two-sided minimum support structure would significantly decrease processing times. This is because it would be possible to assume mesh spacings, allowing traditional infill generation methodologies to be used. Alternatively, more robust cell ordering within the meshing process could allow efficiency gains to be made. Multi-core processing can also improve process runtime.

For the purposes of investigation into fabrication, the initial case study results using baselined parameter values were used. These were chosen over the tuned results as the practical fabrication limitations considered what was currently available (with regards to materials and nozzles).

8.3 Manufacture

For manufacture, Ultimaker S3 [149] and Ultimaker 3 Extended [195] printers were used. These printers were set up to use Polymaker PLA [196] and RS Pro Copper-fill [183] filament using a print head with two nozzles. The PLA was deposited using normal Ultimaker AA print cores, whilst the copper-fill was deposited using the Ultimaker CC print core [197] or 3D Solex Everlast core [190]. The only modifications made to the printers was the use of PrintBite+ as the build plate surface [198].

Each case study was fabricated using a layer height of 0.1 mm, with a brim, support (if required) and otherwise consistent settings with the Cura defaults. This was done to ensure that the process was consistent across parts and with that which a design office would likely use. The exception to this was retraction which was controlled by the Python slicer. This allowed control over the number of retractions, with this only being allowed between material and layer changes. Controlling retraction in this way reduced the overall number of retractions. This reduces the chance of material grinding. The downside of doing this is that material "oozing" – where material seeps out of the nozzle when it shouldn't be – will be more apparent. The effect of this is shown in Figure 8.3 for case study A. It is shown that the surface quality reduces and material strands are left around the part. It may be possible to overcome this through a more robust path planning methodology that allows continuous deposition of each material. This would reduce the number of retractions over any given length of material, but was considered out of scope for a proof of concept tool.

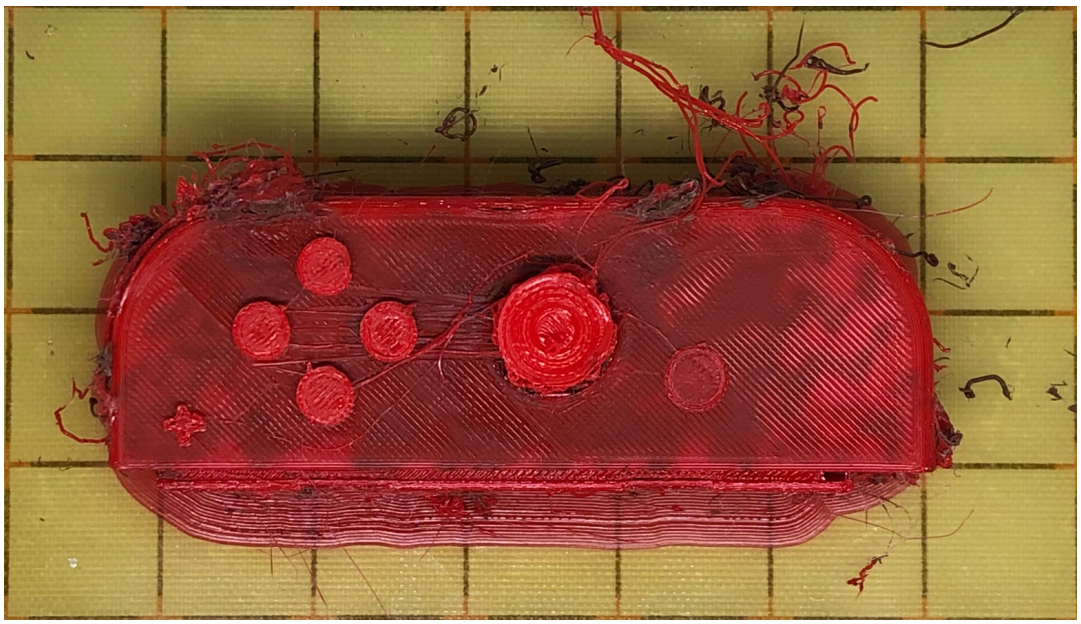

Figure 8.3: The finished deposition on the build plate for case study A. Oozing is evident with strands of material surrounding the deposition.

It is recognised that process parameters (that control the MEX deposition directly) will have an impact on the deposition mass. This is discussed by Afonso et al. in literature [199]. It is shown that process parameters affect the results by a significant amount. However, it was more useful – at this stage – to understand what is achievable using general settings.

This was done as the calibration of material, machine and environmental conditions would be practically unviable for the hypothesised use cases. As such, the only calibration that was done ensured that the materials printed with sufficient quality using the manufacturer's print settings.

During fabrication the process was found to generally work as anticipated, at least for case studies A and C. Issues around material oozing were observed, though these were expected. One unexpected issue was observed in case study B, however – this is presented in Figure 8.4. The issue is observed as the support structure collapsing. This is caused through the use of an STL representation for the shell, and the Ansys mesh definition for the internal volume. This led to a small gap forming between the shell and initialisation of infill structure, that meant the infill depositions did not adhere as expected. For this reason, some of the high-density cells were also not deposited as expected, though those surrounded/supported by other high-density cells were generally unaffected. This occurred at ~ 50% into the fabrication of case study B, and so it was expected that deposition in the upper half of the drill will be reduced. To overcome this in future depositions, overlap of the shell and support structure definition is recommended.

One other area of improvement identified was that surrounding deposition time, which was much greater than anticipated.This is because of the way that the printer interprets gcode and accelerates between movements. Although the shell, support (structure and infill structure) and brim printed as expected, the high-density cells were deposited much more slowly. This was because the printer was forever accelerating from rest (in x and y) whilst depositing many small lengths. It should be possible to overcome this through improved print path planning techniques, that deposit material across multiple cells in continuous movements. It is further hypothesised that print quality would further improve. This was briefly investigated, and did improve the print quality and time see Figure 8.5), but the tool was judged to be suitable for the purposes of process demonstration.

Figure 8.4: In-process issues with support structure deposition in case study B.

Figure 8.5: MEX fabrications of case study A with a conventional print (left), an initial fabrication with breakthrough from the interior and holes (center), and the final fabrication demonstrating a lack of retraction and oozing (right).

The three case studies took roughly 8 hours (up from 2.1 hours), 9 days (up from 1.3 days), and 8 hours (up from 2.5 hours) respectively. However, it is thought each of these print times could be halved with improved high-density cell deposition. If this were possible, fabrication time would decrease by ~50-100%, depending on part, as the printer's average speed would be higher and the number of movements could be reduced.

8.4 Results

The fabricated parts (post support removal but with no other post-processing) are presented in Figure 8.6, with case studies A, B and C presented left to right. Figures 8.7 to 8.9 further show each print individually, with defects highlighted. There were artefacts in each of the parts that were not evident in the conventional MEX equivalents. All of these issues could be attributed to the lack of retraction used. It was thought beneficial to develop the manufacturing method to allow for retraction in future iterations of the model.

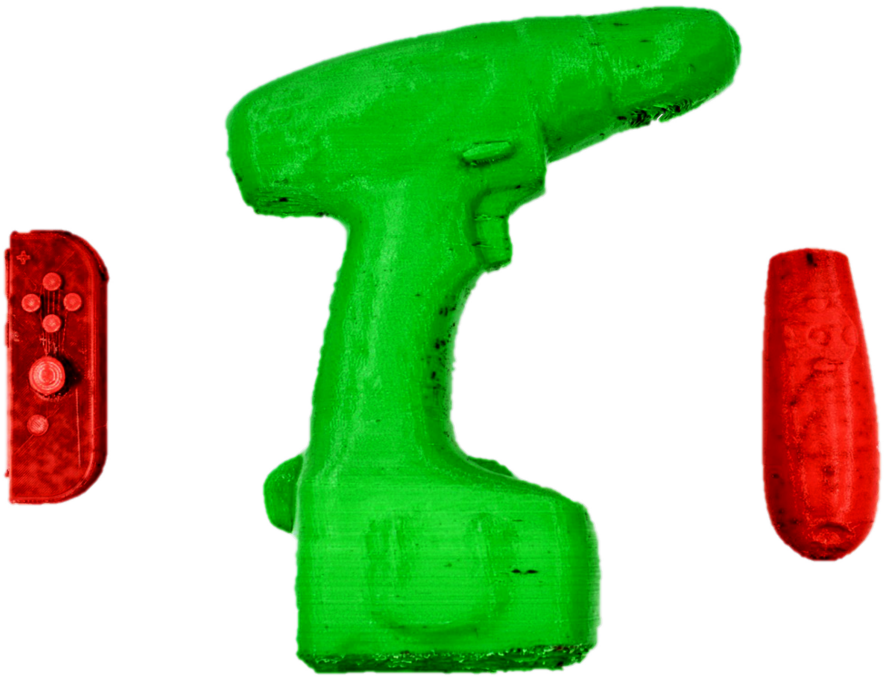

Figure 8.6: Fabricated case study products with A, B and C presented left to right.

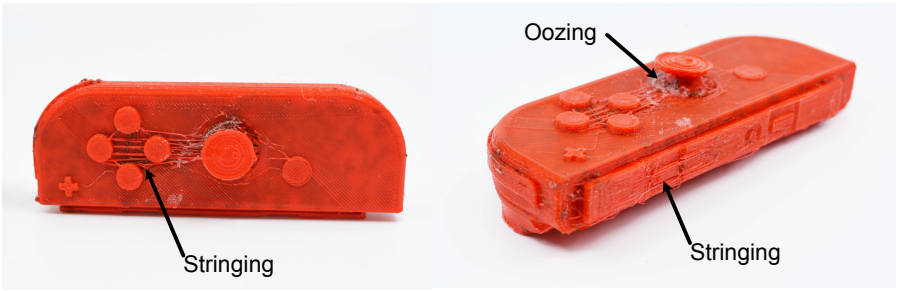

Figure 8.7: Fabricated case study product A with defects highlighted.

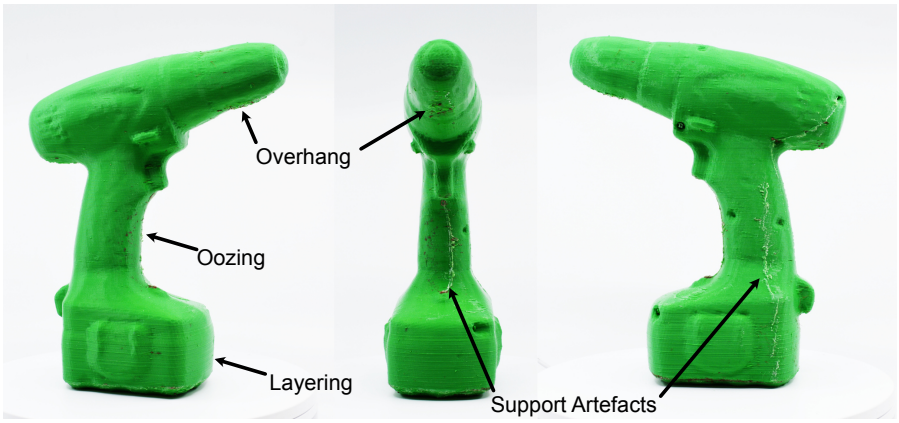

Figure 8.8: Fabricated case study product B with defects highlighted.

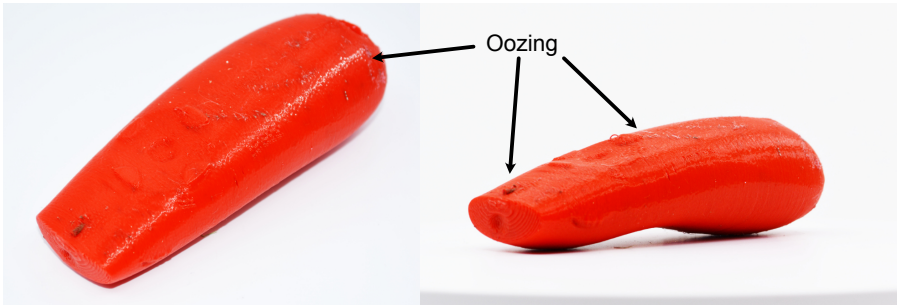

Figure 8.9: Fabricated case study product C with defects highlighted.

The evaluated mass property results for the presented fabrications are presented in Table 8.1. These were found through the same methods as discussed in Section 4.3.1. As previously stated, due to the mass of the products for case studies A and C, the measured RI values for the fabrications are likely to experience significant error. This is because the relative RI of the product is small compared to the RI of the system.

8.5 Discussion of Fabrication Results

It is shown in Table 10.2 that, generally, there is an improvement in the mass property error when comparing the computed conventional and fabricated emulated prototype mass properties. This demonstrates that the method has been successful in allowing MEX prototype mass properties to be better represented in MEX prototypes. However, there are instances where this is not the case.

Table 8.1: Case study fabrication result errors (relative to as-designed product). Conventional (computed) and computed emulation results also provided for reference.

	Product	Objective Function Value	Mass Error	CoM Error			RI Error		
				x	y	z	xx	yy	zz
Conventional (Computed)	A	52.8	-49.6%	-0.3%	-2.7%	0.3%	-87.6%	-38.0%	-67.7%
	B	92.9	-74.2%	0.2%	-3.7%	14.2%	-77.5%	-77.6%	-74.7%
	C	65.4	-34.5%	-1.2%	5.7%	24.0%	-60.6%	-63.9%	-92.4%
Computed Emulation	A	0.8	0.0%	-0.1%	-0.3%	-0.4%	-80.1%	-15.4%	-54.8%
	B	2.5	-0.1%	0.1%	-1.2%	1.1%	-32.5%	-30.6%	-27.8%
	C	28.9	-0.1%	-1.0%	6.1%	21.8%	-45.3%	-49.9%	-89.8%
Fabricated Emulation	A	8.3	5.8%	0.6%	-1.9%	0.0%	499.3%	-83.5%	259.9%
	B	49.6	-32.3%	-1.6%	-6.2%	-1.0%	-49.1%	-45.7%	-45.3%
	C	31.9	-5.2%	-0.9%	-0.6%	25.2%	169.8%	115.5%	75.9%

Although case studies A and C demonstrated mass errors of ± 5%, the mass error for case study B was significantly greater than expected. This was because of the issue presented in Figure 8.4, where the internal, supporting infill structure had collapsed. This meant that, especially in the upper section of the product, the high-density material could not be adequately deposited into the product. For a similar reason, the y-axis CoM position for case B was found to be further back than anticipated, as most of the forward mass was located in the upper portion of the volume. Future work should focus on ensuring that the supporting infill is deposited more reliably.

It is also worth noting that there is a general increase in absolute error between computational emulation and fabricated emulation. Therefore, it is likely that the method will be limited by the process variability, rather than the numerical analysis. There are likely mechanisms that could be leveraged to improve this accuracy, although this was out-of-scope due to the increased expertise required from a user. This is discussed in greater depth in Chapter 10.

The cost of fabricating the prototypes with the emulated mass properties was another important consideration. For the three case study parts, this is presented in Table 8.2 through reference to the material costs of fabrication. This costing is broken down by shell, high-density cells and low-density cells. As expected, for each case study product, the cost of material used in fabrication (relative to the conventional MEX fabrication) increases. This is shown in the ratio column.

Table 8.2: Material cost for the three case study prototypes with emulated mass properties.

Case Study	**Cost**				
	Shell	High Density Cells	Low Density Cells	Total	Ratio (rel. to conventional)
A	£ 0.73	£ 2.91	£ 0.33	£ 3.97	2.98
B	£ 17.06	£ 91.41	£ 1.84	£ 110.31	6.59
C	£ 1.28	£ 2.50	£ 0.62	£ 4.40	2.08

Case study B has both the highest absolute material cost and the largest multiplier relative to the conventional MEX fabrication. Principally, this was because the volume requires the largest increase in mass, with this driven by the material cost of the high-density cells. With present technology, it was not thought possible to improve this, though it may be possible to reduce this cost with future improvements in available materials.

The effect of failed prints was not considered within the costing completed and presented. For this reason, the effective cost of fabrication for each is likely to be higher than presented. For the cases considered, case B is likely to be the most affected by failed prints due to its size (and therefore extended print time). Future work should therefore ensure that the fabrication is as reliable as possible, with the issues around the support infill structure of particular concern at this stage.

Ensuring that the fabrication is as reliable as possible will also improve the fabrication time of the prototypes, which have also increased, as previously discussed. Although the process is highly-automated, and therefore the number of person-hours required to make the prototype is relatively unaffected, the absolute fabrication time has gone up to 8 hours (up from 2.1 hours), 9 days (up from 1.3 days), and 8 hours (up from 2.5 hours) for each of the case studies respectively. Other future work should try to improve this, also as discussed previously.

8.6 Chapter Summary

The three case study products were fabricated successfully, with clear improvement over conventional fabrications. However, issues remain around the geometric accuracy of fabrications, accuracy of fabricated infill and efficiency of fabrication. Each of these issues have been discussed in more detail, and potential methods for improvement have been proposed. As a proof-of-concept, what has been fabricated was considered acceptable, confirming that the method allows mass property emulation to be embedded in the MEX workflow (RQ 3).

Future work may also look at developing methods for ensuring consistency in deposition mass between the computed and physical depositions. This work should build on that presented, as well as that by Afonso *et al.* [199]. However, a singular set of parameters to use for the MEX process could not be proposed, with an individual's material, printer and environmental conditions affecting the results.

Chapter 9
Discussion

9.1 Chapter Overview

The work detailed so far presents a methodology for the emulation of mass properties within MEX properties. However, the implications of this work have not been discussed in detail. Within this chapter, generisability, accuracy, effect on process, and effect on prototyping are discussed.

9.2 Variable Infill Methodology Review

A method has been presented that allows a user - intended to be a designer - to fabricate a prototype using MEX with emulated mass properties. In this work, the mass properties of interest were found to be mass and CoM position. Through emulating these mass properties, the feel of MEX prototypes of consumer goods can be improved. This enables a greater level of information to be generated through the use of the prototype, especially for those that require a high-level of user-interaction (such as games controllers, tools, instruments and other consumer goods). To do this, a multi-stage process has been developed that leverages the current MEX process. This is shown in Figure 9.1.

The theoretical accuracy has been shown to be ~ 1% using the baseline parameter set. This parameter set is thought likely to be the best option for ease of use for designers. This could be improved to ~ 0.1% in most instances if the parameter values were adjusted on a case-by-case basis. However, the adjusted parameter values considered within this work neglected practical limitations including nozzle size and secondary MDR. Future technical developments may improve this.

Physical emulation accuracy also demonstrated improvements relative to conventional fabrications. Although the accuracy wasn't as good as theoretically predicted, this may be improved through calibration of the MEX process (as discussed in literature [199]) and improved print path planning. Improvements in print path planning may also enable improvements in print time and quality - with the associated manufacturing defects summarised in Figure 9.2 - that were highlighted as further limiting factors.

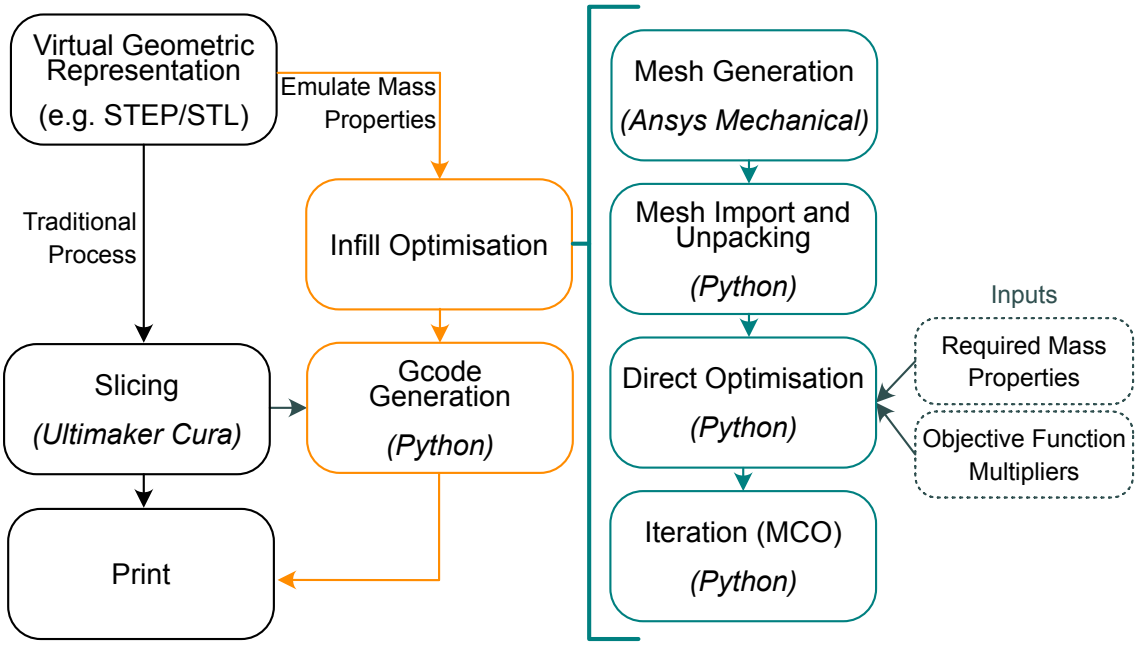

Figure 9.1: Flowchart showing the overall process that a designer follows to apply the process in its state at the time of writing.

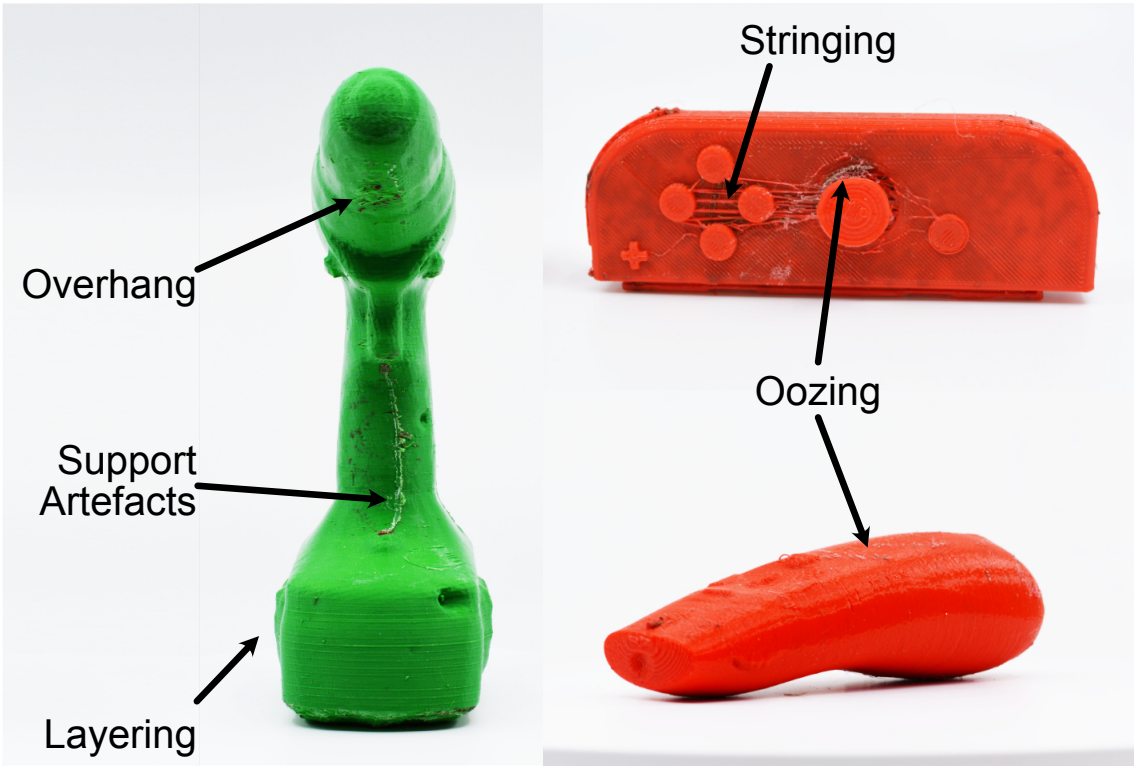

Figure 9.2: The three case study products with print quality issues summarised.

Revisiting the PDS in Figure 5.1 it is clear that a majority of the requirements have been met. The exceptions are F1 and F8. F1 - concerning the integration of the method in the MEX process - has somewhat been met, though it is likely that some calibration would be required (as discussed previously). Although this may be overcome, it is not as seamless as had been hoped at the outset of the project and may require extra work from a user. Similarly, F8 - concerning the retention of the prototype mass properties throughout the prototype life - was met for case studies A and C, but was not met for case study B. This was due to the support material failing in-process, and therefore requires further development to avoid this issue in future work. It was thought the most appropriate means to do this would be to update the shell geometry definition used, and improve the print path planning (as discussed).

It may also be sensible to update the criteria used in the PDS and Pugh matrix (see Table 5.2). For example, it has been shown that the print time has increased considerably for the three case studies considered. Although the process is automated - so the effect is reduced - this may reduce prototyping efficiency and negatively impact the design process. Further, design fixation may increase. For these reasons, the PDS and Pugh matrix may be updated to include print time. It may also be updated to consider weighting the criteria as deemed fit. As an example, emulation accuracy appears to have less of an effect than anticipated - with the worst method (variable infill) demonstrably achieving successful emulation.

The criteria (or weightings) may also be updated once an understanding of the appropriate emulation accuracy is developed (discussed further within this chapter). If a lower emulation accuracy is appropriate, then it may be possible to use a quicker, cheaper method of emulation. Hence, these criteria may be reviewed in future work.

9.3 Generalisability of Method

The developed emulation method has been developed with general applicability in mind, with the considered case studies demonstrating that the method can be applied to a wide array of products. However, the work is currently positioned to target hand-held products, intended for user-interaction. This was done as these were thought the most likely products that the methodology would be applied to. There exists, however, a set of products for which emula-

tion of mass properties would be beneficial yet are not interacted with by users. For example, motors, crank shafts or other products that will undergo motion. For these products, the assumption that principal RI can be neglected does not hold true. For this reason, modifications to the process may be required. It is thought this could be achieved through additional considerations in the application of the probability distribution across the internal volume. For example, changing the probability distribution to be related to both the distance and square-distance of a cell from the target position. For most handheld, consumer products, however, the process would be applicable and provide satisfactory results.

9.4 Accuracy of Method

It has been shown that the accuracy of the computational emulation process is sufficiently accurate based on the work presented in Chapter 8. The fabricated case studies demonstrate greater error than is expected from the computational process. The computational accuracy is, currently, appropriate for the application. It is, however, recognised that it has not been possible to determine whether the fabricated product emulation accuracy is sufficient for the given application(s). To do this, it is thought a significant study would be required, investigating the error that can be perceived by users. This is likely to be product and use case specific and is not undertaken here. Instead, it is likely that any future application should have a calibration stage where required accuracy is assessed. Although this would have a cost overhead associated with it, doing so may mean that computational and fabrication costs are reduced.

9.5 Effect on Material Extrusion Pre-Process

Due to how the process was developed, the emulation method should have a minimal effect on the design process. In essence, the only additional step is for the developed method to be applied. However, there are instances where the design and pre-processing of a product may have an effect.

9.6 Effect on Prototype Mechanical Properties

Although the prototypes that leverage this method did not require careful control of mechanical properties, the processes effects on them should be considered. The most significant change in this regard, was to have the main supporting infill structure now oriented in one direction. This meant that there was a single direction load path. This will reduce the prototype's torsional and tensile strength (in the neglected axis). Further, the z-axis tensile strength may be reduced due to oozing reducing the adhesion between layers.

9.7 Limitation to Product Volume

The emulation of CoM positions in axes that required large relative movement from the GC(where the moment arm required approaches the volume boundary) was challenging. Although the associated products would often be edge cases they are an important consideration. Primarily, this was because they would benefit most from mass property emulation in early-stage design. This is due to the error being larger for these products when using conventional fabrication methods. The primary cause is that sufficient mass cannot be placed far enough away from the GC. This is due to the product mass and volume envelope being restrictive or due to inadequate material density options. For the latter, it may be possible to develop alternative materials, while the former is a fundamental limitation. However, it may be possible to improve the presented methodology through applying limitations to the internal volume CoM search method.

From a design perspective, a user may decide that small changes to the form of a prototype are acceptable. If the laser pointer from case C is considered, it may be possible to elongate the lower geometry to allow the required CoM target to fall within the geometry (thus allowing the target CoM to be achieved). To do this would currently require manual modification, though it may be possible to automatically generate this geometry in future toolchains. It is recognised that this is unlikely to be appropriate in all instances, but may be suitable when combined with the use of virtual reality or similar (when the visual of the prototype is less important in the real world).

9.8 User Process

For a general example, a user is now required to use three additional tools – Ansys, the emulation script and the slicing script. In addition, the user is required to provide the intended mass properties. Although this appears significant, the hypothesised expertise required to leverage the methods is low - with much of these process highly automated. Further, it is thought that the tools could be integrated into a single toolchain – discussed in Section 10.4.2. It should also be possible to avoid the use of Ansys through the use of open-source meshing methods in future work.

9.9 Effect on Prototype Fabrication Process

Due to the nature of the process development, the effect on the fabrication process is limited. Compared to a conventional MEX process, only two principal modifications are required:

1. The use of a secondary print material is suggested, with this ideally done using a secondary nozzle on the print head,
2. A hardened second nozzle for use with abrasive materials that are currently able to provide a higher material density.

Other process effects are discussed herein.

9.9.1 Calibration of Fabrication Process

Afonso *et al.* [199] previously discussed how changing MEX parameters affects the deposited mass with part production. To be confident of the deposition mass, it is therefore necessary to calibrate the hardware used (machine, material and environment). Within this work, this was not considered. This was due to the proposed use of the technology in design office settings, potentially by non-expert users and/or under tight time constraints. As such, the fabrication process presented was completed using standard Cura print parameters with the manufacturer material settings. The only exception to this was on retraction, which may be improved

in future work. It was generally demonstrated that the error, although not as good as the computed result, remained small. Further, improvement is clear compared to the conventional result.

9.9.2 Fabrication Quality and Time

As was shown in Figure 9.2, as well as in Chapter 8, there were several issues with the observable print quality of the fabricated case studies. These were often due to stringing and material oozing - caused by the lack of retraction. Issues with support, layering and overhangs were also observed.

Also in Chapter 8, the print times of the case studies was found to be significantly longer than for conventional MEX fabrications (8 hours up from 2.1 hours, 9 days up from 1.3 days, and 8 hours up from 2.5 hours for the case studies A, B and C respectively). This was fundamentally due to two reasons. The first was that the increase in deposited material volume required the process to take longer. The second, and more controllable, was due to an issue with the print path planning.

The developed fabrication methodology generates gcode on a cell-by-cell basis. Although this ensures that every cell will be considered, and will be printed using consistent machine code, it does not allow for the efficient movement between cells. Whereas conventional slicing software will calculate the most efficient path for the deposition head to move through, the developed method will generate many small movements that often require the head to accelerate in an orthogonal axis. This is inefficient, stopping the deposition head from accelerating to normal printing speed and requiring many retractions. Both print quality and print time could therefore be improved through the use of a more efficient print path. It was thought that this could be done using existing software and was therefore not investigated further within this work.

9.10 Effect on Prototyping Activity

The developed method enables the highly-automated MEX prototyping of designs with emulated mass properties. This would improve the feel of the prototype, allowing a greater level of information to be disseminated and, therefore, improve the learning from the process. There is scope for improving this with calibration of the MEX process for accurate mass deposition. Further, it has been demonstrated that alternative mass properties to the as-designed product's mass properties can be prototyped. This allows rapid investigation into the effect of a product's mass properties on user-interaction without full product redesign. This is possible using a completely automated process with minor modification to the MEX process.

This comes at the cost - both time and economic - increasing compared to equivalent, conventional MEX fabrications. It has also not been possible to assess whether the accuracy of emulation is sufficient. Although future work may reduce the costs and develop a baseline understanding of the required accuracy, it is unlikely they will be completely overcome. As such, use of the method should be targeted to ensure appropriate allocation of resources throughout the design process.

9.11 Chapter Summary

The implications of the developed process were assessed and their effect considered. This was done at a high level - i.e. how the process can be applied - and for aspects within the process itself. It is thought that the process presents a successful proof-of-concept method for the emulation of mass properties in prototypes, with a high-level of accuracy numerically achieved. Although physical fabrication accuracy wasn't as good as predicted, there are clear routes to improve this whilst also reducing fabrication time and cost. Fabrication quality and representation of computed result would likely be improved through the same methods. Before undertaking this work, it is recommended that required emulation accuracy is assessed, as the developed process may already be suitably accurate.

For application to prototypes, the process should be used where there is clear benefit to ensure efficient allocation of resources. This is because the process will normally require greater fabrication time and resources. However, where user-interaction is important, there is clear benefit over existing techniques.

Chapter 10
Conclusions and Future Work

10.1 Chapter Overview

The thesis has presented the development of a method to allow for mass properties to be emulated in MEX prototypes. This chapter concludes the thesis; reviewing the initial aims and research questions to ascertain whether the work has met the original goal and outlining future work based on learning developed.

10.2 Thesis Overview

The work undertaken to answer the RQs and demonstrate fulfilment of the aim is presented throughout the 10 chapters of this thesis.

Chapter 1 introduces the work, the aim and the RQs. Further, a breakdown on the work is presented.

Chapter 2 then discusses and presents relevant literature around prototyping, a cornerstone of the work. Examples of prototypes where the "feel" of the prototype is deemed important are discussed. It is also shown that the rapid fabrication of prototypes is a key part of the design process, and that one method to enable this is the use of AM.

Chapter 3 progresses this work, reviewing the state of the art in AM, with a focus on the technologies used for prototyping. MEX is identified as the most widely used technology, with explanation of its function provided, and core limitations and advantages discussed. The chapter concludes by reviewing the issues the conventional MEX process demonstrates in enabling the emulation of product mass properties in the associated prototypes.

This knowledge is then used in the work presented in **Chapter 4**, that assesses how mass properties are perceived by users of products and prototypes. This is done through several means, including; industry interview, user study, literature review and biomechanic analysis. It is shown that the mass and CoM of a product are important, perceivable mass properties whilst principal RI is not as noticeable for most handheld applications.

Chapter 5 evaluates potential methods for emulating mass properties, now that it is understood how they are perceived. The considered methods included the use of lumped masses, particulates and fluids, and the use of variable infill. It is found that a variable infill methodology - where cellwise infill is changed through a body within the MEX process - is preferred through application of a conventional design process. Principally, this is because the process required little change to the current MEX process, no additionally fabrication of parts, and could continue to be fully automated. Initial process setup considerations are discussed, with a finite volume mesh and binary cell composition identified to be favourable for progression of the method.

Chapter 6 then starts to develop the variable infill method, and baselines the work for a primitive form factor (a cube). To do this, various optimisation and evaluation methods are assessed, with a directed optimisation approach employed. This method uses the mass properties as variables within an optimisation process, allowing the method to work independently of geometric form. This was important to improve computational efficiency and enable application to currently undefined, complex geometric forms. An initial set of controlling parameters are identified, and their individual effects assessed on emulation accuracy. A set of baseline values for these controlling parameters were then decided upon and presented.

This is then progressed in **Chapter 7** with the developed method applied to three case study products. These were a games controller, electric hand drill, and laser pointer. It was shown that mass properties may be computationally emulated to within ~1% using the baseline parameter set. A sensitivity analysis is then undertaken that aimed to improve the computed result, demonstrating mass property emulation to within ~0.1% of the as-designed properties (in most instances).

Chapter 8 investigates the fabrication of the three case study products, with a slicing method and fabricated parts produced. It is shown that the as-fabricated products demonstrate significantly worse error in mass property emulation compared to the computed result. Methods for improving this are discussed; such as the calibration of the MEX process or maturing the print path planning. However, it is recognised that understanding of the required emulation accuracy should lead this to ensure efficiency of resource allocation.

Chapter 9 discusses the implications and intricacies of the method developed with respect to process intricacies and effect of process on prototyping. **Chapter 10** concludes the thesis with a review of the aim and RQs, and closes with suggestion of future work that may be carried out.

10.3 Conclusion

To finish this thesis, a review of the thesis aim was undertaken through assessment of the RQs. The thesis aim was stated in Chapter 1 as:

Improve the influence of mass properties in user-interaction of MEX prototypes.

To do this, three RQs are answered throughout this thesis. From this, a method for emulating mass properties in MEX prototypes has been developed. Excellent computational accuracy has been shown, with fabrication results also demonstrating improvement over conventional methods. The anwers to the RQs through the thesis are summarised within the proceeding sections, more explicitally demonstrating that the thesis aim has been fulfilled.

10.3.1 Research Question 1

RQ 1 was presented in Chapter 1 as:

How important are mass properties of MEX prototypes?

To investigate the answer to RQ1, initial work identified and assessed key literature to provide context to the problem. From this work, it was clear that the feel of a prototype is particularly important in user-centric product prototyping (Chapter 4). Further, analysis of the biomechanics demonstrates that principal product RI is often of negligible importance for handheld products – agreeing with literature. Finally, a user study was completed demonstrating that the mass properties of MEX prototypes are clearly recognised as properties for

improvement. Therefore, although it has not been possible to quantify the effective importance of each mass property within prototyping, it has been possible to conclude that mass properties are important considerations.

10.3.2 Research Question 2

RQ 2 was:

How can mass properties be emulated in MEX prototypes?

In Chapter 5, three methods for mass property emulation in MEX prototypes were identified and assessed. There were variable infill, particulates, and lumped masses. Each of these methods were explained, and the hypothetical advantages and disadvantages discussed. The chapter concludes with the decision to use a methodology cantered around the variable infill methodology – where the MEX machine deposits material within the internal volume to achieve the mass properties. This provided the foundation to the answer to RQ2.

Chapters 6 and 7 then developed, baselined, and applied the variable infill methodology. This work demonstrated, through consideration of process limitations, what is theoretically possible – with application to a games controller, an electric hand drill and a laser pointer. It is shown that, except for the z-axis CoM accuracy for the laser pointer, significant improvement could be achieved in the mass and CoM positional accuracy. The z-axis CoM position of the laser pointer could not be significantly improved due to the relative offset between CoM and GC. Principal RI is also improved, though not directly optimised, which should be a net positive for application to consumer goods.

Fabrication of the computed distributions in Chapter 8 demonstrated that the errors generally worsen compared to the computed accuracy. This was due to MEX process variability and hardware calibration affecting the deposited mass, although process specific issues were also identified. This said, improvement relative to conventional MEX fabrications was evident in all instances.

10.3.3 Research Question 3

RQ 3 focussed on how the process may be embedded into the current MEX process:

How can mass property emulation be embedded into the MEX process?

Due to the nature of the method adopted and development process, the method could be inherently embedded into the MEX process. The only extra considerations were (in most instances) for the process to use a secondary material and for this process to possibly increase wear on the deposition nozzle.

To ensure that it was possible to do this, a slicer was developed in Python that outputs a combination of original code and Cura output (Chapter 8). It was found that, although future improvements are possible, standard desktop MEX machines are capable of fabricating the required prototypes.

10.3.4 Contributions

In conclusion, the following contributions are made by this work in fulfillment of the aim:

1. The construction of a set of user and industrial data demonstrating that mass properties are important considerations in early-stage prototyping.
2. An assessment of the effect of principal rotational inertia on a user's perception of a prototype such that rotational inertia could be neglected in emulation methods.
3. An assessment of the potential emulation methods that may be integrated into the current material extrusion 3D printing workflow.
4. The development and characterisation of a method to allow mass properties to be emulated in material extrusion prototypes using variable infill density.
5. The application of the developed method to a series of case studies, demonstrating applicability in real-world cases and tuning of the method.
6. The development of a fabrication method for 3D printed prototypes with emulated mass properties by variable infill.

10.4 Future Work

Although a viable methodology has been presented, scope for improvement was recognised. Some of the clear potential future work streams are presented herein.

10.4.1 Alternative Emulation Methods

Investigation of the use of alternative emulation methods in MEX prototypes should be undertaken. This is suggested to be methods that have previously been proposed in Chapter 5. For example, the use of standard parts as lumped masses may provide benefit for near-net mass properties to be achieved to sufficient accuracy. The work should target the relevant disadvantages – principally complication of integration into the MEX process for this example.

In addition, it would be interesting to investigate whether any of the methods could be combined such that the process advantages may be leveraged, and the disadvantages overcome. If an example is considered where lumped masses and variable infill is combined; the main mass modification can be achieved through the use of large lumped mass(es), whilst the fine control of CoM can be achieved using variable infill. This should reduce overall fabrication time and costs, though complexity of fabrication is increased.

10.4.2 Integration of Tools

One of the clear areas for improvement is the integration of design tools developed through this study. Currently, three additional steps are required (over and above the normal MEX process) that:

1. Generate CHEXA mesh
2. Compute a volume-wide cell composition
3. Generate bespoke g-code.

For the purposes of this work – which was for a proof-of-concept – Ansys Mechanical and Python were used. To improve this workflow, integration of tools into a single toolchain would be beneficial. This would improve process efficiency and further decrease the user expertise required.

To enable the toolchain to be integrated, Ultimaker Cura could be leveraged (or another slicer). To do this, the Python based API should allow an add-in to be developed with little modification to the current scripts.

10.4.3 Infill Structure Development

In case study B, issues with the supporting infill structure were observed (as seen in Chapter 8). This was primarily due to the way that the infill structure blended with the shell – exaggerated in the work due to the use of separate shell and internal volume meshes. Future work could improve upon this by considering the interface more closely, ensuring that the infill is properly deposited and thereby allowing the high-density cells to be properly supported. This may additionally need greater support material to be deposited within the internal volume.

Additionally, the supporting infill structure could be generated based upon the location of the high-density cells. This would allow greater support to be provided where necessary, whilst keeping the overall infill mass low. The slicing process may be complicated by this, but closer integration into Cura may allow the pre-built slicing methods to be leveraged. This would reduce the expertise required (and other associated overheads).

10.4.4 Development of Materials

Finally, future work may investigate the development of high-density, low-cost materials intended for deposition in MEX prototypes to manipulate mass properties. It has already been shown that the use of higher density materials is beneficial to the accuracy of the emulation. Further, cost has demonstrably increased in all cases considered. Current MEX materials may allow for higher density depositions – such as the BASF Ultrafuse material [189] – though this often comes with an increase in cost. It is thought that one of the principal challenges is as-

sociated with how metal particulates are suspended in the thermoplastic. For this application, it may be possible to use larger metal particulates, which would be averaged out over the deposition (as all deposition will be internal). However, a transition to larger nozzle machines may be required to accommodate (and avoid blockages). On the other hand, the use of a higher density material may decrease costs, despite increased material costs, as the deposition volume reduces. This reduces process time, required energy (assuming same processing parameters) and should reduce the chance of print failure.

10.4.5 Understanding of Required Accuracy

Development of an understanding for the required mass property emulation accuracy has not yet been undertaken. Through improved understanding of the required accuracy, the process efficiency can be improved by targeting higher accuracy, reduced costs, reduced print time or otherwise. To do this, a user study is likely required that considers a range of users, products, MEX representations and use cases. This was considered outside of scope for this project, as the methodology can be tailored to provide improved accuracy or efficiency as needed. However, application of the methodology would benefit from this work.

10.5 Thesis Summary

It has been shown, through the consideration of the RQs originally presented in Chapter 1, that the thesis aim has been fulfilled. The study has demonstrated a viable methodology that allows for the emulation of mass properties in MEX prototypes. This has been assessed to be useful in prototyping for products intended for user-interaction. To do this, a process that leverages the automated deposition of infill within MEX prototypes has been used. The process has been generalised, as much as practicable, to allow a non-expert designer to use the method without specialist equipment. Areas for improvement and future work have also been identified and discussed. These include the development of additional materials, integration of toolchain, and investigation of alternative emulation methods.

References

[1] S. Houde and C. Hill. “What do Prototypes Prototype?” In: *Handbook of Human-Computer Interaction* (1997). Publisher: Elsevier, pp. 367–381. DOI: 10.1016/b978-044481862-1.50082-0.

[2] B. Camburn et al. “Design prototyping methods: State of the art in strategies, techniques, and guidelines”. In: *Design Science* 3 (Schrage 1993 Apr. 3, 2017), e13. DOI: 10.1017/dsj.2017.10.

[3] D. G. Ullman. *The Mechanical Design Process*. 2010.

[4] James Dyson Foundation. *Dyson Design Process Box*. Dyson Design Process Box. Pages: 32. 2019. (Visited on 10/04/2019).

[5] S. Dowling. *Frustration and failure fuel Dyson’s success*. en. Mar. 2013. URL: https://www.bbc.com/future/article/20130312-failure-is-the-best-medicine (visited on 07/10/2022).

[6] J. Blomkvist and S. Holmlid. “Existing Prototyping Perspectives: Considerations for Service Design”. In: *Nordic Design Research Conference* (June 2011). ISBN: 2222222222222, pp. 1–10.

[7] M. Buchenau and J. F. Suri. “Experience prototyping”. In: *Proceedings of the conference on Designing interactive systems processes, practices, methods, and techniques - DIS ’00*. Issue: October ISSN: 3037782250. New York, New York, USA: ACM Press, 2000, pp. 424–433. DOI: 10.1145/347642.347802.

[8] K. T. Ulrich and S. D. Eppinger. *Product Design and Development*. McGraw-Hill, 2016.

[9] B. Hallgrimsson. *Prototyping and Modelmaking for Product Design*. Laurence King Publishing, 2012.

[10] L. S. Jensen et al. “Prototyping in mechatronic product development: How prototype fidelity levels affect user design input”. In: *Proceedings of International Design Conference, DESIGN* 3 (2018). ISBN: 9789537738594, pp. 1173–1184. DOI: 10.21278/idc.2018.0415.

[11] E. Gerber. “Prototyping: Facing Uncertainty through Small Wins”. In: *DS 58-9: Proceedings of ICED 09, the 17th International Conference on Engineering Design, Vol. 9, Human Behavior in Design, Palo Alto, CA, USA, 24.-27.08.2009* (2009), pp. 333–342.

[12] C. Lauff, D. Kotys-Schwartz, and M. E. Rentschler. “Perceptions of Prototypes: Pilot Study Comparing Students and Professionals”. In: ASME 2017 International Design Engineering Technical Conferences and Computers and Information in Engineering Conference. American Society of Mechanical Engineers Digital Collection, Nov. 3, 2017. DOI: 10.1115/DETC2017-68117.

[13] D. Mathias et al. “Accelerating product prototyping through hybrid methods: Coupling 3D printing and LEGO”. In: *Design Studies* (2019). DOI: 10.1016/j.destud.2019.04.003.

[14] M. McCurdy et al. “Breaking the Fidelity Barrier: An Examination of Our Current Characterization of Prototypes and an Example of a Mixed-Fidelity Success”. In: *Proceedings of the SIGCHI Conference on Human Factors in Computing Systems*. Series Title: CHI ’06. New York, NY, USA: Association for Computing Machinery, 2006, pp. 1233–1242. DOI: 10.1145/1124772.1124959.

[15] J. Sauer and A. Sonderegger. “The influence of prototype fidelity and aesthetics of design in usability tests: Effects on user behaviour, subjective evaluation and emotion”. In: *Applied Ergonomics* (2009). DOI: 10.1016/j.apergo.2008.06.006.

[16] C. Donati and M. Vignoli. “How tangible is your prototype? Designing the user and expert interaction”. In: (2015). DOI: 10.1007/S12008-014-0232-5.

[17] C. Hamon et al. “Virtual or Physical Prototypes? Development and Testing of a Prototyping Planning Tool”. In: Jan. 1, 2014.

[18] J. Verlinden and I. Horváth. “Analyzing opportunities for using interactive augmented prototyping in design practice”. In: *AI EDAM* 23.3 (Aug. 2009). Publisher: Cambridge University Press, pp. 289–303. DOI: 10.1017/S0890060409000250.

[19] A. Wiethoff et al. “Paperbox: a toolkit for exploring tangible interaction on interactive surfaces”. In: *Proceedings of the 9th ACM Conference on Creativity & Cognition*. C&C ’13. New York, NY, USA: Association for Computing Machinery, June 17, 2013, pp. 64–73. DOI: 10.1145/2466627.2466635.

[20] L. Erik. “A Review of Virtual Prototyping Approaches for User Testing of Design Solutions”. In: 2015.

[21] Sculpteo. *The State Printing of 3D Printing 2021*. 2021.

[22] ASTM International. *Standard terminology for additive manufacturing technologies : designation F2792-12a*. West Conshohocken, PA: ASTM International, 2012.

[23] B. Redwood, F. Schöffer, and B. Garret. *The 3D Printing Handbook: Technologies, Design and Applications*. 3D Hubs B.V., 2017.

[24] M. Goudswaard et al. “REVISITING PROTOTYPING IN 2020: A SNAPSHOT OF PRACTICE IN UK DESIGN COMPANIES”. In: *Proceedings of the Design Society* 1 (Aug. 2021). Publisher: Cambridge University Press, pp. 2581–2590. DOI: 10.1017/pds.2021.519.

[25] H. Felton, J. Yon, and B. Hicks. “LOOKS LIKE BUT DOES IT FEEL LIKE? INVESTIGATING THE INFLUENCE OF MASS PROPERTIES ON USER PERCEPTIONS OF RAPID PROTOTYPES”. In: *Proceedings of the Design Society: DESIGN Conference* 1 (May 11, 2020). Publisher: Cambridge University Press, pp. 1425–1434. DOI: 10.1017/dsd.2020.111.

[26] R. Cross and R. Bower. “Effects of swing-weight on swing speed and racket power”. In: *Journal of Sports Sciences* 24.1 (Jan. 1, 2006). Publisher: Routledge, pp. 23–30. DOI: 10.1080/02640410500127876.

[27] L. S. Jensen, A. G. Özkil, and N. H. Mortensen. “Prototypes in engineering design: Definitions and strategies”. In: *Proceedings of International Design Conference, DESIGN* DS 84 (2016), pp. 821–830.

[28] K. Schneider. “Prototypes as assets, not toys. Why and how to extract knowledge from prototypes. (Experience report)”. In: *Proceedings of IEEE 18th International Conference on Software Engineering*. ISSN: 02705257. IEEE Comput. Soc. Press, 1996, pp. 522–531. DOI: 10.1109/ICSE.1996.493446.

[29] M. Beaudouin-Lafon and W. E. Mackay. “Prototyping Tools and Techniques”. In: *The Human–Computer Interaction Handbook* (2003), pp. 1081–1104. DOI: 10.1201/b11963-ch-47.

[30] E. J. Christie et al. “Prototyping strategies: Literature review and identification of critical variables”. In: *ASEE Annual Conference and Exposition, Conference Proceedings* (2012). ISBN: 9780878232413. DOI: 10.18260/1-2--21848.

[31] J. A. Drezner. *The Nature and Role of Prototyping in Weapon System Development*. Santa Monica, CA: RAND Corporation, 1992.

[32] I. Goldfarb and I. Kondratova. “Visual Interface Design Tool for Educational Courseware.” In: 2004, pp. 272–277.

[33] K. Otto and K. Wood. *Product Design: Techniques in Reverse Engineering and New Product Development*. 2001.

[34] K. Lindow and A. Sternitzke. “The Evolution from Hybrid to Blended to Beyond Prototyping”. In: *Rethink! Prototyping: Transdisciplinary Concepts of Prototyping* (Jan. 1, 2016). Publisher: Springer, Cham ISBN: 9783319244396, pp. 85–87. DOI: 10.1007/978-3-319-24439-6_7.

[35] M. C. Yang. “A study of prototypes, design activity, and design outcome”. In: *Design Studies* 26.6 (2005), pp. 649–669. DOI: 10.1016/j.destud.2005.04.005.

[36] R. Hannah, A. Michaelraj, and J. D. Summers. “A Proposed Taxonomy for Physical Prototypes: Structure and Validation”. In: *Volume 1: 34th Design Automation Conference, Parts A and B*. Vol. Volume 1: Series Title: International Design Engineering Technical Conferences and Computers and Information in Engineering Conference. ASMEDC, Jan. 1, 2008, pp. 231–243. DOI: 10.1115/DETC2008-49976.

[37] M. B. Wall, K. T. Ulrich, and W. C. Flowers. “Making Sense of Prototyping Technologies for Product Design”. In: vol. 3rd Intern. Series Title: International Design Engineering Technical Conferences and Computers and Information in Engineering Conference. 1991, pp. 151–158. DOI: 10.1115/DETC1991-0042.

[38] M. Jensen, S. Balters, and M. Steinert. “Measuring prototypes-a standardized quantitative description of prototypes and their outcome for data collection and analysis”. In: *Proceedings of the International Conference on Engineering Design, ICED* 2 (DS 80-02 2015), pp. 1–14.

[39] L. J. Leifer and M. Steinert. “Dancing with ambiguity: Causality behavior, design thinking, and triple-loop-learning”. In: *Information Knowledge Systems Management* 10.1 (2011). Publisher: IOS Press, pp. 151–173. DOI: 10.3233/IKS-2012-0191.

[40] T. Hess and J. D. Summers. “Case study: Evidence of prototyping roles in conceptual design”. In: *Proceedings of the International Conference on Engineering Design, ICED* 1 DS75-01 (August 2013). ISBN: 9781904670445, pp. 249–258.

[41] D. Mathias et al. “Characterising the affordances and limitations of common prototyping techniques to support the early stages of product development”. In: *Proceedings of International Design Conference, DESIGN* 3 (2018). ISBN: 9789537738594, pp. 1257–1268. DOI: 10.21278/idc.2018.0445.

[42] J. Menold, K. Jablokow, and T. Simpson. “Prototype for X (PFX): A holistic framework for structuring prototyping methods to support engineering design”. In: *Design Studies* 50 (2017), pp. 70–112. DOI: https://doi.org/10.1016/j.destud.2017.03.001.

[43] G. G. Wang. “Definition and review of virtual prototyping”. In: *Journal of Computing and Information Science in Engineering* 2.3 (2002), pp. 232–236. DOI: 10.1115/1.1526508.

[44] C. Voss and L. Zomerdijk. “Innovation in experiential services–an empirical view”. In: (2007).

[45] Merriam-Webster. *Fidelity | Definition of Fidelity by Merriam-Webster*. URL: https://www.merriam-webster.com/dictionary/fidelity (visited on 11/22/2021).

[46] E. R. Coutts, A. Wodehouse, and J. Robertson. “A Comparison of Contemporary Prototyping Methods”. In: *Proceedings of the Design Society: International Conference on Engineering Design* 1.1 (July 26, 2019), pp. 1313–1322. DOI: 10.1017/dsi.2019.137.

[47] E. Gerber and M. Carroll. “The psychological experience of prototyping”. In: *Design Studies* 33.1 (Jan. 1, 2012), pp. 64–84. DOI: 10.1016/j.destud.2011.06.005.

[48] J. Rudd, K. Stern, and S. Isensee. “Low vs. high-fidelity prototyping debate”. In: *Interactions* 3.1 (1996), pp. 76–85. DOI: 10.1145/223500.223514.

[49] F. Egger. *Lo-Fi vs. Hi-Fi Prototyping: how real does the real thing have to be?* Telono. Jan. 19, 2000. URL: https://www.telono.com/en/publications-en/lo-fi-vs-hi-fi-prototyping-how-real-does-the-real-thing-have-to-be/ (visited on 11/23/2021).

[50] J. K. Liker and R. M. Pereira. “Virtual and Physical Prototyping Practices: Finding the Right Fidelity Starts With Understanding the Product”. In: *IEEE Engineering Management Review* 46.4 (2018). Conference Name: IEEE Engineering Management Review, pp. 71–85. DOI: 10.1109/EMR.2018.2873792.

[51] T. F. Schubert et al. “The impact of a prototype exemplar on design creativity: A case study in novice designers”. In: *ASEE Annual Conference and Exposition, Conference Proceedings* (2012). ISBN: 9780878232413. DOI: 10.18260/1-2--22064.

[52] V. K. Viswanathan and J. S. Linsey. “Role of Sunk cost in engineering idea generation: An experimental investigation”. In: *Journal of Mechanical Design, Transactions of the ASME* 135.12 (2013), pp. 1–12. DOI: 10.1115/1.4025290.

[53] R. J. Youmans. “The effects of physical prototyping and group work on the reduction of design fixation”. In: *Design Studies* 32.2 (2011), pp. 115–138. DOI: 10.1016/j.destud.2010.08.001.

[54] C. Lauff, J. Menold, and K. L. Wood. “Prototyping Canvas: Design Tool for Planning Purposeful Prototypes”. In: *Proceedings of the Design Society: International Conference on Engineering Design* 1.1 (July 2019). Publisher: Cambridge University Press, pp. 1563–1572. DOI: 10.1017/dsi.2019.162.

[55] P.-A. Arrighi and C. Mougenot. “Towards user empowerment in product design: a mixed reality tool for interactive virtual prototyping”. In: *Journal of Intelligent Manufacturing* 30.2 (Feb. 1, 2019), pp. 743–754. DOI: 10.1007/s10845-016-1276-0.

[56] T. Fröhlich et al. “VRBox: A Virtual Reality Augmented Sandbox for Immersive Playfulness, Creativity and Exploration”. In: *Proceedings of the 2018 Annual Symposium on Computer-Human Interaction in Play*. CHI PLAY ’18. New York, NY, USA: Association for Computing Machinery, Oct. 23, 2018, pp. 153–162. DOI: 10.1145/3242671.3242697.

[57] L. Kent, C. Snider, and B. Hicks. “Mixed Reality Prototyping: Synchronicity and Its Impact on a Design Workflow”. In: *Proceedings of the Design Society* 1 (August 2021), pp. 2117–2126. DOI: 10.1017/pds.2021.473.

[58] L. Kent et al. “Mixed reality in design prototyping: A systematic review”. In: *Design Studies* 77 (2021). Publisher: Elsevier Ltd, p. 101046. DOI: 10.1016/j.destud.2021.101046.

[59] L. Kent, C. Snider, and B. Hicks. *Engaging Citizens with Urban Planning Using City Blocks, a Mixed Reality Design and Visualisation Platform*. Springer International Publishing, 2019. 51-62. DOI: 10.1007/978-3-030-25999-0_5.

[60] F. Zorriassatine et al. “A survey of virtual prototyping techniques for mechanical product development”. In: *Proceedings of the Institution of Mechanical Engineers, Part B: Journal of Engineering Manufacture* 217.4 (Apr. 1, 2003). Publisher: IMECHE, pp. 513–530. DOI: 10.1243/095440503321628189.

[61] B. Macomber and M. Yang. “The role of sketch finish and style in user responses to early stage design concepts”. In: *Proceedings of the ASME Design Engineering Technical Conference* 9 (2011). ISBN: 9780791854860, pp. 567–576. DOI: 10.1115/DETC2011-48714.

[62] ISO International Organization for Standardization. *ISO 10303-242:2020 - Industrial automation systems and integration — Product data representation and exchange — Part 242: Application protocol: Managed model-based 3D engineering*. Pages: 11. 2020.

[63] S. P. S. Leino, T. Koivisto, and A. Riitahuhta. “Value of virtual prototyping -a strategic resource based view”. In: *Proceedings of the International Conference on Engineering Design, ICED* 4 DS75-04 (August 2013). ISBN: 9781904670476, pp. 249–258.

[64] H. Aoyama and Y. Kimishima. “Mixed reality system for evaluating designability and operability of information appliances”. In: *International Journal on Interactive Design and Manufacturing (IJIDeM)* 3.3 (Aug. 1, 2009), pp. 157–164. DOI: 10.1007/s12008-009-0070-z.

[65] E. Akaoka, T. Ginn, and R. Vertegaal. “DisplayObjects: prototyping functional physical interfaces on 3d styrofoam, paper or cardboard models”. In: *Proceedings of the fourth international conference on Tangible, embedded, and embodied interaction*. TEI ’10. New York, NY, USA: Association for Computing Machinery, Jan. 24, 2010, pp. 49–56. DOI: 10.1145/1709886.1709897.

[66] G. Cascini et al. “Exploring the use of AR technology for co-creative product and packaging design”. In: *Computers in Industry* 123 (Dec. 1, 2020), p. 103308. DOI: 10.1016/j.compind.2020.103308.

[67] T. L. Woods et al. “Pilot Study Using the Augmented Reality Sandbox to Teach Topographic Maps and Surficial Processes in Introductory Geology Labs”. In: *Journal of Geoscience Education* 64.3 (Aug. 19, 2016). Publisher: Routledge, pp. 199–214. DOI: 10.5408/15-135.1.

[68] L. Kent and Design and Manufacturing Futures Lab. *City Blocks – Urban Planning Through Play – Design and Manufacturing Futures Lab*. Design and Manufacturing Futures Lab. 2018. URL: https://dmf-lab.co.uk/blog/cityblocks/ (visited on 11/22/2021).

[69] D. Jones et al. “Characterising the Digital Twin: A systematic literature review”. In: *CIRP Journal of Manufacturing Science and Technology* 29 (May 1, 2020), pp. 36–52. DOI: 10.1016/j.cirpj.2020.02.002.

[70] J. Perret and E. Vander Poorten. “Touching Virtual Reality: A Review of Haptic Gloves”. In: *ACTUATOR 2018; 16th International Conference on New Actuators*. June 2018, pp. 1–5.

[71] M. Deininger et al. “Does prototype format influence stakeholder design input?” In: *DS 87-4 Proceedings of the 21st International Conference on Engineering Design (ICED 17) Vol 4: Design Methods and Tools, Vancouver, Canada, 21-25.08.2017* (2017). ISBN: 9781904670926, pp. 553–562.

[72] M. C. Frank, R. A. Wysk, and S. B. Joshi. “Rapid Prototyping Using CNC Machining”. In: ASME 2003 International Design Engineering Technical Conferences and Computers and Information in Engineering Conference. American Society of Mechanical Engineers Digital Collection, 2003, pp. 245–254. DOI: 10.1115/DETC2003/DFM-48157.

[73] *Home | Official LEGO® Shop GB*. URL: https://www.lego.com/en-gb/ (visited on 11/22/2021).

[74] *MINDSTORMS® | Themes | Official LEGO® Shop GB*. URL: https://www.lego.com/en-gb/themes/mindstorms (visited on 11/24/2021).

[75] D. Boa, D. Mathias, and B. Hicks. “Evolving LEGO: Prototyping requirements for a customizable construction kit”. In: *DS 87-4 Proceedings of the 21st International Conference on Engineering Design (ICED 17) Vol 4: Design Methods and Tools, Vancouver, Canada, 21-25.08.2017* (2017). ISBN: 9781904670926, pp. 397–306.

[76] D. Mathias. “Investigating and Characterising the Coupling of LEGO and 3D Printing”. In: (October 2019).

[77] *MakerBeam - Think Build Enjoy*. MakerBeam. URL: https://www.makerbeam.com/?source=facebook (visited on 11/22/2021).

[78] J. Hur et al. “Hybrid rapid prototyping system using machining and deposition”. In: *Computer-Aided Design*. Rapid Technologies: Solutions for Today and Tomorrow 34.10 (Sept. 1, 2002), pp. 741–754. DOI: 10.1016/S0010-4485(01)00203-2.

[79] L. Lennings. “Selecting Either Layered Manufacturing or CNC Machining to Build Your Prototype .” In: (1997), pp. 1–9.

[80] J. W. Schmidt. “CNC Machining - The Other Rapid Prototyping Technology”. In: SAE International Congress and Exposition. Feb. 24, 1997, p. 970368. DOI: 10.4271/970368.

[81] T. Schmitz et al. “The application of high-speed CNC machining to prototype production”. In: *International Journal of Machine Tools and Manufacture* 41.8 (June 1, 2001), pp. 1209–1228. DOI: 10.1016/S0890-6955(01)00005-0.

[82] M. B. Wall, K. T. Ulrich, and W. C. Flowers. “Evaluating prototyping technologies for product design”. In: *Research in Engineering Design* 3.3 (Sept. 1992), pp. 163–177. DOI: 10.1007/BF01580518.

[83] I. Campbell, D. Bourell, and I. Gibson. “Additive manufacturing: rapid prototyping comes of age”. In: *Rapid Prototyping Journal* 18.4 (Jan. 1, 2012). Publisher: Emerald Group Publishing Limited, pp. 255–258. DOI: 10.1108/13552541211231563.

[84] Jean-Claude André. *From Additive Manufacturing to 3D/4D Printing 1*. DOI: 10.1002/9781119428510.

[85] Sculpteo. *The State of 3D Printing 2017*. 2017, pp. 1–40.

[86] C. Moreau. *The State of 3D Printing 2018*. Publication Title: Sculpteo the state of 3D printing 2018. 2018, pp. 1–40.

[87] Sculpteo. *The State of 3D Printing 2019*. Issue: April. 2019, p. 26.

[88] Sculpteo. *The State of 3D Printing 2020*. 2020, p. 23.

[89] *3D printing prototypes: How to improve your manufacturing process?* Sculpteo. URL: https://www.sculpteo.com/en/3d-learning-hub/3d-printing-business/3d-printing-prototypes/ (visited on 10/25/2022).

[90] I. Gibson et al. “Introduction and Basic Principles”. In: *Additive Manufacturing Technologies*. Ed. by I. Gibson et al. Cham: Springer International Publishing, 2021, pp. 1–21. DOI: 10.1007/978-3-030-56127-7_1.

[91] S. Kumar. “Additive Non-layer Manufacturing”. In: *Additive Manufacturing Processes*. Ed. by S. Kumar. Cham: Springer International Publishing, 2020, pp. 159–170. DOI: 10.1007/978-3-030-45089-2_10.

[92] ISO/TC 261. *ISO/ASTM 52900:2021: Additive manufacturing — General principles — Fundamentals and vocabulary*. ISO. Nov. 2021. URL: https://www.iso.org/cms/render/live/en/sites/isoorg/contents/data/standard/07/45/74514.html (visited on 11/24/2021).

[93] B. Kelly et al. “Computed Axial Lithography (CAL): Toward Single Step 3D Printing of Arbitrary Geometries”. In: (May 16, 2017). arXiv: 1705.05893.

[94] R. Liu et al. “13 - Aerospace applications of laser additive manufacturing”. In: *Laser Additive Manufacturing*. Ed. by M. Brandt. Woodhead Publishing Series in Electronic and Optical Materials. Woodhead Publishing, Jan. 1, 2017, pp. 351–371. DOI: 10.1016/B978-0-08-100433-3.00013-0.

[95] P. Gradl, O. Mireles, and N. Andrews. *Introduction to Additive Manufacturing for Propulsion Systems*. Aug. 21, 2019. DOI: 10.13140/RG.2.2.13113.93285.

[96] Ultimaker. *3D Printing Success Stories*. 2019. URL: https://ultimaker.com/learn/stories (visited on 05/04/2020).

[97] B. Blakey-Milner et al. “Metal additive manufacturing in aerospace: A review”. In: *Materials & Design* 209 (Nov. 1, 2021), p. 110008. DOI: 10.1016/j.matdes.2021.110008.

[98] R. Leal et al. “Additive manufacturing tooling for the automotive industry”. In: *The International Journal of Advanced Manufacturing Technology* 92.5 (Sept. 1, 2017), pp. 1671–1676. DOI: 10.1007/s00170-017-0239-8.

[99] MANUFACTUR3D. *Formula 1 & FIA use Additive Manufacturing to build 50% scaled models to test their 2021 Car Regulations*. MANUFACTUR3D. Aug. 27, 2019. URL: https://manufactur3dmag.com/formula-1-fia-use-additive-manufacturing-to-build-50-scaled-models-to-test-their-2021-car-regulations/ (visited on 11/29/2021).

[100] M. Schmitt, R. M. Mehta, and I. Y. Kim. “Additive manufacturing infill optimization for automotive 3D-printed ABS components”. In: *Rapid Prototyping Journal* 26.1 (Jan. 6, 2020). Publisher: Emerald Group Publishing Ltd., pp. 89–99. DOI: 10.1108/RPJ-01-2019-0007.

[101] *Introducing the "faster than Formula 1" hypercar with a 3D printed gearbox*. 3D Printing Industry. June 29, 2021. URL: https://3dprintingindustry.com/news/introducing-the-faster-than-formula-1-hypercar-with-a-3d-printed-gearbox-192132/ (visited on 11/29/2021).

[102] B. I. Wawrzyniak and J. Tangudu. “Design Analysis of High Power Density Additively Manufactured Induction Motor”. In: SAE 2016 Aerospace Systems and Technology Conference. Sept. 20, 2016, pp. 2016–01–2063. DOI: 10.4271/2016-01-2063.

[103] N. Simpson et al. “Additive Manufacturing of Shaped Profile Windings for Minimal AC Loss in Electrical Machines”. In: *IEEE Transactions on Industry Applications* 56.3 (May 2020). Conference Name: IEEE Transactions on Industry Applications, pp. 2510–2519. DOI: 10.1109/TIA.2020.2975763.

[104] *BOSEbuild: Accelerating design and testing phases with 3D printed parts*. ultimaker.com. URL: https://ultimaker.com/learn/bosebuild-accelerating-design-and-testing-phases-with-3d-printed-parts (visited on 11/29/2021).

[105] H. Dodziuk. “Applications of 3D printing in healthcare”. In: *Kardiochirurgia i Torakochirurgia Polska = Polish Journal of Cardio-Thoracic Surgery* 13.3 (Sept. 2016), pp. 283–293. DOI: 10.5114/kitp.2016.62625.

[106] E. Rezvani Ghomi et al. “Future of additive manufacturing in healthcare”. In: *Current Opinion in Biomedical Engineering* 17 (Mar. 1, 2021), p. 100255. DOI: 10.1016/j.cobme.2020.100255.

[107] D. D. Camacho. “Applications of Additive Manufacturing in the Construction Industry”. In: (2018).

[108] H. Felton, R. Hughes, and A. Diaz-Gaxiola. “Negligible-cost microfluidic device fabrication using 3D-printed interconnecting channel scaffolds”. In: *PLOS ONE* 16.2 (Feb. 3, 2021). Ed. by Z. Li. Publisher: Public Library of Science, e0245206. DOI: 10.1371/journal.pone.0245206.

[109] *Heineken: Ensuring production continuity with 3D printing*. ultimaker.com. URL: https://ultimaker.com/learn/heineken-ensuring-production-continuity-with-3d-printing (visited on 11/29/2021).

[110] *3D printing custom refractory mold cores for industrial ceramics*. ultimaker.com. URL: https://ultimaker.com/learn/3d-printing-custom-refractory-mold-cores-for-industrial-ceramics (visited on 11/29/2021).

[111] X. Zhang and F. Liou. “Chapter 1 - Introduction to additive manufacturing”. In: *Additive Manufacturing*. Ed. by J. Pou, A. Riveiro, and J. P. Davim. Handbooks in Advanced Manufacturing. Elsevier, Jan. 1, 2021, pp. 1–31. DOI: 10.1016/B978-0-12-818411-0.00009-4.

[112] I. Gibson et al. “Design for Additive Manufacturing”. In: *Additive Manufacturing Technologies*. Ed. by I. Gibson et al. Cham: Springer International Publishing, 2021, pp. 555–607. DOI: 10.1007/978-3-030-56127-7_19.

[113] *Transformation in 3D Printing: How A Walnut-Sized Fuel Nozzle Changed The Way GE Aviation Builds Jet Engines | GE News*. URL: https://www.ge.com/additive/stories/transformation-3d-printing-how-walnut-sized-fuel-nozzle-changed-way-ge-aviation-builds-jet (visited on 11/29/2021).

[114] *Complex geometries are possible with 3D printing | EOS*. URL: https://www.eos.info/en/industrial-3d-printing/advantages/complex-geometries (visited on 11/29/2021).

[115] *Bugatti - World premiere: brake caliper from 3-D printer*. URL: https://www.bugatti.com/media/news/2018/world-premiere-brake-caliper-from-3-d-printer/ (visited on 11/29/2021).

[116] J. Gopsill et al. “Achieving Responsive and Sustainable Manufacturing Through a Brokered Agent-Based Production Paradigm”. In: *Sustainable Design and Manufacturing*. Ed. by S. G. Scholz, R. J. Howlett, and R. Setchi. Smart Innovation, Systems and Technologies. Singapore: Springer, 2022, pp. 24–33. DOI: 10.1007/978-981-16-6128-0_3.

[117] K. Rainey. *3-D Printer Could Turn Space Station into ’Machine Shop’*. NASA. Apr. 3, 2015. URL: http://www.nasa.gov/mission_pages/station/research/news/3D_in_space (visited on 11/29/2021).

[118] S. Loff. *International Space Station’s 3-D Printer*. NASA. Feb. 25, 2015. URL: http://www.nasa.gov/content/international-space-station-s-3-d-printer (visited on 11/29/2021).

[119] Z. Zhu et al. “A review of hybrid manufacturing processes – state of the art and future perspectives”. In: *International Journal of Computer Integrated Manufacturing* 26.7 (July 1, 2013). Publisher: Taylor & Francis _eprint: https://doi.org/10.1080/0951192X.2012.749530, pp. 596–615. DOI: 10.1080/0951192X.2012.749530.

[120] G. A. Roth et al. “Potential occupational hazards of additive manufacturing”. In: *Journal of Occupational and Environmental Hygiene* 16.5 (May 4, 2019). Publisher: Taylor & Francis _eprint: https://doi.org/10.1080/15459624.2019.1591627, pp. 321–328. DOI: 10.1080/15459624.2019.1591627.

[121] Q. Zhang et al. “Characterization of Particle Emissions from Consumer Fused Deposition Modeling 3D Printers”. In: *Aerosol Science and Technology* 51 (2017), p. 0. DOI: 10.1080/02786826.2017.1342029.

[122] D. E. Jones et al. “Early Stage Digital Twins for Early Stage Engineering Design”. In: *Proceedings of the Design Society: International Conference on Engineering Design* 1.1 (2019), pp. 2557–2566. DOI: 10.1017/dsi.2019.262.

[123] F. Calignano et al. “Overview on Additive Manufacturing Technologies”. In: *Proceedings of the IEEE* 105.4 (Apr. 2017). Conference Name: Proceedings of the IEEE, pp. 593–612. DOI: 10.1109/JPROC.2016.2625098.

[124] B. Caulfield, P. E. McHugh, and S. Lohfeld. “Dependence of mechanical properties of polyamide components on build parameters in the SLS process”. In: *Journal of Materials Processing Technology* 182.1 (Feb. 2, 2007), pp. 477–488. DOI: 10.1016/j.jmatprotec.2006.09.007.

[125] P. Guo et al. “Study on microstructure, mechanical properties and machinability of efficiently additive manufactured AISI 316L stainless steel by high-power direct laser deposition”. In: *Journal of Materials Processing Technology* 240 (Feb. 1, 2017), pp. 12–22. DOI: 10.1016/j.jmatprotec.2016.09.005.

[126] M. Goudswaard, B. Hicks, and A. Nassehi. “Towards the democratisation of design: a generalised capability model for FDM”. In: *Int. J. Agile Systems and Management* 13.1 (2020), pp. 79–101. DOI: 10.3233/978-1-61499-898-3-125.

[127] M. K. Thompson et al. “Design for Additive Manufacturing: Trends, opportunities, considerations, and constraints”. In: *CIRP Annals* 65.2 (Jan. 1, 2016), pp. 737–760. DOI: 10.1016/j.cirp.2016.05.004.

[128] W. Liu, Z. Zhu, and S. Ye. “A decision-making methodology integrated in product design for additive manufacturing process selection”. In: *Rapid Prototyping Journal* 26.5 (2020), pp. 895–909. DOI: 10.1108/RPJ-06-2019-0174.

[129] A. Boschetto and L. Bottini. “Accuracy prediction in fused deposition modeling”. In: (2014), pp. 913–928. DOI: 10.1007/s00170-014-5886-4.

[130] C. Li, J. Liu, and Y. Guo. “Prediction of Residual Stress and Part Distortion in Selective Laser Melting”. In: *Procedia CIRP* 45 (Jan. 1, 2016). Publisher: Elsevier, pp. 171–174. DOI: 10.1016/J.PROCIR.2016.02.058.

[131] T. Mukherjee, W. Zhang, and T. DebRoy. “An improved prediction of residual stresses and distortion in additive manufacturing”. In: *Computational Materials Science* 126 (Jan. 1, 2017). Publisher: Elsevier, pp. 360–372. DOI: 10.1016/J.COMMATSCI.2016.10.003.

[132] J. Francis and L. Bian. “Deep Learning for Distortion Prediction in Laser-Based Additive Manufacturing using Big Data”. In: *Manufacturing Letters* 20 (Apr. 1, 2019), pp. 10–14. DOI: 10.1016/j.mfglet.2019.02.001.

[133] I. Gibson et al. “Post-Processing”. In: *Additive Manufacturing Technologies*. Ed. by I. Gibson et al. Cham: Springer International Publishing, 2021, pp. 457–489. DOI: 10.1007/978-3-030-56127-7_16.

[134] I. Gibson et al. “Materials for Additive Manufacturing”. In: *Additive Manufacturing Technologies*. Ed. by I. Gibson et al. Cham: Springer International Publishing, 2021, pp. 379–428. DOI: 10.1007/978-3-030-56127-7_14.

[135] *Wohlers Associates publishes 2021 annual State of 3D Printing report*. 3D Printing Industry. Mar. 17, 2021. URL: https://3dprintingindustry.com/news/wohlers-associates-publishes-2021-annual-state-of-3d-printing-report-186439/ (visited on 11/29/2021).

[136] T. Wohlers et al. *Wohlers Report 2021: 3D Printing and Additive Manufacturing Global State of the Industry*. Wohlers Associates, Incorporated, 2021.

[137] *The Devil Is In The Details: How GE Found A Way To Bring 3D Printing To Mass Production | GE News*. URL: https://www.ge.com/news/reports/devil-details-3d-printed-part-jet-engine-part-now (visited on 11/29/2021).

[138] B. Redwood. *Additive manufacturing technologies: An overview*. 3D Hubs. URL: https://www.hubs.com/knowledge-base/additive-manufacturing-technologies-overview/ (visited on 11/24/2021).

[139] *LightSPEE3D 3D Metal Printer*. SPEE3D. Nov. 4, 2019. URL: https://www.spee3d.com/product/lightspee3d/ (visited on 11/25/2021).

[140] I. Gibson et al. “Material Jetting”. In: *Additive Manufacturing Technologies*. Ed. by I. Gibson et al. Cham: Springer International Publishing, 2021, pp. 203–235. DOI: 10.1007/978-3-030-56127-7_7.

[141] 3D Hubs. *3D Printing Trends 2020*. 3D Hubs, 2020.

[142] P. Siemiński. “Chapter 7 - Introduction to fused deposition modeling”. In: *Additive Manufacturing*. Ed. by J. Pou, A. Riveiro, and J. P. Davim. Handbooks in Advanced Manufacturing. Elsevier, Jan. 1, 2021, pp. 217–275. DOI: 10.1016/B978-0-12-818411-0.00008-2.

[143] *Official Doodle Pen | 3D Printing Pen Art*. Doodle Pen. URL: https://www.doodlepen.co.uk/ (visited on 11/25/2021).

[144] Ultimaker. *Ultimaker Cura: Powerful, easy-to-use 3D printing software*. 2021. URL: https://ultimaker.com/software/ultimaker-cura (visited on 06/23/2021).

[145] *PrusaSlicer | Original Prusa 3D printers directly from Josef Prusa*. URL: https://www.prusa3d.com/page/prusaslicer_424/ (visited on 11/25/2021).

[146] *Enabling the full potential of 3D printing*. 3MF Consortium. URL: https://3mf.io/ (visited on 11/25/2021).

[147] M. Fernandez-Vicente et al. “Effect of Infill Parameters on Tensile Mechanical Behavior in Desktop 3D Printing”. In: *3D Printing and Additive Manufacturing* 3.3 (Sept. 1, 2016). Publisher: Mary Ann Liebert, Inc., publishers, pp. 183–192. DOI: 10.1089/3dp.2015.0036.

[148] J. Villacres, D. Nobes, and C. Ayranci. “Additive manufacturing of shape memory polymers: effects of print orientation and infill percentage on mechanical properties”. In: *Rapid Prototyping Journal* 24.4 (May 14, 2018). Publisher: Emerald Group Publishing Ltd., pp. 744–751. DOI: 10.1108/RPJ-03-2017-0043.

[149] Ultimaker. *Ultimaker S3: Easy-to-use 3D printing starts here*. 2020. URL: https://ultimaker.com/3d-printers/ultimaker-s3 (visited on 05/12/2021).

[150] *Original Prusa i3 MMU2S upgrade kit (for MK2.5 & MK3S/+) | Original Prusa 3D printers directly from Josef Prusa*. URL: https://www.prusa3d.com/product/original-prusa-i3-mmu2s-upgrade-kit-for-mk2-5-mk3s-org/ (visited on 11/29/2021).

[151] 3D Jake UK. *Flashforge Creator Pro*. 3DJake UK. URL: https://www.3djake.uk/flashforge/creator-pro (visited on 11/29/2021).

[152] *Palette 3 Pro*. Mosaic Manufacturing. URL: https://www.mosaicmfg.com/products/palette-3-pro (visited on 11/29/2021).

[153] P. F. Flowers et al. "3D printing electronic components and circuits with conductive thermoplastic filament". In: *Additive Manufacturing* 18 (Dec. 1, 2017), pp. 156–163. DOI: 10.1016/j.addma.2017.10.002.

[154] M. L. Smith and J. F. Jones. "Dual-extrusion 3D printing of anatomical models for education". In: *Anatomical Sciences Education* 11.1 (2018). _eprint: https://onlinelibrary.wiley.com/doi/pdf/10. pp. 65–72. DOI: 10.1002/ase.1730.

[155] *Multi-Material 3D Printing Guide*. All3DP. Aug. 11, 2019. URL: https://all3dp.com/2/multi-material-3d-printing-an-overview/ (visited on 11/29/2021).

[156] Prusa Research. "Original PRUSA I3 MK35S+". In: (2021).

[157] *What 3D Printer Nozzle Size Should I Use? - The Pros and Cons...* rigid.ink. URL: https://rigid.ink/blogs/news/what-3d-printer-nozzle-size-should-i-use-the-pros-and-cons (visited on 11/29/2021).

[158] *Olsson Ruby Nozzle: Review the Specs*. All3DP. Feb. 14, 2021. URL: https://all3dp.com/2/olsonn-ruby-nozzle-review-specs/ (visited on 11/29/2021).

[159] C. Bell. *3D Printing with Delta Printers*. Apress, 2015.

[160] B. M. Schmitt et al. "A Comparative Study of Cartesian and Delta 3D Printers on Producing PLA Parts". In: *Materials Research* 20 (Feb. 5, 2018). Publisher: ABM, ABC, ABPol, pp. 883–886. DOI: 10.1590/1980-5373-MR-2016-1039.

[161] M. Ratiu, D. M. Anton, and D. C. Negrau. "Experimental study on the settings of Delta and Cartesian 3D printers for samples printing". In: *IOP Conference Series: Materials Science and Engineering* 1169.1 (Aug. 2021). Publisher: IOP Publishing, p. 012026. DOI: 10.1088/1757-899X/1169/1/012026.

[162] *3D printing technology – Delta versus Cartesian - Tractus3D*. URL: https://tractus3d.com/knowledge/learn-3d-printing/3d-printing-technology-delta-versus-cartesian/ (visited on 11/29/2021).

[163] F. M. Mwema and E. T. Akinlabi. "Basics of Fused Deposition Modelling (FDM)". In: *Fused Deposition Modeling: Strategies for Quality Enhancement*. Ed. by F. M. Mwema and E. T. Akinlabi. SpringerBriefs in Applied Sciences and Technology. Cham: Springer International Publishing, 2020, pp. 1–15. DOI: 10.1007/978-3-030-48259-6_1.

[164] *70525 | Polymaker 1.75mm Black PLA 3D Printer Filament, 1kg | RS Components*. URL: https://uk.rs-online.com/web/p/3d-printing-materials/2009387/?cm_mmc=UK-PLA-DS3A-_-google-_-CSS_UK_EN_Computing_%26_Peripherals_Whoop-_-3D+Printing+Materials_Whoop-_-2009387&matchtype=&aud-827175561347:pla-305759255199&gclid=Cj0KCQiAkZKNBhDiARIsAPsk0Wio8KfJq8lQAMWAcjL0BMlPaTz6tDHu53W4SNuF9wcB&gclsrc=aw.ds (visited on 11/29/2021).

[165] *Continuous Carbon Fiber - High Strength 3D Printing Material*. Markforged. URL: https://markforged.com/materials/continuous-fibers/continuous-carbon-fiber (visited on 11/29/2021).

[166] Markforged. *Markforged Metal X*. 2019. URL: https://markforged.com/metal-x/.

[167] Desktop Metal. *Desktop Metal*. 2019. URL: https://www.desktopmetal.com/.

[168] *Filaments.directory Releases Results of 2018 3D Printing Filament Survey*. 3DPrint.com | The Voice of 3D Printing / Additive Manufacturing. Apr. 18, 2018. URL: https://3dprint.com/210552/filaments-directory-2018-survey/ (visited on 11/30/2021).

[169] T. C. Kershaw, K. Hölttä-otto, and Y. S. Lee. "The Effect of Prototyping and Critical Feedback on Fixation in Engineering Design". In: *33rd Annual Meeting of the Cognitive Science Society* (2011), pp. 807–812.

[170] *Abrasive filaments*. Learn ColorFabb. July 28, 2017. URL: https://learn.colorfabb.com/abrasive-filaments/ (visited on 11/29/2021).

[171] *Definition of mass | Dictionary.com*. en.

[172] M. Levi. *The Mathematical Mechanic: Using Physical Reasoning to Solve Problems*. Princeton University Press, 2009.

[173] S. R. Mitchell, R. Jones, and M. King. “Head speed vs. racket inertia in the tennis serve”. In: *Sports Engineering* 3.2 (May 1, 2000). Publisher: Springer Nature, pp. 99–110. DOI: 10.1046/j.1460-2687.2000.00051.x.

[174] *consumer good | Definition, Types, Examples, & Facts | Britannica*. URL: https://www.britannica.com/topic/consumer-good (visited on 12/07/2021).

[175] J. L. du Bois, N. A. J. Lieven, and S. Adhikari. “Error analysis in trifilar inertia measurements”. In: *Experimental Mechanics* 49.4 (2009), pp. 533–540. DOI: 10.1007/s11340-008-9142-4.

[176] Ultimaker. *Ultimaker Drill*. 2017. URL: https://www.youmagine.com/designs/hand-drill (visited on 09/23/2019).

[177] H. Felton. *Ultimaker Hand Drill with mass pockets*. YouMagine. URL: https://www.youmagine.com/designs/ultimaker-hand-drill-with-mass-pockets (visited on 11/30/2021).

[178] Ultimaker. *Technical data sheet PLA*. Pages: 1-3. 2018.

[179] S. J. Hall. *Basic Biomechanics*. Delaware: McGraw-Hill, 2012. 202 - 205 and 210 - 212.

[180] S. Plagenhoef, F. Gaynor Evans, and T. Abdelnour. *Anatomical Data for Analyzing Human Motion*. Volume: 54 Issue: 2. 1983, pp. 169–178.

[181] G. (Pahl et al. *Engineering design: a systematic approach*. 3rd ed. Solid mechanics and its applications. Section: xxi, 617 pages : illustrations ; 24 cm. London: Springer, 2007. xxi, 617.

[182] S. Pugh. *Total design: integrated methods for successful product engineering*. Section: 278 pages. Addison-Wesley, 1990. 278 pp.

[183] RS Components. *RS PRO 2.85mm Copper MT-COPPER 3D Printer Filament, 750g | RS Components*. 2021. URL: https://uk.rs-online.com/web/p/3d-printing-materials/1254348/?cm_mmc=UK-PLA-DS3A-_-google-_-CSS_UK_EN_Computing_%26_Peripherals_Whoop-_-3D+Printing+Materials_Whoop-_-1254348&matchtype=&aud-842313741498:pla-304675461982&gclid=CjwKCAjw8cCGBhB6EiwAgORey9m9fO (visited on 06/21/2021).

[184] The Engineering Toolbox. *Metals and Alloys - Densities*. URL: https://www.engineeringtoolbox.com/metal-alloys-densities-d_50.html (visited on 12/20/2021).

[185] *Specification*. 3MF Consortium. URL: https://3mf.io/specification/ (visited on 02/05/2022).

[186] *Membership*. 3MF Consortium. URL: https://3mf.io/membership/ (visited on 02/05/2022).

[187] *Iron-filled Metal Composite PLA*. ProtoPlant, makers of Proto-pasta. URL: https://www.proto-pasta.com/products/magnetic-iron-pla (visited on 12/18/2021).

[188] Proto Pasta. *Stainless Steel PLA*.

[189] BASF. *TDS Ultrafuse 316L*. May 2019.

[190] *3D Solex Hardcore Everlast UM3 – S3 -S5*. URL: https://3dsolex.com/product/s5-hardcore-60-sapphire-everlast/ (visited on 02/17/2021).

[191] H. Felton, J. Yon, and B. Hicks. "Improving Feel in 3D Printed Prototypes: A Numeric Methodology for Controlling Mass Properties Using Infill Structures". In: *Design Studies* (In Review).

[192] H. Taha. *Operations Research: an Introduction, Global Edition*. Harlow, UNITED KINGDOM: Pearson Education, Limited, 2017.

[193] A. W. Mohamed. "Solving large-scale global optimization problems using enhanced adaptive differential evolution algorithm". In: *Complex & Intelligent Systems* 3.4 (Dec. 1, 2017), pp. 205–231. DOI: 10.1007/s40747-017-0041-0.

[194] K. Tang et al. "Benchmark Functions for the CEC'2010 Special Session and Competition on Large-Scale". In: *undefined* (2009).

[195] *Ultimaker 3*. ultimaker.com. URL: https://ultimaker.com/3d-printers/ultimaker-3 (visited on 03/19/2022).

[196] *70540 | Polymaker 2.85mm Grey PLA 3D Printer Filament, 1kg | RS Components*. URL: https://uk.rs-online.com/web/p/3d-printing-materials/2009426 (visited on 03/19/2022).

[197] *Ultimaker print cores and add-ons*. ultimaker.com. URL: https://ultimaker.com/3d-printers/ultimaker-print-cores-and-addons (visited on 03/19/2022).

[198] *PrintBite+ An Excellent 3D Print Surface for your 3D Printer*. URL: https://flex3drive.com/printbite/ (visited on 02/17/2021).

[199] J. A. Afonso et al. “Influence of 3D printing process parameters on the mechanical properties and mass of PLA parts and predictive models”. In: *Rapid Prototyping Journal* 27.3 (Apr. 2, 2021), pp. 487–495. DOI: 10.1108/RPJ-03-2020-0043.

Appendix A
Publication Abstracts

Improving Feel in 3D Printed Prototypes: A Numeric Methodology for Controlling Mass Properties Using Infill Structures

Felton, H., Yon, J. and Hicks, B.

To Be Confirmed

(In Review)

Product prototypes often have mass properties significantly different to the product they represent. This affects both functional performance and stakeholder perception of the prototype. Within this work, emulation of mass properties for a primitive object (a cube) is considered, developing a baseline method and parameter set. The developed method is then applied and tuned to three case study products, demonstrating that relevant product mass properties could be numerically emulated to within ~1% of the target values. This was achieved using typical material extrusion technology with no physical or process modification. It was observed that emulation accuracy is dependent on the relative displacement of the centre of mass from the geometric centre.

Negligible-cost microfluidic device fabrication using 3D-printed interconnecting channel scaffolds

Felton, H., Hughes, R., Diaz Gaxiola, A.

PLOS One

(3rd February 2021)

This paper reports a novel, negligible-cost and open-source process for the rapid prototyping of complex microfluidic devices in polydimethylsiloxane (PDMS) using 3D-printed interconnecting microchannel scaffolds. These single-extrusion scaffolds are designed with interconnecting ends and used to quickly configure complex microfluidic systems before being embedded in PDMS to produce an imprint of the microfluidic configuration. The scaffolds are printed using common Material Extrusion (MEX) 3D printers and the limits, cost and reliability of the process are evaluated. The limits of standard MEX 3D-printing with off-the-shelf printer modifications is shown to achieve a minimum channel cross-section of 100×100 μm. The paper also lays out a protocol for the rapid fabrication of low-cost microfluidic channel moulds from the thermoplastic 3D-printed scaffolds, allowing the manufacture of customisable microfluidic systems without specialist equipment. The morphology of the resulting PDMS microchannels fabricated with the method are characterised and, when applied directly to glass, without plasma surface treatment, are shown to efficiently operate within the typical working pressures of commercial microfluidic devices. The technique is further validated through the demonstration of 2 common microfluidic devices; a fluid-mixer demonstrating the effective interconnecting scaffold design, and a microsphere droplet generator. The minimal cost of manufacture means that a 5000-piece physical library of mix-and-match channel scaffolds (100 μm scale) can be printed for ~$0.50 and made available to researchers and educators who lack access to appropriate technology. This simple yet innovative approach dramatically lowers the threshold for research and education into microfluidics and will make possible the rapid prototyping of point-of-care lab-on-a-chip diagnostic technology that is truly affordable the world over.

Looks like but does it feel like? Investigating the influence of mass properties on user perceptions of rapid prototypes

Felton, H., Yon, J. and Hicks, B.

Design 2020

(11th June 2020)

Prototyping is a key part of the design process, with artefacts increasingly fabricated using 3D printing methods. However, these printed parts often lack internal structure and the mass properties of the artefact – mass, balance and moments of inertia – differ from the design. It is hypothesised that a stakeholder's assessment of a design is affected by this misrepresentation. The work presented demonstrates that mass properties have a significant effect on stakeholder perception of prototypes. This is done through a study of University of Bristol students and consultation with industry.

Appendix B
Alternative Concept Selection

Table B.1: Pugh matrix considering the identified methods for mass property emulation in MEX product prototypes. The matrix is baselined to the small lumped masses method.

	Small, regular masses	Variable infill	Large, bespoke masses	Standard parts	Particulates	Fluids
Automation	0	+	-	+	+	-
Ease of use	0	+	-	+	+	-
Safety	0	0	0	0	-	0
Cost/kg	0	+	0	+	+	+
Hardware cost	0	+	-	+	+	+
Emulation accuracy (Material Density)	0	-	0	-	-	-
Retention	0	+	0	+	0	-
Total	0	4	-3	4	2	-2

Appendix C
Effects of the Central Limit Theorem

The effects of the central limit theorem, for the work discussed within this thesis, are two-fold:

1. Increasing the number of discrete options a continuum is broken down into reduces the variance of samples taken from this.
2. Increasing the number of discrete compositions a cell within a continuum may take reduces the variance of samples taken from this.

Each of these effects are presented here.

C.1 Number of Compositions

To investigate the better option, a simple example is used. Three random number generators are used. The first of these has 11 possible outputs: 0, 10, 20, 30 etc. up to 100 (inclusive). Each value has a 1 in 11 chance of being the output. The second has 101 outputs: 0 through 100. Each value has a 1 in 101 chance of being output. Finally, the last has two outputs: 0 and 100, each with a 1 in 2 chance of being selected. Figure C.1 shows the derived normal distribution of averages (for a sample size of 10). This effect is commonly known as the central limit theorem.

It is clear from Figure C.1 that the use of a distribution with fewer outputs leads to the results having greater variance. For the mass property emulation problem, this is advantageous, as it promotes exploration.

C.2 Number of Cells

A two-dimensional area is considered as a simple analogue to the forms detailed within the rest of this thesis, as in Figure C.2. It is possible to break this area into several smaller cells. Figure C.2 shows three different cell breakdowns – with 4, 25 and 100 cells representing the area. It is then possible to consider this in a similar way to the emulation method – where individual cells can be “filled”. Through doing this randomly with a target fill factor of 0.5 (the

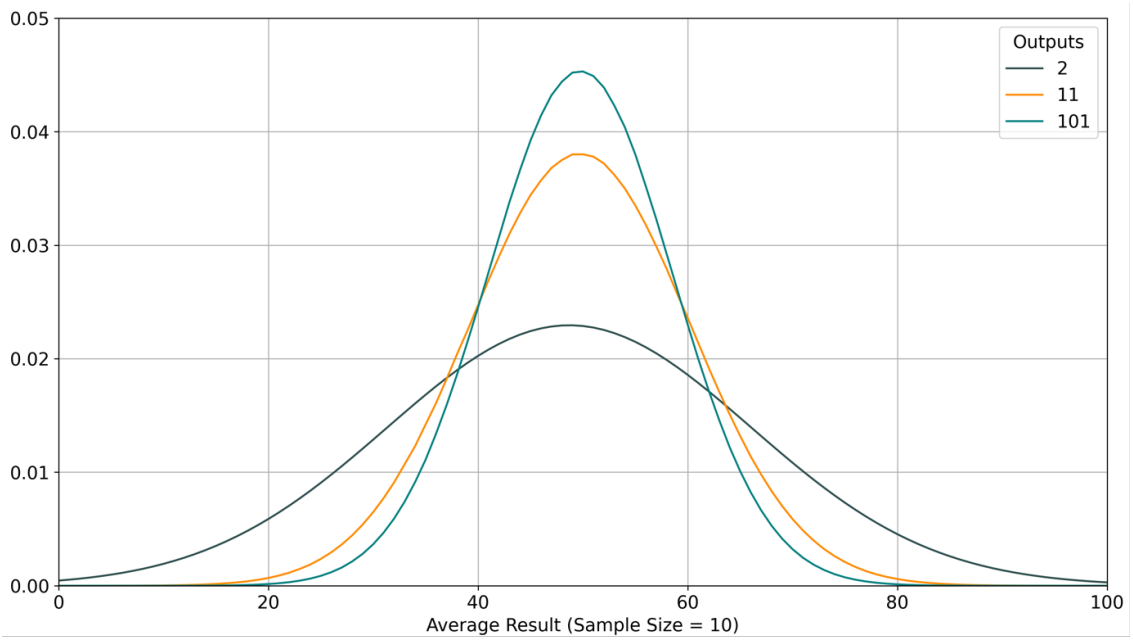

Figure C.1: Normal distribution derived from average sample results (sample size = 10) for three different systems using 100 samples, intended to show the effect of cell composition on variability in result.

proportion of the total area filled), it is possible to identify a distribution of results for the fill factor and average fill position. The mean and standard deviation for these distributions is shown in Table C.1.

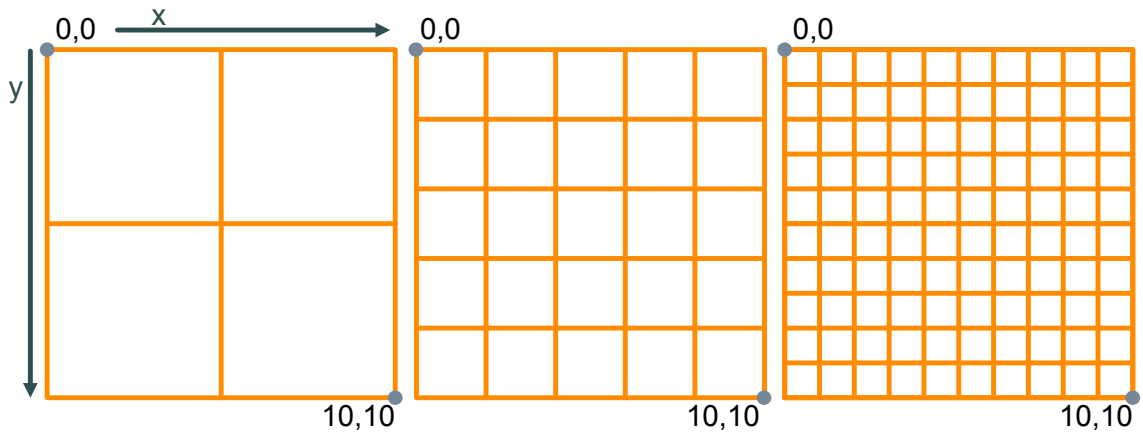

Figure C.2: Graphical breakdown of the area showing the distribution of cells.

Table C.1: Results from the test case demonstrating the reduction in standard deviation of distribution when increasing the number of cells.

Property		Number of Cells		
		4	25	100
Mean	Fill Factor	0.502	0.510	0.499
	Mean X Position	4.961	5.012	5.021
	Mean Y Position	4.919	5.077	4.954
Standard Deviation	Fill Factor	0.254	0.095	0.050
	Mean X Position	1.545	0.577	0.307
	Mean Y Position	1.536	0.607	0.280

As the number of cells defining the volume increases, the standard deviation of the results reduces – both for fill factor and mean fill position. This directly applies to the emulation process, with the exception that the emulation method will be applied to three-dimensional space. It is then clear that to search a solution space more broadly it is important to have as few cells as possible. This must, however, be balanced with the need to:

- Reduce the effect of individual cells on the fill factor.
- Improve the accuracy of geometric form (relative to the as-designed product).

As such, it would be advantageous to allow the number of cells to be larger, whilst developing a method to properly investigate and search the solution space.

Appendix D
User Study Results

Table D.1: Results from the user study depicted in Chapter 4.

Participant	Scores (Drill 1/2/3)	Q2 Answers	Q2 Discussion	Q3 Answers	Q3 Discussion
1	4	Too Heavy	1 was too light	Functional drill	The larger chuck referred to the length
	5	Drill bit long		Larger chuck	
	1			Placement for forefinger should improve	
2	3	Too lightweight		CoG (centre of gravity) closer to grip	Better control, easier to guide
	3			Slightly longer grip	Tad too heavy
	4				Heavier to grip
3	3	The weight is spread across, very unstable		Make very slightly lighter	Same location of mass
	1	Too light, reduced precision		More space for the hand on the grip	Drill 3 was too heavy
	5				
4	2	Far too light		Better grip	"Top Heavy"
	3	Hard to move precisely due to its mass		More weight in handle - better balance	
	5				
5	4	It has not proper centre of mass	Refers to 3	Make a bit heavier, as it feels too light	
	3	Heavy	Would like the CoM to move down towards the grip		
	3		Talks of inertia		
6	2	Too unrealistically light		Realistic but too heavy -> smaller motor and battery	Confirmed the reference to the light was regarding visual, not mass
	4			Improve design of the handle and focus most of the weight here	Mentioned balance
	5			Add light in the front	
7	5	Heavier		Lighter	
	4				
	2				
8	4	Too heavy	Lots of effort to move	Shorter drill bit (to improve accuracy)	
	5	Hard to control	Referenced inertia	Comfier grip (e.g. rubber)	
	3	Drill bit too long			
9	5	Weight (too heavy)	"Manoeuvre" refers to inertia	A taller handle	Light and easy
	4	Hard to manoeuvre			Moves well
	2				Feels good
10	3	Bad grip		Make it stable - poor base	Add mass
	4	Heavy		A tad bit heavier	
	2				
11	3	Lightweight		Grip unhandle	Grip should be rubber (or similar)
	2	Unstable bottom		More space to hold drill area	Bigger grip
	4				Balance is amazing
12	3	Weight distribution	Heavy at back		No obvious improvements
	5	Bit too heavy			Like Drill 2 - not too light
	2				Grip is good
13	1	Not heavy enough		Make it more stable when standing	
	4				
	3				
14	2	Too light	Reference to inertia - drill bit led movement	Balance the drill to make it more accurate	Balance refers to the drill rolling in use
	3	Felt less accurate			They would like the mass moved forward
	4				
15	4	Weight	Lighten	Grip	Unsafe grip
	5		Off-balance		Change grip to rubber
	2				
16	5	Weight	Too heavy	Smaller drill	Refers to length of bit
	3		Balance was top heavy		Smaller drill bit (diameter) preferred
	2				Feels okay
17	3	Heavy (wasn't expecting that)	Balance - top heavy		No improvements observed
	5				Thought drill 2 was neither too heavy nor too light
	2				
18	3	Heavy, bulky	Bad balance (movement)	Lighter weight	Weight reduction to improve precision in use
	5				
	2				
19	3	The body of the drill is too heavy, difficult to control it	Top heavy	Make the handle a little bit heavy	Centre of gravity to handle
	4		Referenced inertia making it harder to control		
	2				
20	2	Either too heavy or too light (depends on drill)		Bigger handle	Taller handle preferred
	4	Weight not distributed evenly			
	2				
21	2	Size of grip		Improve grip size	
	3	Lack of weight		Slightly less weight	
	4				
22	3	Too light	Referred to RI when discussing turning	Make it heavier (closer to normal drill weight)	Moved the centre of gravity to handle
	1	Didn't resist turning		Balance the drill with battery	Preferred Drill 3, but 1 was better balanced
	4	Was expecting different weight distribution			Drill 1 was seen as flimsy
23	3	Weight too far back		Bigger handle	
	4	Quite heavy		Weight centered	
	2	Handle small		Drill quite long	
24	2	Too light		More even weight distribution (more in the battery end)	
	3	Trigger too far forward		Longer handle	
	4	Handle too small		Thicker handle	
25	5	Heavy		Decrease the thickness of the grip	
	3				
	1				